

**A NOVEL ROLE FOR 5-hmC IN THE REGULATION OF
CANCER TESTIS GENE EXPRESSION IN CANCER AND
MESENCHYMAL TO EPITHELIAL TRANSITION**

**A THESIS SUBMITTED TO
THE DEPARTMENT OF MOLECULAR BIOLOGY AND GENETICS
AND THE GRADUATE SCHOOL OF ENGINEERING AND SCIENCE
OF BILKENT UNIVERSITY
IN PARTIAL FULFILLMENT OF THE REQUIREMENTS
FOR THE DEGREE OF
DOCTOR OF PHILOSOPHY**

**BY
SİNEM YILMAZ ÖZCAN
DECEMBER, 2014**

I dedicated my thesis to my mum and dad for the endless love they gave, my husband and son for being the meaning of my life.

I certify that I have read this thesis and that in my opinion it is fully adequate, in scope and in quality, as a thesis for the degree of Doctor of Philosophy.

Assis. Prof. Dr. Ali O. Güre

(Advisor)

I certify that I have read this thesis and that in my opinion it is fully adequate, in scope, and in quality, as a thesis for the degree of Doctor of Philosophy.

Assoc. Prof. Dr. Işık Yuluğ

I certify that I have read this thesis and that in my opinion it is fully adequate, in scope, and in quality, as a thesis for the degree of Doctor of Philosophy.

Assis. Prof. Dr. Stefan Fuss

I certify that I have read this thesis and that in my opinion it is fully adequate, in scope, and in quality, as a thesis for the degree of Doctor of Philosophy.

Assoc. Prof. Dr. Sreeparna Banerjee

I certify that I have read this thesis and that in my opinion it is fully adequate, in scope, and in quality, as a thesis for the degree of Doctor of Philosophy.

Prof. Dr.Can Akçalı

Approved for the Graduate School of Engineering and Science

Prof. Dr. Levent Onural

Director of the Graduate School of Engineering and Science

ABSTRACT

A NOVEL ROLE FOR 5-hmC IN THE REGULATION OF CANCER TESTIS GENE EXPRESSION IN CANCER AND MESENCHYMAL TO EPITHELIAL TRANSITION

Sinem YILMAZ ÖZCAN

Ph.D. in Molecular Biology and Genetics

Supervisor: Assist. Prof. Dr. Ali O. Güre

December 2014

Cancer/testis (CT) genes show highly restricted expression among normal tissues, limited to germ cells in the testis and ovary, and to trophoblast cells, but are frequently expressed in various cancers. Other than a clear association with promoter-specific demethylation and histone deacetylation, the specific mechanisms by which these genes are expressed are currently unknown. In this study, we tested various mechanisms including promoter- and region-specific epigenetic mechanisms to gain a better understanding of CT gene expression.

To better study the epigenetic mechanisms regulating CT gene expression, we searched for a model that dynamically expresses CT genes. As a result of preliminary bioinformatic efforts and literature search, we chose to study CT gene expression in Caco-2 spontaneous differentiation model. We showed that *PAGE-2, -2B* and *SPANX-B* genes were up-regulated significantly as Caco-2 cells differentiated. Differentiation was also characterized as a mesenchymal to epithelial transition as evidenced by the decrease in mesenchymal markers (*Fibronectin1*, *Vimentin* and *Transgelin*) and the concomitant increase in epithelial markers (*E-cadherin*, *Claudin 4* and *Cdx2*). CT protein (*SPANX-B* and *PAGE-2, -2B*) positive cells were positive for epithelial protein (*Cdx2*), and negative for mesenchymal proteins (*Fibronectin1*, *Vimentin*). Although we could not find a significant difference in promoter proximal DNA demethylation of CT genes, we identified that promoter proximal DNA was hydroxymethylated with a gradual increase in hydroxymethylation as cells differentiated. The change in hydroxymethylation level was concordant with an increase in TET enzyme levels and co-localization of TET2 protein with CT proteins in the corresponding cells. Besides, we found that promoters of CT genes lost EZH2, H3K27me3 and HP1 marks as CT genes were up-regulated. Reversal of differentiation resulted in loss of CT and TET gene expression and EMT induction. Thus, for the first time, we describe dynamic expression of CT genes in association with DNA hydroxymethylation in mesenchymal to epithelial transition.

In addition to promoter-proximal alterations, we thought that epigenetic alterations leading to CT gene expression in cancer could occur within larger regions containing CT

genes, but with clear boundaries. As genes that do not show an expression pattern similar to CT genes can be located within their proximity, we hypothesized that there could be clear boundaries between neighbouring regions containing CT genes and those with non-CT type expression patterns. We, therefore, identified 2 genes; *ALAS2* and *CDRI*, in close proximity to two different CT genes (*PAGE-2,-2B* and *SPANX-B*), which were downregulated in cancer, and thus showed an expression pattern opposite to that of these two CT genes. *ALAS2* and *CDRI* were downregulated in lung and colon cancer cell lines compared to healthy counterparts. We found that the downregulation of *ALAS2* and *CDRI* in cancer cell lines, in contrast to CT genes, was independent of DNA hypomethylation. We also found that *ALAS2* and *CDRI* downregulation in cancer was possibly related to decreased levels of hydroxymethylation in promoter proximal regions. As the upregulation of *PAGE-2,-2B* and *SPANX-B* genes was associated with increased hydroxymethylation at promoter-proximal regions, these two groups of genes, despite their close proximity were found to be controlled inversely albeit possibly by the same mechanisms. We tested if ectopic upregulation of *ALAS2* and *CDRI* in cancer cell lines would result in a tumor-suppressive effect, but were unable to find any. As both genes are located about 200 and 50 kbs from *SPANX-B* and *PAGE-2*, we propose that there might be a boundary within these regions that could possibly have an insulator-like function to help distinguish the two very different epigenetic events occurring in tumorigenesis.

As almost all CT genes map within highly homologous inverted repeats it is possible that 3 dimensional chromosomal structures formed around these repeats underlie the common epigenetic mechanism responsible for coordinate CT gene expression. To test for this hypothesis, we analyzed expression of various transcripts identified within and outside the NY-ESO-1 repeat region. However, we could not find a correlation between the presence of such transcripts and CT gene expression patterns.

Keywords: Cancer testis genes, *PAGE-2,-2B*, *SPANX-B*, DNA hydroxymethylation, mesenchymal to epithelial transition

ÖZET

KANSERDE VE MEZENKİMALDEN EPİTELE GECİŞ SÜRECİNDE

5-hmC'NİN KANSER TESTİS GEN İFADESİNDEKİ ÖZGÜN ROLÜ

Sinem YILMAZ ÖZCAN

Moleküler Biyoloji ve Genetik Doktora Tezi

Tez Yöneticisi: Yard. Doç. Dr. Ali O. Güre

Aralık 2014

Kanser testis (KT) genleri normal dokular içinde sınırlı şekilde sadece yumurtalık ve testislerdeki eşey üreme hücreleri ve trofoblast hücrelerinde ifade edilirken, pek çok kanserde sıklıkla ifade edildiği gözlenmiştir. Promotor bölgesine özgü DNA demetilasyonu ve histon deasetilasyonu ile ilgili açık bir ilişki haricinde bu genlerin ifade edilmesindeki spesifik mekanizmalar bilinmemektedir. Bu çalışmada KT gen ifadesini daha iyi anlayabilmek için KT genlerini bulunduran promotor bölgelerine özgü ve alana sınırlı epigenetik mekanizmaları test ettik.

KT gen ifadesi varlığında ve yokluğundaki epigenetik mekanizmaları daha iyi çalışabilmek için, KT genlerini dinamik olarak ifade eden bir model aradık. Öncü biyoinformatik analizler ve literatür araştırması sonucunda, KT genlerini Caco-2 farklılaşmasında incelemeyi seçtik. *PAGE-2*, *-2B* ve *SPANX-B* gen ifadelerinin farklılaşan Caco-2 hücrelerinde anlamlı şekilde arttığını gösterdik. Mezenkimal belirteç gen ifadeleri (*Fibronectin1*, *Vimentin* ve *Transgelin*) azaldığı ve eş zamanlı olarak epitel belirteç gen ifadeleri (*E-cadherin*, *Claudin 4* ve *Cdx2*) arttığı için farklılaşma mezenkimalden epitele geçiş süreci olarak tanımlanmıştır. Bunun yanı sıra, KT proteinlerini (*SPANX-B* ve *PAGE-2*, *-2B*) bulunduran hücrelerin epitel belirteç proteinini (*CDX2*) de bulundurduğu, mezenkimal belirteç proteinlerini (*Fibronectin1* ve *Vimentin*) de bulundurmadığını gösterdik. Farklılaşmış Caco-2 hücrelerinde artan KT genlerinin promotor yakınındaki DNA bölgelerinde anlamlı demetillasyon gözlemlenmemekle birlikte bu bölgelerde hidroksimetilasyon seviyelerinde aşamalı bir artış tespit edilmiştir. Promotor yakını bölgelerdeki hidroksimetilasyon seviyesindeki artış aynı zamanda TET enzim seviyesindeki artış ile ve de TET2 proteini ve KT proteinlerinin aynı hücrelerdeki konumlanması ile uyumlu bulunmuştur. Bunların yanı sıra, KT gen ifadesi ile birlikte KT genlerinin promotor bölgelerindeki *EZH2* ve *HP1* proteinlerinin işgali ve *H3K27me3* işareti azalmıştır. Caco-2 farklılaşması tersine döndürüldüğünde KT ve TET gen ifadelerinin azalması ve epitelden mezenkimala geçiş ile sonuçlanmıştır. Böylece bu çalışma ile ilk defa KT genlerinin dinamik ifadesi gösterilmiş, bu süreç mezenkimalden epitele geçiş ve DNA hidroksimetilasyonu ile açıklanmıştır.

Promotor yakını bölgelerdeki deęişimlerin yanısıra, kanserde KT gen ifadesine sebep olan epigenetik deęişikliklerle alternatif epigenetik deęişikliklerin aynı anda sınırları belli farklı bölgelerde meydana geldiğini düşündük. KT genleri ve KT genlerine komşuluk eden ama KT gen ifade paterninden farklı gen ifadesine sahip olan genler arasında sınırlar olabileceğini hipotezledik. Boylece, KT genlerine (*PAGE-2*, *-2B* ve *SPANX-B*) komşuluk eden ve kanserde gen ifadesi azalan 2 geni, *ALAS2* ve *CDRI*'i, bulduk. *ALAS2* ve *CDRI* gen ifadelerinin sağlıklı dokulara kıyasla kolon ve akciğer kanseri hücre hatlarında azaldığını gösterdik. *ALAS2* ve *CDRI* gen ifadelerinin kanser hücre hatlarındaki azalışlarının KT gen ifadesinden farklı olarak DNA metilasyonundan bağımsız olduğunu bulduk. Kanserde *ALAS2* ve *CDRI* gen ifadesi azalışlarının promotor yakını bölgelerdeki artan hidroksimetilasyon seviyesi ile kuvvetli ihtimal ilişkili olabileceğini gözlemledik. *PAGE-2*, *-2B* ve *SPANX-B* gen ifadelerindeki artış da DNA hidroksimetilasyonu ile ilişkili bulunmuştur, bu iki grup genlerinin farklı ifade paternlerine rağmen. Kanser hücre hatlarındaki *ALAS2* ve *CDRI* gen ifadelerinin çarpıcı azalışına rağmen, bu genlerin kanser hücrelerindeki ektopik ifadeleri sonucu hücre canlılığı ölçümlerinde anlamlı bir deęişiklik bulunmamıştır. *ALAS2* ve *CDRI*, sırasıyla *PAGE-2*, *-2B* ve *SPANX-B* genlerine 200 ve 50 kbs uzaklıkta konumlandığından, bu bölgeler arasında farklı epigenetik olayların meydana gelmesinde etkili yalıtkan bir sınır bulunduğunu önermekteyiz.

KT genlerinin neredeyse tamamı yüksek homolojik benzerliği bulunan tekrar bölgelerinde konumlandığından, bu tekrar bölgelerinin katlanarak 3 boyutlu yapılar oluşturması ve bu yapıların eş güdümlü KT gen ifadesinden sorumlu mekanizma olması muhtemeldir. Bu hipotezi test etmek için, *NY-ESO-1* genini içeren tekrar bölgesinin içindeki ve dışındaki genlerin ifadesini inceledik. Ancak anlamlı bir ilişki tespit edemedik.

Anahtar sözcükler: Kanser testis genleri, *PAGE-2*, *-2B*, *SPANX-B*, DNA hidroksimetilasyonu, mezenkimalden epitele geçiş

ACKNOWLEDGEMENT

I would like to owe my sincere gratitude to my advisor Assist. Prof. Dr. Ali O. Güre for not only guiding me in this work but also improving my thinking in this journey and helping me to find my way in the scientific area. He helped with his wide knowledge and experience but also let me to express myself, try and sometimes even fail in this period.

I would like to express my very great appreciation to Assoc. Prof. Dr. Sreeparna Banerjee and Dr. Aslı Sade Memişoğlu for their mental and physical support in this nice collaboration. It was such an important chance for me to work with them since it taught me a lot about being in a productive collaboration.

I would like to extend my appreciation to my thesis follow up committee members Assoc. Prof. Dr. Işık Yuluğ and Assis. Prof. Dr. Stefan Fuss. They always participated with their important critics and motivated me to do further during my PhD study.

I am grateful to Kerem Mert Şenses, Barış Küçükkaraduman, Dilan Çelebi and Yasemin Kaygusuz for their joyful and indispensable contributions to this study. This work could not be completed without their help.

I also would like to thank all past and present members of Gure lab; Kerem Mert Şenses, Şükrü Atakan, Barış Küçükkaraduman, Alper Poyraz, Seçil Demirkol , Waqas Akbar, Mehdi Ghassemi, Murat İşbilen, Duygu Akbaş, Derya Dönertaş, Aydan Bulut Karşlıoğlu since we altogether generated a perfect and amusing working environment.

I am especially grateful to my friends in Bilkent, Kerem Mert Şenses, Şükrü Atakan, Emre Yurdusev, Ceyhan Ceran, Gizem Ölmezer, İrem Gürbüz, Eylül Harputlugil, Merve Aydın, Ece Akhan Güzelcan since they were always with me and this journey was meaningful with them. Gurbet Karahan, Nilüfer Sayar and Dilan Çelebi were more than a friend and became a part of my family during these six years, though I am thankful for their companionship.

I would like to express my very great appreciation to all Bilkent MBG family. Bilge Kılıç, Füsun Elvan, Sevim Baran, Yıldız Karabacak, Yavuz Ceylan and Abdullah Ünnü made this department as a home for all of us.

Undoubtedly, I am grateful to my mother Nuray Yılmaz and father Duran Yılmaz for being beside me and believing me in all stages of my educational life. I do not know how to thank my husband Tahsin Özcan since he always supported me with patience and stood by me during tough times. Finally, I would like to thank my baby boy Ege to being my little sunshine at the end of this long journey.

I was supported by TÜBİTAK BİDEB 2211 scholarship during my PhD study; thereby I would like to thank TÜBİTAK to giving me this opportunity.

Table of Contents

ABSTRACT	iv
ÖZET	vi
ACKNOWLEDGEMENT	viii
List of Figures:.....	xiv
List of Tables:	xvii
Abbreviations:.....	xviii
1 INTRODUCTION	1
1.1 CANCER TESTIS GENES	1
1.1.1 Expression Patterns of Cancer Testis Genes.....	1
1.1.2 Genomic Structure of Cancer Testis Genes	3
1.1.3 Epigenetics of Cancer Testis Genes.....	3
1.1.4 Cancer Testis Gene Expression in Stem Cells	5
1.1.5 Cancer Testis Gene Expression during Epithelial to Mesenchymal Transition.....	5
1.2 CACO-2 SPONTANEOUS DIFFERENTIATION MODEL.....	6
1.3 DNA HYDROXYMETHYLATION AS EPIGENETIC CONTROL MECHANISMS OF GENE EXPRESSION.....	8
1.4 AIM AND HYPOTHESIS.....	12
2 MATERIALS AND METHODS.....	13
2.1 MATERIALS.....	13
2.1.1 General Chemicals	13
2.1.2 Instruments.....	24
2.1.3 Cell Lines and Tissue Culture Reagents	25
2.2 SOLUTIONS AND MEDIA	27
2.2.1 General Solutions.....	27
2.2.2 Cell Culture Solutions.....	29
2.3 METHODS	30
2.3.1 Cancer cell culture techniques	30
2.3.2 RNA isolation with TRIzol.....	30
2.3.3 DNA Isolation with Phenol-Chloroform-Isoamylalcohol Extraction	31

2.3.4	Identification of CT-proximal down-regulated genes in cancer compared to healthy counterparts by Cancer Genome Anatomy Project.....	31
2.3.5	Q RT-PCR Experiments with Taqman Probe Chemistry	32
2.3.6	Sequencing of sodium bisulphite treated tumor cell lines' and normal tissues' DNAs	32
2.3.7	Plasmid constructions	33
2.3.8	Generation of stable cell lines.....	34
2.3.9	β -Galactosidase Staining Assay.....	35
2.3.10	MTT Cell Viability Assay	35
2.3.11	Spontaneous differentiation and dedifferentiation of Caco-2 cell line	36
2.3.12	In silico analysis of CT gene expression during Caco-2 spontaneous differentiation	36
2.3.13	Total RNA isolation and DNaseI treatment.....	36
2.3.14	cDNA synthesis	37
2.3.15	Q RT-PCR of CT genes	37
2.3.16	<i>In silico</i> identification of differentially expressed mesenchymal and epithelial genes during Caco-2 spontaneous differentiation	37
2.3.17	Q RT-PCR of mesenchymal and epithelial marker genes	38
2.3.18	Promoter methylation analysis.....	38
2.3.19	Hydroxymethylated DNA Immunoprecipitation	39
2.3.20	Immunofluorescence microscopy	39
2.3.21	Protein Isolation.....	40
2.3.22	Western Blotting.....	40
2.3.23	Chromatin Immunoprecipitation (ChIP).....	40
2.3.24	<i>In vitro</i> treatment of tumor cell lines with 5-aza-2-deoxycytidine	41
2.3.23	Q RT-PCR Experiments with SYBR Green chemistry for noncoding RNA expression in NY-ESO-1 repeat region	42
3	RESULTS:.....	43

3.1 EPIGENETIC MECHANISMS LEADING CANCER TESTIS GENE EXPRESSION IN CACO-2 SPONTANEOUS DIFFERENTIATION MODEL.....	43
3.1.1 Cancer Testis gene expression in Caco-2 spontaneous differentiation model:.....	43
3.1.2 Characterization of Caco-2 spontaneous differentiation in association with MET and CT gene expression:.....	45
3.1.3 Epigenetic mechanisms underlying CT gene expression in Caco-2 spontaneous differentiation:	57
3.2 REGION SPECIFIC EPIGENETIC MECHANISMS OF CANCER TESTIS (CT) AND CT PROXIMAL GENE EXPRESSION.....	66
3.2.1 Analysis of CT proximal genes down-regulated in cancer by CGAP:	66
3.2.2 The down-regulation in mRNA expression of CT proximal genes; <i>ALAS2</i> and <i>CDR1</i> and CT gene expression in cancer:	67
3.2.3 The promoter proximal DNA methylation of <i>ALAS2</i> and <i>CDR1</i> genes in normal tissues and colon and lung cancer cell lines:.....	71
3.2.4 The response of CT proximal genes; <i>ALAS2</i> , <i>CDR1</i> and CT genes; <i>PAGE-2,-2B</i> , <i>SPANX-B</i> to 5-aza-2'-deoxycytidine treatment in cancer cell lines:	76
3.2.5 The promoter proximal DNA hydroxymethylation of <i>ALAS2</i> and <i>CDR1</i> genes in normal tissues, colon and lung cancer cell lines:	77
3.2.6 The gene expression of <i>TET</i> enzymes in normal tissues and colon and lung cancer cell lines:.....	78
3.2.7 The result of ectopic expressions of <i>ALAS2</i> and <i>CDR1</i> genes in cancer cell lines in cell viability manner:	79
3.2.8 <i>ALAS2</i> and <i>CDR1</i> expression in Caco-2 spontaneous differentiation model	82
3.3 GENE EXPRESSION INSIDE AND OUTSIDE OF A CANCER TESTIS GENE-CONTAINING REPEAT REGION	84
3.3.1 Uncoordinated expression of <i>NY-ESO-1</i> , <i>IκBG</i> and the noncoding RNAs in NY-ESO-1 containing repeat region:.....	84
4 DISCUSSION AND CONCLUSION.....	86
5 FUTURE PERSPECTIVES.....	92
6 REFERENCES	93
APPENDIX A.....	101
APPENDIX B	105

APPENDIX C	109
7 PUBLICATION	120

List of Figures:

FIGURE 1.1.1 1: THE EXPRESSION PATTERN OF CT-X GENES IN NORMAL TISSUES AND CANCER.....	2
FIGURE 1.2 1: DIFFERENTIALLY EXPRESSED GENES IN CACO-2 SPONTANEOUS DIFFERENTIATION.....	8
FIGURE 1.3 1: ACTIVE DNA DEMETHYLATION.....	10
FIGURE 1.3 2: PASSIVE DNA DEMETHYLATION	10
FIGURE 3.1.1 1: CT GENE EXPRESSION INCREASES DURING CACO-2 SPONTANEOUS DIFFERENTIATION.....	43
FIGURE 3.1.1 2: CACO-2 CELLS DIFFERENTIATE DURING 30 DAYS POST CONFLUENCE CULTURING.....	44
FIGURE 3.1.1 3: AMONG 6 CT GENE FAMILIES; THE GENE EXPRESSIONS OF <i>PAGE-2,-2B</i> AND <i>SPANX-B</i> INCREASE IN CACO-2 SPONTANEOUS DIFFERENTIATION.	45
FIGURE 3.1.2 2: CT GENE MRNA LEVELS INCREASE CONCOMITANT WITH MESENCHYMAL TO EPITHELIAL TRANSITION.....	47
FIGURE 3.1.2 3: INCREASE IN CDX-2 (34 KDA, EPITHELIAL PROTEIN) AND SPANX-B (12 KDA, CT PROTEIN), THE DECREASE IN TRANSGELIN (23 KDA), FIBRONECTIN (263 KDA) AND VIMENTIN (54 KDA) (MESENCHYMAL PROTEINS) AT THE PROTEIN LEVEL BY WESTERN BLOT EXPERIMENT IN 3 DIFFERENT DIFFERENTIATION SETS.....	48
FIGURE 3.1.2 4: DECREASE IN MRNA LEVELS OF MESENCHYMAL MARKER GENES (VIM, FN1 AND TAGLN) AND INCREASE IN MRNA LEVEL OF EPITHELIAL MARKER GENE (CDX2) EXIST IN PROTEIN LEVEL AS WELL.....	49
FIGURE 3.1.2 5: INCREASE IN MRNA LEVELS OF CT GENES (<i>SPANX-B</i> AND <i>PAGE-2,-2B</i>) EXISTS IN PROTEIN LEVEL AS WELL.....	50
FIGURE 3.1.2 6: DOUBLE IMMUNOFLUORESCENCE STAINING AT DAY 0 SHOWS THAT VIMENTIN POSITIVE CELLS ARE NEGATIVE FOR <i>SPANX-B</i> PROTEIN AND <i>SPANX-B</i> POSITIVE CELLS ARE NEGATIVE FOR VIMENTIN PROTEIN.....	51
FIGURE 3.1.2 7: DOUBLE IMMUNOFLUORESCENCE STAINING AT DAY 0 SHOWS THAT VIMENTIN POSITIVE CELLS ARE NEGATIVE FOR <i>PAGE-2,-2B</i> PROTEIN AND <i>PAGE-2,-2B</i> POSITIVE CELLS ARE NEGATIVE FOR VIMENTIN PROTEIN.....	52
FIGURE 3.1.2 8: DOUBLE IMMUNOFLUORESCENCE STAINING SHOWS THAT CDX2 PROTEIN CO-LOCALIZES WITH <i>SPANX-B</i> PROTEIN IN THE CORRESPONDING CELLS DURING DIFFERENTIATION.....	53
FIGURE 3.1.2 9: DOUBLE IMMUNOFLUORESCENCE STAINING SHOWS THAT CDX2 PROTEIN CO-LOCALIZES WITH <i>PAGE-2,-2B</i> PROTEIN IN THE CORRESPONDING CELLS DURING DIFFERENTIATION.....	54
FIGURE 3.1.2 10: DOUBLE IMMUNOFLUORESCENCE STAINING AT DAY 0 SHOWS THAT FIBRONECTIN POSITIVE CELLS ARE NEGATIVE FOR <i>SPANX-B</i> PROTEIN AND <i>SPANX-B</i> POSITIVE CELLS ARE NEGATIVE FOR FIBRONECTIN PROTEIN.	55
FIGURE 3.1.2 11: DOUBLE IMMUNOFLUORESCENCE STAINING AT DAY 0 SHOWS THAT FIBRONECTIN POSITIVE CELLS ARE NEGATIVE FOR <i>PAGE-2,-2B</i> PROTEIN AND <i>PAGE-2,-2B</i> POSITIVE CELLS ARE NEGATIVE FOR FIBRONECTIN PROTEIN.	56

FIGURE 3.1.3 1: THE PROMOTER PROXIMAL DNA REGIONS OF 3 CT GENES ARE HEAVILY HYPERMETHYLATED.....	58
FIGURE 3.1.3 2: THE AMOUNT HYDROXYMETHYLATED DNA INCREASES IN THE PROMOTER PROXIMAL REGIONS OF <i>PAGE-2</i> AND <i>SPANX-B</i> GENES DURING CACO-2 SPONTANEOUS DIFFERENTIATION.....	59
FIGURE 3.1.3 3: MRNA LEVELS OF <i>TET</i> GENES (<i>TET1</i> , <i>TET2</i> , <i>TET3</i>), RESPONSIBLE FOR 5HMC RESIDUE GENERATION, INCREASE DURING CACO-2 SPONTANEOUS DIFFERENTIATION.....	60
FIGURE 3.1.3 4: A POSSIBLE SMALL VARIANT OF TET2 PROTEIN IS FOUND TO BE INCREASED IN CACO-2 DIFFERENTIATION CONSISTENTLY IN 3 DIFFERENT DIFFERENTIATION SETS.	61
FIGURE 3.1.3 5: A POSSIBLE TRUNCATED FORM OF TET2 IS GENERATED WITH CA ⁺² DEPENDENT CALPAINS.	62
FIGURE 3.1.3 6: DOUBLE IMMUNOFLUORESCENCE STAINING SHOWS THAT TET2 PROTEIN CO-LOCALIZES WITH <i>SPANX-B</i> AND <i>PAGE-2,-2B</i> PROTEINS IN CACO-2 CELLS DURING DIFFERENTIATION.....	63
FIGURE 3.1.3 7: BINDING OF (A) EZH2, H3K27ME3 AND (B) HP1 TO THE PROMOTERS OF <i>PAGE-2B</i> , <i>PAGE-2</i> AND <i>SPANX-B</i> DECREASES DURING DIFFERENTIATION SHOWN BY CHIP WITH THE INDICATED ANTIBODIES OR CONTROL IGG.	64
FIGURE 3.1.3 8: AS THE DEDIFFERENTIATION OCCURS, CELLS GAIN MESENCHYMAL CHARACTER, DOWN-REGULATE CTS AND TET ENZYMES AT THE SAME TIME.	65
FIGURE 3.2.1 1: THE GENOMIC LOCATION OF <i>ALAS2</i> AND <i>CDR1</i> GENES WITH RESPECT TO PROXIMAL CANCER-TESTIS ANTIGENS; <i>PAGE-2,-2B</i> AND <i>SPANX-B</i> RESPECTIVELY.	67
FIGURE 3.2.2 1: THE MRNA EXPRESSION OF <i>ALAS2</i> GENE IS SHOWN IN NORMAL TISSUES AND A PANEL OF COLON AND LUNG CANCER CELL LINES BY TAQMAN PROBE BASED Q RT-PCR. <i>GAPDH</i> GENE WAS USED AS ENDOGENOUS CONTROL. ALTHOUGH <i>ALAS2</i> EXPRESSION WAS DETECTED IN VARIABLE AMOUNTS IN ALL HEALTHY TISSUES, IN NONE OF THE TESTED LUNG AND COLON CANCER CELL LINES <i>ALAS2</i> MRNA EXPRESSION EXISTED.	68
FIGURE 3.2.2 2: THE MRNA EXPRESSIONS OF <i>PAGE-2,-2B</i> GENES PROXIMAL TO <i>ALAS2</i> ARE SHOWN IN NORMAL TISSUES AND A PANEL OF COLON AND LUNG CANCER CELL LINES BY TAQMAN PROBE Q RT-PCR.	69
FIGURE 3.2.2 3: THE MRNA EXPRESSION OF <i>CDR1</i> GENE IS SHOWN IN NORMAL TISSUES AND A PANEL OF COLON AND LUNG CANCER CELL LINES BY TAQMAN PROBE Q RT-PCR.	70
FIGURE 3.2.2 4: THE MRNA EXPRESSION OF <i>SPANX-B</i> GENE PROXIMAL TO <i>CDR1</i> IS SHOWN IN NORMAL TISSUES AND A PANEL OF COLON AND LUNG CANCER CELL LINES BY TAQMAN PROBE Q RT-PCR.....	71
FIGURE 3.2.3 1: THE ORGANIZATION OF <i>ALAS2</i> GENE; PROMOTER, EXON-INTRON STRUCTURE AND BISULPHITE SEQUENCING RESULT OF THE ANALYZED CPG RESIDUES ARE SHOWN.	73

FIGURE 3.2.3 2: THE ORGANIZATION OF CDR1 GENE; PROMOTER, EXON-INTRON STRUCTURE AND BISULPHITE SEQUENCING RESULT OF THE ANALYZED CPG RESIDUES ARE SHOWN.	75
FIGURE 3.2.4 1: THE RESPONSE OF CT GENES AND CT PROXIMAL GENES TO 5-AZA-2'- DEOXYCYTIDINE TREATMENT IS SHOWED BY Q RT-PCR.	77
FIGURE 3.2.5 1: THE AMOUNT HYDROXYMETHYLATED DNA IN THE PROMOTER PROXIMAL REGIONS OF CT GENES AND CT-PROXIMAL GENES ARE SHOWN.	78
FIGURE 3.2.6 1: THE MRNA LEVELS OF <i>TET</i> GENES (<i>TET1</i> , <i>TET2</i> , <i>TET3</i>) IN COLON CANCER AND LUNG CANCER CELL LINES WITH RESPECT TO NORMAL COUNTERPARTS.	79
FIGURE 3.2.7 1: 3 CANDIDATE CLONES ARE IDENTIFIED AS A RESULT OF B- GALACTOSIDASE STAINING EXPERIMENT PERFORMED AFTER PCDNA4/TO/LACZ TRANSFECTION TO STABLE CLONES EXPRESSING TET REPRESSOR.	80
FIGURE 3.2.7 2: <i>ALAS2</i> GENE EXPRESSION IN TETRACYCLINE TREATED CLONES COMPARED TO UNTREATED AND UNTRANSFECTED CLONES.	81
FIGURE 3.2.7 3: THE CELL VIABILITY RESULTS ARE MEASURED BY MTT ASSAY AFTER ECTOPIC EXPRESSION OF <i>ALAS2</i> AND <i>CDR1</i> GENE.	82
FIGURE 3.3.1 1: THE LOCALIZATION OF PRIMERS HITTING <i>IKBG</i> , <i>NY-ESO-1</i> AND 3 NONCODING RNA GENES IN NY-ESO-1 REPEAT REGION.	85
FIGURE 3.3.1 2: THE EXPRESSIONS OF NONCODING RNAS IN REPEAT REGION, <i>IKBG</i> AND <i>NY-ESO-1</i> IN NY-ESO-1 POSITIVE (MAHLAVU, SK-LC-17 AND MDA-MB157) AND NEGATIVE CELL LINES (HCT116, SW20 AND MCF-7) ARE ANALYZED BY Q RT-PCR.	85
FIGURE 4 1: THE PROPOSED WINDOW OF EMT AND THE SUGGESTED EXPRESSION PATTERNS OF CT GENES IN EMT.	91

List of Tables:

TABLE 2.1.1 1: LIST OF CHEMICALS ENZYMES KITS.....	13
TABLE 2.1.1 2: LIST OF CONSTRUCTS AND VECTORS.....	17
TABLE 2.1.1 3: LIST OF POSITIVE AND NEGATIVE CONTROLS	18
TABLE 2.1.1 4: PRIMERS USED	19
TABLE 2.1.1 5: LIST OF ANTIBODIES USED IN IF STAINING AND WESTERN BLOTTING	22
TABLE 2.1.1 6: LIST OF ANTIBODIES USED IN CHIP	23
TABLE 2.1.2 1: LIST OF INSTRUMENT.....	24
TABLE 2.1.3 1: LIST OF CELL CULTURE REAGENTS	25
TABLE 3.2.3 1: THE METHYLATION STATUS OF <i>ALAS2</i> PROMOTER IN ANALYZED NORMAL TISSUES AND CANCER CELL LINES SHOWN AS PERCENT METHYLATION	74
TABLE 3.2.3 2: THE METHYLATION STATUS OF <i>CDR1</i> PROMOTER IN ANALYZED NORMAL TISSUES AND CANCER CELL LINES SHOWN AS PERCENT METHYLATION	76

Abbreviations:

CT	Cancer testis
5-AZA	5-aza-2-deoxycytidine
LINE1	Long interspersed elements
EZH2	Enhancer of zeste homolog 2
DNMT	DNA methyltransferase
LSD1	Lysine-specific demethylase 1
BORIS	Brother of the Regulator of Imprinted Sites
LAGE	L antigen family member 1
NY-ESO-1	New York esophageal squamous cell carcinoma 1
MAGE-A	Melanoma-associated antigens
SSX	Synovial sarcoma, X breakpoint 2
SPAN-X	Sperm protein associated with the nucleus
PAGE	P antigen family
MSC	Mesenchymal stem cell
hESC	Human embryonic stem cell
IL13RA	Interleukin 13 receptor, alpha 1
SOX2	Sex-determining region Y (SRY)-Box2
CSC	Cancer stem cell
EMT	Epithelial to mesenchymal transition
HMLE	Human mammary epithelial cell
TGF- β	Transforming growth factor beta
ECM	Extracellular matrix
DKO	Double knockout
GAPDH	Glyceraldehyde 3-phosphate dehydrogenase
TAGLN	Transgelin
FN1	Fibronectin 1
VIM	Vimentin
CDX2	Caudal type homeobox 2
CLDN4	Claudin 4
CDH1	E-Cadherin
TET	Ten-eleven translocation methylcytosine dioxygenase
I κ B γ	
ALAS2	Aminolevulinate, delta-, synthase 2
CDR1	Cerebellar degeneration-related protein 1
HP-1	Heterochromatin protein 1
PBS	Phosphate buffered saline
SAGE	Serial analysis of gene expression
EST	Expressed sequence tag
SDS	Sodium dodecyl sulphate
PVDF	Polyvinylidene fluoride
ECL	Enhanced chemiluminescence

ChIP	Chromatin immunoprecipitation
hMEDIP	Hydroxymethylated DNA immunoprecipitation
CGAP	Cancer genome anatomy project
DNMTi	DNA methyltransferase inhibitor
IF	Immunofluorescence
H3K27me3	Histone 3 Lysine 27 trimethylation
5Mc	5-methylcytosine
5hmC	5-hydroxymethylcytosine

1 INTRODUCTION

1.1 CANCER TESTIS GENES

1.1.1 Expression Patterns of Cancer Testis Genes

Cancer testis (CT) antigens are tumor-associated antigens that are activated in various human tumors from different origins. Cancer testis antigen gene expression is restricted to germ cells in testis and ovary and in trophoblast cells among healthy tissues [1]. Due to the aberrant gene expression in cancer and the restricted expression pattern in healthy tissues, CT genes are considered as a model to study epigenetic mechanisms behind gene expression and complex gene regulation processes.

Up to now, more than 140 CT genes belonging to at least 70 gene families have been identified by different methodologies such as T-cell epitope cloning, serological analysis of recombinant cDNA expression libraries and representational difference analysis [2,3].

CT genes have variable expression in different types of cancer. Melanoma, ovarian, bladder and non-small cell lung cancers have high CT gene expression, whereas breast and prostate cancers have moderate CT gene expression. Hematological malignancies such as lymphomas and leukemia, renal, colon and pancreatic cancers were identified as low CT expressing cancers[4] [5]. By using genome wide survey expression for 153 CT genes in normal and cancer expression libraries, Hofmann et al. classified CT genes in 3 groups; testis-restricted, testis/brain restricted and testis selective [6].

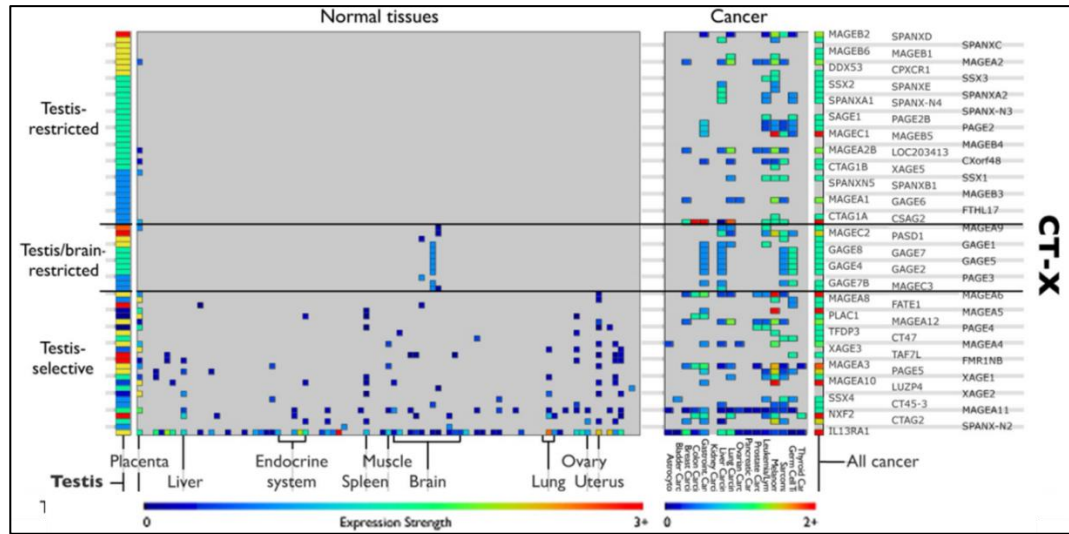


Figure 1.1.1: The expression pattern of CT-X genes in normal tissues and cancer
 CT genes on chromosome X are mainly expressed in testis and placenta among normal tissues. CT-X gene expression is detected in brain and in some of the normal tissues at very low levels albeit. Various CT genes are induced and detected in cancer tissues. Adopted from [6]. (Hofmann et al. PNAS, 105, 51, 2008 Genome-wide analysis of cancer/testis gene expression. Copyright (2008) National Academy of Sciences, U.S.A.)

Gure et al. found that the analyzed nine CT genes (*LAGE1*, *NY-ESO-1*, *MAGE-A1*, *MAGE-A3*, *MAGE-A4*, *MAGE-A10*, *CT7*, *SSX2* and *SSX4*) were coordinately expressed in non-small cell lung cancer. According to the study, the frequency of expression of a second CT antigen by a tumor already expressing a CT antigen was higher than the expression frequency if these two events were independent. The study also showed significant correlation between CT expression and larger tumours' and later stages of disease [7]. The associations between CT expression and different variables such as metastatic disease, poor survival and advanced tumour type have been established in many studies [5].

It has been previously shown that CT genes except *SPAN-X* were expressed in earlier stages of spermatogenesis such as spermatogonia and primary spermatocytes. CT gene expression seen at oogonia was similarly in the earlier stages of oogenesis. In the later stages of both spermatogenesis and oogenesis, CT gene expression was diminished [8].

1.1.2 Genomic Structure of Cancer Testis Genes

Cancer testis genes can be classified as the ones encoded from Chromosome X, CT genes and the ones encoded from chromosomes other than Chromosome X, non-CT genes. Most of the CT genes are members of multigene families and each family is composed of proximally located and highly homologous genes that vary from 3 (*NY-ESO*) to more than 12 (*MAGE*) genes. The multigene families exist on well-defined clusters that either form a direct or inverted repeat on Chromosome X [4,5]. In 2004, Warburton and his colleagues published the first genome wide inverted repeat structure of human genome identified by a software package named Inverted Repeat Finder program. The most dramatic result they obtained was the abundance of large and highly homologous inverted repeat regions containing CT genes on chromosome X. 10 of 20 inverted repeats that they identified on X-chromosome contained a gene expressed in testis tissue [9]. Since inverted repeats have the capacity to form self organizing loops and is a common property of majority of CT genes, the possible roles of repeats and loop formation on gene expression is an important question. The effect of the repeat structure on gene expression was proposed by Bredenbeck et al. They showed that gene expression inside the repeat region was coordinated compared to the gene expression outside the repeat region coding *MAGEA* and *CSAG* genes [10]. A direct physical link between gene expression and repeat structure, however, is still to be identified.

1.1.3 Epigenetics of Cancer Testis Genes

CT gene expression regulation is primarily epigenetic in nature. As well as promoter DNA hypermethylation in normal somatic tissues lacking CT gene expression, promoter DNA hypomethylation of CT genes in various CT expressing tumors have been shown in various studies. Induction of CT genes with the DNA hypomethylating agent, 5-aza-2'-deoxycytidine (5-AZA), in cancer cell lines is an important evidence of DNA methylation as a leading epigenetic mechanism controlling CT gene expression [1,11-15]. In addition to promoter and proximal promoter DNA hypomethylation, CT gene expression is associated with global DNA hypomethylation when *MAGEA11* expression and LINE1 methylation are studied [16]. The DNA methylation status of CT

genes shows intra- and inter-tumour heterogeneity [14,15]. Thus the clinical usages of DNA methylation inhibitors have importance in CT based immunotherapy studies. Role of histone acetylation in CT gene expression was revealed with synergistic effects of histone deacetylase inhibitors with DNA hypomethylating agent [11,17]. Recently role EZH2 and histone methylation on the expressions of *GAGE* and *MAGE* genes was presented in breast cancer cell lines. S-adenosylhomocysteine hydrolase inhibitor named 3-deazaneplanocin was previously shown to disrupt EZH2 complex. The combination of DNA hypomethylating agents with 3-deazaneplanocin resulted with enhancing expressions of *GAGE* and *MAGE* type CT genes [18]. In another study the inhibition of histone methyltransferase (KMT6) and histone demethylases (KDM1 and KDM5B) improved the effect of DNA hypomethylating agent deoxyazacytidine on expressions of *NY-ESO-1*, *MAGE-A1* and *MAGE-A3* genes in lung cancer cell lines. Thereby, incorporation of histone methylation in epigenetic regulation of CT genes was verified [19]. The synergistic effect of histone methylation and DNA demethylation was shown recently with the combined treatment of DNMT inhibitor and LSD1 inhibitor. LSD1 inhibitor inhibited demethylation of H3K4me2 and H3K4me1 and could synergistically activate CT gene expression when used with DNMT inhibitor[20]. The dominant function of DNA methylation in CT gene expression mechanisms compared to histone marks was suggested in works of De Smet et al. They generated a methylated *MAGEA1/hph* construct that was resistant to hygromycin upon stable re-activation. By either treating the generated clone with histone acetyltransferase inhibitor or by depleting DNA methyltransferase-1, they showed hygromycin resistant cells developed DNA hypomethylation and active histone marks[21]

The transcription factor BORIS was established as a candidate for the regulation of CT genes. The occupancy of BORIS in *NY-ESO-1* promoter was associated with gene expression [22]. The induction of BORIS resulted in the induction of *MAGE-A3* and *MAGE-A1* genes [23,24]. However in another study, BORIS overexpression with an adenoviral system did not induce CT genes, neither were promoter and global DNA demethylation levels altered [25]. Thus the role of BORIS in CT gene expression is controversial.

1.1.4 Cancer Testis Gene Expression in Stem Cells

CT gene expression in stem cells and whether CT genes have a role in stem cell differentiation pathways are interesting questions. Expression of various CT genes (*NRAGE*, *NY-ESO-1*, *MAGE-1* and *SSX*) has been detected in undifferentiated mesenchymal stem cells [26,27]. In addition to the CT gene expression in mesenchymal stem cells, melanoma and glioma cancer stem cells also express many CT genes (*MAGE*, *GAGE*, *NY-ESO-1* and *SSX* families) according to different studies[28-30].

CT gene expression (*SSX*, *NY-ESO-1* and *N-BAGE*) was observed in undifferentiated mesenchymal stem cells (MSC). CT gene expression was attenuated as MSCs differentiate to adipocytes and osteocytes [31]. In addition to MSCs, expressions of *MAGE-D1*, *-D2* genes in human embryonic stem cells (hESC) and expressions of *GAGEs*, *MAGE-A3*, *-A6*, *-A4*, *-A8* genes in human embryoid body cells were described by Lifantseva et al.[32]. In contrast, Loriot et al. showed that various CT genes either had very low or no expression in human embryonic cell lines compared to melanoma cell lines and testis by Q RT-PCR[33]. Whether CT gene expression being present in hESCs is controversial, the expression of CT genes in cancer stem cells (CSC) was demonstrated by showing the expression of *MAGED3*, *-D1*, *IL13RA*, *SPANXA* and *SPANXC* in CD133 and SOX2 positive CSCs derived from glioma cells lines and tissues [30].

1.1.5 Cancer Testis Gene Expression during Epithelial to Mesenchymal Transition

The relation between CSCs and epithelial to mesenchymal transition (EMT) process was characterized by Mani et al. EMT was induced in non-transformed immortalized human mammary epithelial cells (HMLEs) either by ectopically expressing Snail or Twist or TGF β 1 exposure. These cells started to resemble mesenchymal cells by expressing mesenchymal markers (*N-cadherin*, *Vimentin*, *Fibronectin*) and down-regulating epithelial markers (*E-cadherin*) and gained the ability to form mammospheres which was highly observed in human breast CSCs. EMT induced HMLEs was enriched in CD44^{high}/CD24^{low} population showing a strong association with normal human breast epithelial stem cells and human breast CSCs. The

study was further improved by establishing the high expression levels of mesenchymal markers and the low expression levels of epithelial markers in CD44^{high}/CD24^{low} cells isolated from patient tissue samples. [34]

According to these two observations; CT gene expression in glioma CSCs and the association of EMT with CSCs, there might be a connection between CT gene expression and EMT phenotype.

In literature, there were two papers confirming the relation of CT gene expression with EMT process. Contrary to the expectation, both of them claimed that CT gene expression was associated with the epithelial phenotype but not the mesenchymal phenotype in EMT. In the study conducted by Gupta et al., the gene expression in transformed HMLE in response of either salinomycin (shown to be effective on mesenchymal type of cells in tumor) or paclitaxel (shown to be effective on epithelial type of cells in tumor) was analyzed. *MAGE-A1* gene was up-regulated in salinomycin treatment which eliminated the mesenchymal cells and down-regulated in paclitaxel treatment which eliminated the epithelial cells [35]. Similarly, the result of another study done by Thomson et al. claimed that CT (*SPANXA1*, *-A2*, *SPANX-B1*, *-B2*, *SPANXC*, *MAGEA8*, *SOX2*) gene expression was diminished in two EMT models generated by stable transfection of Snail gene and TGF- β exposure[36].

The up-regulation of *MAGE-A1* gene in epithelial enriched population and the down-regulation of various CT genes in two important EMT models proved that CT gene expression might be related with epithelial phenotype in EMT.

1.2 CACO-2 SPONTANEOUS DIFFERENTIATION MODEL

To associate CT gene expression with epithelial phenotype of a cell, we used Caco-2 spontaneous differentiation model. Caco-2 and HT29 cell lines were derived from colorectal tumors and well known with their capabilities to differentiate into mature intestinal cells, such as enterocyte, mucus and M cells. Because of their differentiation potential, they became important tools for in vitro structural and

functional studies of the intestine cells [37]. At low seeding density, Caco-2 cells exhibit proper cell division and generate normal unpolarized and undifferentiated cells [38]. Under standard culture conditions and upon cell to cell contact formation, in 20 to 30 days differentiation process starts. Caco-2 cells stop dividing and become a monolayer of polarized epithelial cells. In addition to tight junctions, apical and basal-lateral membranes appear and cells resemble to polarized enterocytes both in structural and functional manner. Even though Caco-2 cells are derived from colon, they express hydrolyase enzymes and transport ions and water similar to enterocytes do [39]. It is important to note that although Caco-2 cells are valuable model for mimicking the differentiation taking place from crypts to villus, these cells are malignant and belonging to colon tissue but not small intestine [37].

In order to identify this model in depth and identify the transcriptional regulation during the enterocytic differentiation, two important studies have been done by Halbleib and Sääf et al. Caco-2 differentiation was generated by growing the cells on permeable filter supports for 26 days in this study. As well as the microscopic investigation, microarray experiments performed with RNAs isolated at different time points during differentiation were used for clarification of the differentiation process. Halbleib et al. showed that as well as apical brush border assembly (such as myosin 1A), many other proteins required for epithelial junctional complexes (Occludin, Claudin 1, protocadherins and desmosomal cadherins,) were regulated in transcriptional levels. The transcriptional regulation in some of extracellular matrix proteins (Laminin-1, Laminin-5), and intermediate filament proteins (Keratin-20, Keratin-18) were also established. This study claimed that the transcriptional regulation had an important role on Caco-2 cells being differentiate into a fully functional enterocyte in vitro without the effect of stromal cells and signals normally present in vivo[40]. In the other study carried by Sääf et al., according to microarray data there were two distinct clusters named prepolarization (samples from 0 to 4 days) and polarization cluster (samples from 4 to 26 days) which were formed by the difference in gene regulation at day 4. When the gene expression pattern during Caco-2 differentiation was compared with normal colon and colorectal cancer samples, there were two clusters; tumor and normal epithelial cluster. While prepolarized cells remained in tumor clusters, polarized cells remained

normal epithelial cluster. Several genes belonging to cell cycle checkpoints, ECM components, Wnt pathway were shown to be differentially regulated between tumor and normal epithelial cluster. As a result of this study, it has been established that differentiated Caco-2 cells resemble more to a normal epithelial cell than a tumor cell [41].

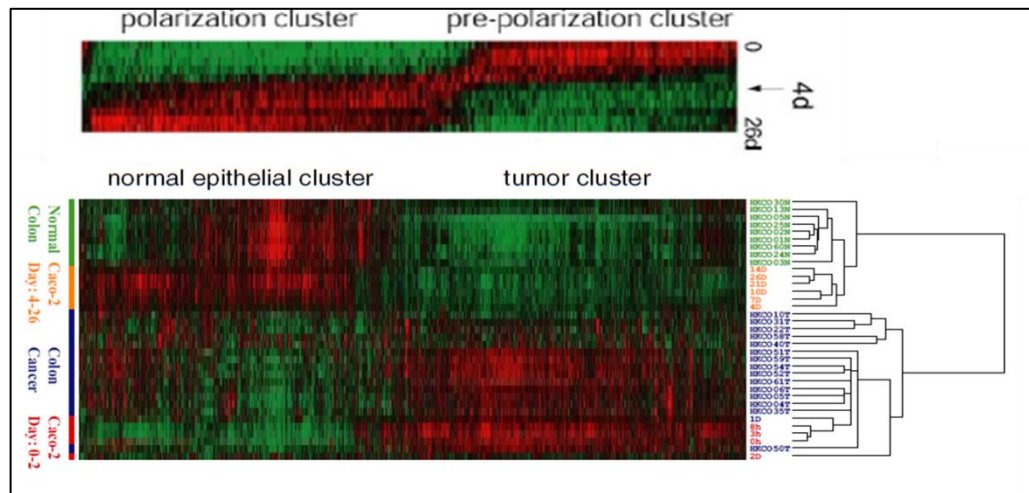


Figure 1.2 1: Differentially expressed genes in Caco-2 spontaneous differentiation. When the gene expression analysis is performed in Caco-2 spontaneous differentiation, there is a dramatic switch in gene expression pattern at day 4 time point. The undifferentiated Caco-2 cells (Day0-2) cluster with colon cancer and the differentiated Caco-2 cells (Day4-26) cluster with normal colon tissue. Adopted from [41].

1.3 DNA HYDROXYMETHYLATION AS EPIGENETIC CONTROL MECHANISMS OF GENE EXPRESSION

With the identification of 5-hydroxymethylcytosine (5-hmC) residue in Purkinje neurons and embryonic stem cells, 5-methylcytosine (5-mC) has become no more the only epigenetic modification of DNA [42,43]. This was groundbreaking information in epigenetics. 5-hydroxymethylcytosine was established as an epigenetic mark on DNA due to its binding partners and unique distribution patterns affecting gene expression with the following studies [43-45]. 5-hmC was shown to inhibit binding of methyl CpG binding protein 2 (MeCP2) to DNA thereby acting oppositely to 5-mC [46]. In addition

to inhibiting MeCP2 binding, 5-hmC has its own binding partners. 5-hmC was found to interact with Mbd3, a chromatin regulator, and this interaction was necessary for Tet1 binding to chromatin and interacting with Mbd3. It was also shown that Mbd3 preferably binds to 5-hmC compared to 5-mC [44]. When the genomic distribution of 5-hmC was investigated in ESCs, it was identified that 5-hmC mainly localized at gene rich, low to moderate CpG containing regions specifically transcription start sites, promoters and gene bodies. The bivalent domains containing both permissive H3K4me3 and repressive H3K27me3 marks were also enriched for 5hmC residues. The role of 5hmC on gene expression was described as activating mainly [43,45,47]. Although recent study claimed that 5hmC could also act as inhibiting transcription in the case of being on distal regulatory sites such as enhancers [48].

Ten eleven translocation family proteins (TET1,-2 and -3) produce 5-hydroxymethylcytosine from 5-methylcytosine. [42,49]. TET enzymes further oxidize and generate 5-formylcytosine and 5-carboxycytosine and 2-oxoglutarate and Fe^{+2} are necessary cofactors for the oxidation reaction [50].

Though 5-hmC is a newly identified residue, its level in human tissues is more than the expected levels. Brain, kidney, liver and colorectal tissues have higher 5-hmC levels and the abundance of 5-hmC declines in the cancerous state [51,52]. Proper functioning of TET enzymes and the level of 5hmC on DNA are very crucial since various mutations of TET2 were reported in hematological malignancies [53].

In addition to its epigenetic functions, 5hmC also act as an intermediate player in DNA demethylation. It exerts its function via two different paths, passive and active DNA demethylation. In passive mechanism, the generated 5hmC from 5mC cannot be recognized by DNMT1, thereby after each cell division cycle DNA become more demethylated [54]. Though in some circumstances cells need to demethylate DNA immediately such as after fertilization or in primordial germ cells [55]. In this case 5-hydroxymethylated cytosine residues are either further oxidized to 5-carboxylcytosine by TET enzymes or deaminated to 5-hydroxymethyluracil by AID/APOBEC enzymes. Then both 5-carboxylcytosine and 5-hydroxymethyluracil are removed from DNA by base excision repair mechanism (BER) [55,56].

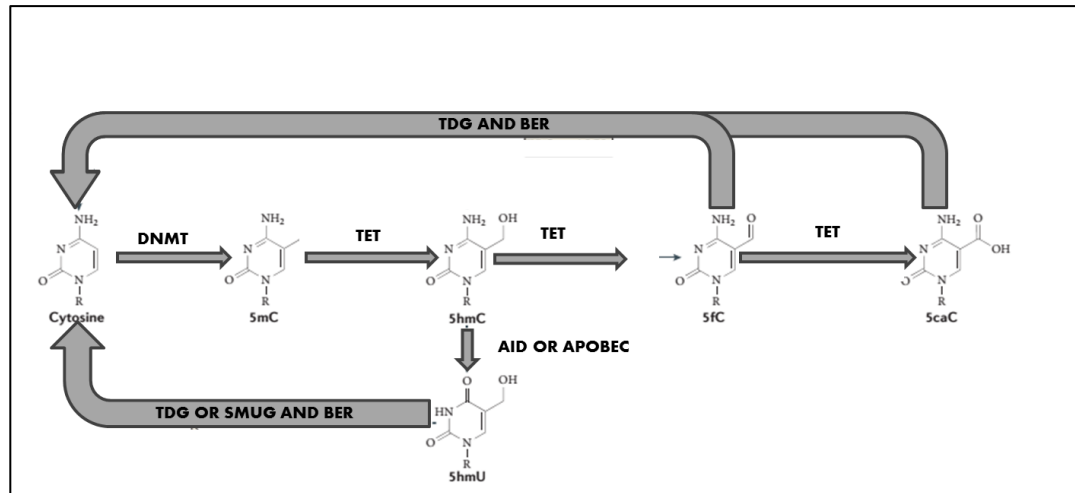


Figure 1.3 1: Active DNA demethylation

TET enzymes oxidize 5-methylcytosine to 5-hydroxymethylcytosine, 5-formylcytosine and 5-carboxycytosine sequentially. 5-formylcytosine and 5-carboxylcytosine is excised by thymine DNA glycosylase (TDG) and cytosine is added with base excision repair (BER) mechanism. In addition, 5-hydroxyuracil can be generated from 5-hydroxymethyl with AID and APOBEC mediated deamination. 5-hydroxyuracil is further be excised with TDG or SMUG and cytosine is added via BER. Adopted from [45].

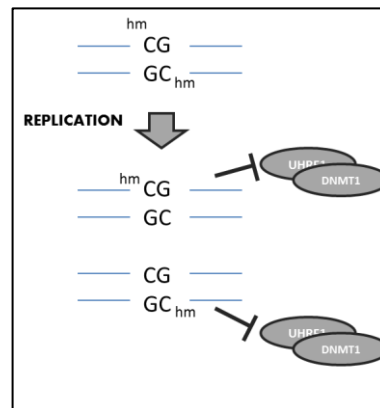


Figure 1.3 2: Passive DNA demethylation

5-hydroxymethylated cytosine inhibits binding of UHRF1 or DNMT1 or both UHRF1 and DNMT1, thereby by each cell division methylated cytosines are lost. Adopted from [45].

All TET enzymes have the ability to hydroxymethylate DNA; however their differential roles were established. In a study done in embryonic germ cell lines (EGCs),

TET1 was essential for the proper methylation of imprinted control regions whereas TET2 was indispensable for the precise reprogramming when ECGs were fused with B cells [57]. The activities of TET1 on transcription start sites and TET2 on gene bodies were established with the gene depletion study performed in mouse embryonic stem cells [58]. TET1 and TET2 deficient double knockout mouse model established TET3 have redundant functions since double knockout animals were viable though having decreased 5hmC levels and impaired imprinting [59].

New functions and novel interactions about the transcriptional role of 5hmC are emerging. Recently, enrichment of 5hmC on the gene bodies of neuronal genes in accompany with loss of H3K27me3 was shown to be essential for neurogenesis [60]. TET2 and TET3 were shown to directly interact with *O*-GlcNAc transferase (OGT). TET2-OGT and TET2/TET3-OGT interactions resulted with *O*-GlcNAcylation of H2B Ser112 and HCF1 which is a component of H3K4 methyltransferase SET1/COMPASS complex respectively [61,62]. OGT was shown to interact with TET3 and *O*-GlcNAcylated TET3. The modified TET3 exported to nucleus and its catalytic activity was inhibited [63].

1.4 AIM AND HYPOTHESIS

Because of their unique cancer-specific expression pattern, studying the regulation of CT gene expression can help reveal the deregulated epigenetic mechanisms during carcinogenesis. Additionally, CT genes can be used as perfect biomarkers for DNA hypomethylation known to occur in cancer. They might be useful in the detection and prognosis of cancer as well.

In this study, we aimed to study both region specific as well as promoter-proximal epigenetic alterations in CT gene expression in cancer. To be able to study the epigenetic basis of CT gene expression, we had three different approaches. In the first approach, we used a model dynamically expressing CT genes; thereby we studied and verified the responsible epigenetic mechanisms relevant to the transition from CT negative to positive gene expression. In the second approach, we studied CT and CT proximal regions with opposite expression patterns in healthy and cancer conditions. Finally we tried to find out an explanation to coordinate CT gene expression in cancer by analyzing CT encoding repeat regions on DNA since repeat demethylation was a known epigenetic event during carcinogenesis.

2 MATERIALS AND METHODS

2.1 MATERIALS

2.1.1 General Chemicals

General laboratory chemicals such as; Methanol, Ethanol, Isopropanol, Chloroform, Formaldehyde, NaCl, tris-base, glycine are analytical grade and purchased from either Sigma-Aldrich (St. Louis, USA) or Calbiochem Merck Millipore (Darmstadt, Germany). The detailed list of the chemicals and kits were shown below.

Table 2.1.1 1: List of chemicals enzymes kits

<i>Name</i>	<i>Catalog number</i>	<i>Company</i>
<i>TRIzol reagent</i>	15596018	Ambion by Life Sciences (CA, USA)
<i>Nuclease free water</i>	AM9930	Ambion by Life Sciences (CA, USA)
<i>DNA-free™ Kit</i>		
<i>DNase Treatment and Removal Reagents</i>	AM1906	Ambion by Life Sciences (CA, USA)
<i>RevertAid First Strand cDNA Synthesis Kit</i>	# K1622	Thermo Scientific Inc. (IL, USA)
<i>DyNAzyme II DNA Polymerase</i>	# F-501S	Thermo Scientific Inc. (IL, USA)
<i>OneTaq Hot Start DNA Polymerase</i>	M0481S	New England BioLabs Inc.
<i>SYBR® Green PCR Master Mix</i>	4309155	Applied Biosystems by Life

		Sciences (CA, USA)
<i>TaqMan® Universal PCR Master Mix</i>	4364338	Applied Biosystems by Life Sciences (CA, USA)
<i>Proteinase K</i>	P2308	Sigma Aldrich (St. Louis, USA)
<i>Phenol:Chloroform:IAA, 25:24:1, pH 6.6</i>	AM9730	Ambion by Life Sciences (CA, USA)
<i>EZ DNA Methylation-Gold™ Kit (Bisulphite Conversion kit)</i>	D5006	Zymo Research (CA, USA)
<i>TA Cloning® Kit, with pCR™2.1 Vector, without competent cells</i>	K2020-40	Invitrogen by Life Sciences (CA, USA)
<i>Phusion® High-Fidelity DNA Polymerase</i>	M0530S	New England BioLabs Inc.
<i>BamHI</i>	R0136S	New England BioLabs Inc.
<i>NotI</i>	R0189S	New England BioLabs Inc.
<i>XbaI</i>	R0145S	New England BioLabs Inc.
<i>HindIII</i>	R0104S	New England BioLabs Inc.
<i>EcoRI</i>	R0101S	New England BioLabs Inc.
<i>T-REx™ System</i>	K1020-01	Invitrogen by Life Sciences
<i>Lipofectamine® 2000 Transfection Reagent</i>	11668-027	Invitrogen by Life Sciences (CA, USA)

<i>TransIT-LT1 Transfection Reagent</i>	MIR 2304	Mirus Bio (Madison, USA)
<i>β-Gal Staining Kit</i>	K1465-01	Invitrogen by Life Sciences(CA, USA)
<i>Cell Proliferation Kit I(MTT)</i>	11 465 007 001	Roche Applied Science (Basel, Switzerland)
<i>FspI</i>	R0135S	New England BioLabs Inc.
<i>EpiSeeker hydroxymethylated DNA Immunoprecipitation (hMeDIP) Kit</i>	ab117134	Abcam (UK)
<i>UltraCruz™ Mounting Medium</i>	sc-24941	Santa Cruz Biotechnology (Texas, USA)
<i>NuPAGE® Novex® 4-12% Bis-Tris Protein Gels, 1.5 mm, 15 well</i>	NP0336BOX	NuPAGE® Novex® by Life Sciences (CA, USA)
<i>Immobilon-P Membrane, PVDF, 0.45 μm, 26.5 cm x 3.75 m roll</i>	IPVH00010	Merck Millipore (MA, USA)
<i>Clarity™ Western ECL Substrate</i>	170-5060	Bio Rad (CA, USA)
<i>5-aza-2-deoxycytidine</i>	A3656	Sigma Aldrich (St. Louis, USA)
<i>Protease inhibitor cocktail</i>	P8340	Sigma Aldrich (St. Louis, USA)

<i>QIAquick Gel Extraction Kit</i>	28706	QIAGEN (CA, USA)
<i>QIAGEN Plasmid Mini Kit</i>	12125	QIAGEN (CA, USA)
<i>QIAGEN Plasmid Midi Kit</i>	12145	QIAGEN (CA, USA)
<i>Precision Plus Protein™ Dual Color Standards</i>	#161-0374	Bio Rad (CA, USA)
<i>Gene Ruler 1 kb DNA Ladder</i>	#SM0311	Thermo Scientific Inc. (IL, USA)
<i>Gene Ruler 100 bp DNA Ladder</i>	# SM0241	Thermo Scientific Inc. (IL, USA)
<i>Kanamycin</i>	60615	Sigma Aldrich (St. Louis, USA)
<i>Carbenicillin</i>	C1613	Sigma Aldrich (St. Louis, USA)
<i>β-Galactosidase</i>	G5635	Sigma Aldrich (St. Louis, USA)

Table 2.1.1 2: List of constructs and vectors

<i>Name</i>	
<i>pcDNA2.1</i>	3.9 kbp vector which bisulphite pcr products were cloned in it with TA cloning procedure.
<i>pcDNA.6TR</i>	6662 bp vector coding tet repressor gene
<i>pcDNA 4/TO/ lacZ</i>	8224 bp control vector containing the gene for β -galactosidase under the control of tet repressor
<i>pcDNA3.1/His/lacZ</i>	Control vector constitutively expressing the gene for β -galactosidase to calculate transfection efficiency
<i>pcDNA 4/TO/ ALAS2</i>	ALAS2 expressing expression vector
<i>pcDNA 4/TO/ CDR1</i>	CDR1 expressing expression vector

Table 2.1.1 3: List of positive and negative controls

<i>Name</i>	<i>Catalog number</i>	<i>Company</i>
<i>Human non-methylated DNA</i>		
<i>HCT116 DKO cells [DNMT1 (-/-) / DNMT3b (-/-)]</i>	D5014-1	Zymo Research (CA, USA)
<i>Human methylated DNA</i>		
<i>SssI methylated</i>	D5014-2	Zymo Research (CA, USA)
<i>HCT116 DKO cells [DNMT1 (-/-) / DNMT3b (-/-)]</i>		
<i>Human Normal Adult Colon Male DNA</i>	D1234090 (Lot no: A805046)	BioChain (CA, USA)
<i>Human Normal Adult Colon Female DNA</i>		BioChain (CA, USA)

Table 2.1.1 4: Primers used

<i>Primer</i>	<i>Sequence</i>	<i>Product</i>	<i>T_m</i>
<i>RT-PCR & Q-RT-PCR</i>			
GAPDH F	5'-TTCTTTTTCGTCGCCAGCCG -3'	78	61.4
GAPDH R	5'-CGACCAAATCCGTTGACTCCGACC -3'		66.1
TAGLN F	5'-ACGGCGGCAGCCCTTTAAACC -3'	122	60.24
TAGLN R	5'-GGCCATGTCTGGGGAAAGAAGGC -3'		59.74
FN1 F	5'-TGTGATCCCGTCGACCAATGCC -3'	131	59.23
FN1 R	5'-TGCCACTCCCAATGCCACG -3'		59.62
VIM F	5'-CCAAGACACTATTGGCCGCTGC -3'	167	60.36
VIM R	5'-GCAGAGAAATCCTGCTCTCCTCGC -3'		59.42
CDX2 F	5'-CGCTTCTGGGCTGCTGCAAACG -3'	262	61.65
CDX2 R	5'-TAGCTCGGCTTTCCTCCGATGG -3'		60.11
CLDN4 F	5'- ACCTGTCCCCGAGAGAGAGTGC- 3'	157	59.4
CLDN4 R	5' -GATTCCAAGCGCTGGGGACGG - 3'		60.11
CDH1 F	5' - TGGGCCAGGAAATCACATCCTACA - 3'	91	57.57
CDH1 R	5'- TTGGCAGTGTCTCTCAAATCCGA - 3'		57.8
TET1 F	5'- ACCTGCAGCTGTCTTGATCG- 3'	186	60.39
TET1 R	5'- ACACCCATGAGAGCTTTTCCC- 3'		60.27
TET2 F	5'- CGCTGAGTGATGAGAACAGACG- 3'	187	61.29
TET2 R	5'- GCTGAATGTTTGCCAGCCTCG- 3'		62.72
TET3 F	5'- GCATGTACTTCAACGGCTGC- 3'	187	60.18
TET3 R	5'- ATTTCTCGTTGGTCACCTGG- 3'		60.27
IκBG F	5'- AGCACAGCGTGCAGGTGGAC- 3'	209	66.55
IκBG R	5'- GAGATCTTCCAGCTGCATTCC- 3'		62.57
NY-ESO-1 F	5'- CAGGGCTGAATGGATGCTGCAGA- 3'	365	66.33
NY-ESO-1 R	5'- GCGCCTCTGCCCTGAGGGAGG- 3'		72.33
Noncoding RNA1 F	5'- CACTGGCCCCAATTAGGAAGAAC- 3'	275	64.55
Noncoding RNA1 R	5'- GAAGGCCTCATATCCCAATTCTAGC- 3'		64.58
Noncoding RNA2 F	5'- TGCATACCCTTCCAGCTGTAGG- 3'	387	64.54
Noncoding RNA2 R	5'- GGAGAAACCTTGGACAATACCCG- 3'		64.55
Noncoding RNA3 F	5'- GTTAAATTAGAGCGCATTCATATTGCG- 3'	176	61.57
Noncoding RNA3 R	5'- CTCACCCACTGCAAACATTCAATG- 3'		62.86
<i>BISULPHITE SEQUENCING</i>			
PAGE-2 1A	5'- TGGTGGTTTATTTTATAGAGGTAGG -3'	342	50.1
PAGE-2 1B	5'- ACCCTTTTCCCTCAAAAACCA -3'		51.87
PAGE-2 2A	5'- TGTTGGTGTTTATGTTTGTGTTAT -3'	216	57.58
PAGE-2 2B	5'- ACCAACTAACTCCTCCACACATT -3'		58.96
PAGE-2B 1A	5'- TGGAAGTGAAAGAAAGGGTGGG -3'	398	54.44
PAGE-2B 1B	5'- CAAAACCTATCCAAAACCAACTAATC -3'		53.2
PAGE-2B 2A	5'- TTGTTGTTGTATTTGTTTGTGTTA -3'	238	56.55
PAGE-2B 2B	5'- CTATCCAAAACCAACTAATCCTC -3'		57.33
SPANX-B 1A	5'- TGGGTTGAAATTTGTTTGGTAGTAGTT -3'	523	53.81

SPANX-B 1B	5'- ACCCTCCCTATACATACCCTCC -3'		53.50
SPANX-B 2A	5'- ATTGTAGGAGGGAAATG-3'	432	52.54
SPANX-B 2B	5'- AAAACAAAACCACACCCT -3'		57.39
ALAS2 1st region 1A	5'- AGATTATATTGTTTTATAAAAAGGTGAG-3'	395	51.5
ALAS2 1st region 1B	5'- CAACTTACTAACA AAAAATCTAAAACC-3'		51.8
ALAS2 1st region 2A	5'- TTTTTAAAGGAGAGGAGATATTAGG-3'	273	55.4
ALAS2 1st region 2B	5'- CTATTACATTCAAATACATTTC-3'		54.5
ALAS2 2nd region 1A	5'- GGGTTTTATTTTTAGTAAGGAAGG-3'	225	54.6
ALAS2 2nd region 1B	5'- CCTAAAAACCAACTAACAAACC-3'		56.1
ALAS2 2nd region 2A	5'- GATATTTTTGGGGTTAATGTAGG-3'	152	56
ALAS2 2nd region 2B	5'- AAAACAACCTCTTACCTATTACCC-3'		55.5
ALAS2 3rd region 1A	5'- ATGTATTAGTTTTTTGATTTAGATAGG-3'	244	51.1
ALAS2 3rd region 1B	5'- AATTCCTTATCCCAATCCTATTAC-3'		52.7
ALAS2 3rd region 2A	5'- TTTTATTATTATAGGGTTGATATGAG-3'	156	51.1
ALAS2 3rd region 2B	5'- TAAACTTAAACTCTATAATTCCC-3'		52.7
CDR1 1st region 1A	5'- TGGTTTTTTAGATTAGTATGTTGG-3'	341	52.5
CDR1 1st region 1B	5'- AAATAAATACAAACACTTTCTAATACC-3'		50
CDR1 1st region 2A	5'- ATTTAAGGAGTTGTAGTTATTATTAG-3'	234	51
CDR1 1st region 2B	5'- CTTCAAATCATATTCATAACTCC-3'		50.7
CDR1 2nd region 1A	5'- TTAAAGGGAATGGTAGTGG-3'	343	52
CDR1 2nd region 1B	5'- CCATTA AAACTAAATACCATCATTATCC-3'		51
CDR1 2nd region 2A	5'- AAATAGATTTTGGTAGTGATAGG-3'	203	52.2
CDR1 2nd region 2B	5'- CTAAATAATAAAACCAATTTAAACCC-3'		50.4
CDR1 3rd region 1A	5'- GGATTATAGAATATGTTAGAATATTTGG-3'	245	50.5
CDR1 3rd region 1B	5'- ATCTTCCTATATCTCCAAATCTTCC-3'		51.9
CDR1 3rd region 2A	5'- GAATGTTAGAAGATTAGTATATTGGAG-3'	166	50
CDR1 3rd region 2B	5'- ATCTCCAAAACCTCCAACATCTAC-3'		52.6
<i>hMEDIP-Q PCR</i>			
PAGE-2 Primer #1 F	5'- GACTCAGCCGGTAGGTCTGC-3'	152	62.3
PAGE-2 Primer #1 R	5'- CTGGGAGGAGCTGGATGACG-3'		62.0
PAGE-2 Primer #2 F	5'- GAGCGCTGGTGGTTTACTCC-3'	173	61.0
PAGE-2 Primer #2 R	5'- TCCTTGCAGACCTCTGTGCG-3'		62.4
PAGE-2B Primer #1 F	5'- AGTCACGAGGCGAATGTCCC-3'	214	62.2
PAGE-2B Primer #1 R	5'- GACCTACCGGCTGAGTCTCG-3'		61.7
PAGE-2B Primer #2 F	5'- AGGTTCTCCACAGACGCAGG-3'	166	61.8
PAGE-2B Primer #2 R	5'- TGTGTGTGGACAGAAGCGG-3'		62.6
SPANX-B Primer#1 F	5'- AACCTACTGTAGACATCGAAGAACC-3'	125	60.1
SPANX-B Primer#1 R	5'- CGTCTTGTGGCCTCATTGGC-3'		62.4
ALAS2 Primer#1 F	5'- GAACACGGCCTGGCACA-3'	229	60.26
ALAS2 Primer#1 R	5'- ATGAACGTACAGCCAAGGG-3'		57.45
CDR1 Primer#1 F	5'- TGCTGGAAGACCTGGAGATA-3'	330	57.45
CDR1 Primer#1 R	5'- CCCTCAAATCCATAGCTTCCG-3'		58.5
<i>PLASMID CONSTRUCTION</i>			

ALAS2 Primer #1 F	5'-ATTATTGGATCCACTTTAGGTTCAAGATGGTGACTGC- 3'	1650	62.
ALAS2 Primer #1 R	5'-ATTATTGCGGCCGCTGGCTTCTCAGGCATAGGTGG- 3'		65.
CDR1 Primer #2 F	5'-ATTATTGGATCCTGGAAGACATGGCTTGGTTGG- 3'	830	62.
CDR1 Primer #2 R	5'-ATTATTGCGGCCGCTGGCTTCTCAGGCATAGGTGG- 3'		65.
<i>SEQUENCING OF pcDNA2.1</i>			
M13 reverse primer	5'- CAGGAAACAGCTATGAC -3'		51.

Table 2.1.1 5: List of antibodies used in IF staining and western blotting

<i>Name of the antibody</i>	<i>Supplier</i>	<i>Catalog number</i>
PRIMARY ANTIBODY		
<i>Anti-fibronectin antibody</i>	Abcam (UK)	ab23750
<i>Anti-vimentin antibody (EPR3776)</i>	Abcam (UK)	ab92547
<i>Anti-transgelin (SM22 alpha) antibody</i>	Abcam (UK)	ab14106
<i>Anti-CDX2 antibody (AMT28)</i>	Abcam (UK)	ab15258
<i>Anti-PAGE-2,-2B antibody (C-13)</i>	Santa Cruz Biotechnology (Texas, USA)	sc-168892
<i>Anti-SPANX-B antibody (N-13)</i>	Santa Cruz Biotechnology (Texas, USA)	sc-162267
<i>Anti-TET2 antibody</i>	Abcam (UK)	ab-94580
<i>Anti-TET2 antibody</i>	Active motif	61389
SECONDARY ANTIBODY		
<i>Alexa Fluor 488 donkey anti-goat IgG (H+L)</i>	Invitrogen by Life Sciences(CA, USA)	A11055
<i>Alexa Fluor 568 donkey anti-rabbit IgG (H+L)</i>	Invitrogen by Life Sciences(CA, USA)	A10042
<i>Alexa Fluor 568 donkey anti-mouse IgG (H+L)</i>	Invitrogen by Life Sciences(CA, USA)	A10037

Table 2.1.1 6: List of antibodies used in ChIP

<i>Name of the antibody</i>	<i>Supplier</i>	<i>Catalog number</i>
<i>PRIMARY ANTIBODY</i>		
<i>Anti-EZH2</i>	Abcam (UK)	ab3748
<i>Anti-HP1</i>	Abcam (UK)	ab77256
<i>Anti-H3K27me3</i>	Abcam (UK)	ab6002

2.1.2 Instruments

Table 2.1.2 1: List of instrument

<i>Name</i>	<i>Company</i>
<i>Applied Biosystem 7500 Q RT PCR Machine</i>	Applied Biosystems by Life Sciences (CA, USA)
<i>Applied Biosystem PCR Machine</i>	Applied Biosystems by Life Sciences (CA, USA)
<i>AutoFlow NU-8500 Water Jacket CO2 Incubator</i>	NuAire (MN, USA)
<i>The STANDARD CO2 incubator</i>	Binder (Tuttlingen, GERMANY)
<i>Centrifuges 5810 and 5810 R</i>	Eppendorf (Hamburg, GERMAY)
<i>Electrophoresis Equipment</i>	
<i>XCell SureLock™ Mini-Cell Electrophoresis System</i>	Life Sciences (CA, USA)
<i>AxioCam MRc5 image capture device</i>	Carl Zeiss (Oberkochen, GERMANY).

2.1.3 Cell Lines and Tissue Culture Reagents

The Caco-2 cell line was obtained from the SAP Enstitusu (Ankara, Turkey). HCT116, SW620, LoVo (colorectal cancer), MDAMB-157, MCF-7 (breast cancer) and Mahlavu (hepatocellular cancer) cancer cell lines were obtained from LGC Standards (Middlesex, UK). A lung cancer cell line, SK-LC-17, was from the Memorial Sloan Kettering Cancer Center (NY, USA).

Plastic cell culture materials such as; petri dishes, T-75 and T-25 cm flasks, multi-well plates, cryotubes were purchased from Greiner Bio-One (Austria) and serological pipettes were purchased from Costar Corporation (Cambridge, England). Other materials were listed below.

Table 2.1.3 1: List of cell culture reagents

<i>Name</i>	<i>Catalog number</i>	<i>Company</i>
<i>RPMI 1640 medium</i>	F 1215	Biochrom AG (Berlin, Germany)
<i>DMEM medium</i>	FG 0415	Biochrom AG (Berlin, Germany)
<i>EMEM medium</i>	BE12-125F	Lonza (USA)
<i>Trypsin-EDTA</i>	SV3003101	HyClone (IL, USA)
<i>L-Glutamine</i>	SH3003401	HyClone (IL, USA)
<i>Penicillin/Streptomycin</i>	SV30010	HyClone (IL, USA)
<i>Non-essential amino acids</i>	SH3023801	HyClone (IL, USA)
<i>Fetal Bovine Serum</i>	S1620	Biowest (Nuaille, FRANCE)
<i>Blasticidin S HCl</i>	A11139-02	Invitrogen by Life Sciences(CA, USA)

<i>Zeocin Selection reagent</i>	R25001	Invitrogen by Life Sciences(CA, USA)
<i>Opti-MEM® I Reduced Serum Medium</i>	31985-062	Invitrogen by Life Sciences(CA, USA)
<i>Tetracycline</i>	87128	Sigma Aldrich (St. Louis, USA)
<i>Tetracycline reduced Fetal Bovine Serum</i>	631106	Clontech (CA,USA)

2.2 SOLUTIONS AND MEDIA

2.2.1 General Solutions

10X PBS

- 25.6 g Na₂HPO₄·7H₂O
- 80 g NaCl
- 2 g KCl
- 2 g KH₂PO₄
- Bring to 1 liter with H₂O.

Lysis Solution for DNA isolation (300 µl):

- 150 µl TE
- Add 150 µl Proteinase K (from 200 µM stock)
- 15 µl SDS (from %10 SDS stock).

LB (500 ml):

- 5 g Tryptone
- 5 g NaCl
- 2.5 g Yeast Extract in 500 ml ddH₂O

LB Agar + Carbenicillin (or Amphotericin)+ IPTG+ X-Gal (500 ml):

- 5 g Tryptone
- 5 g NaCl
- 2.5 g Yeast Extract
- 12.5 g Bacto Agar in 500 ml ddH₂O
- After autoclaving and cooling down the solution
 - Add carbenicillin to make it 1X (from 1000X add 500µl)

- Add 250 μ l IPTG from 1M stock (Final conc= 0.5 mM)
- Add 1000 μ l X-Gal from 40 mg/ml stock (Final conc= 80 μ g/ml)
- Pour the agar in plates

SOC medium (100 ml):

- 2 g Tryptone
- 0.5 g Yeast extract
- 1000 μ l 1M NaCl solution
- 250 μ l 1M KCl solution
- Add 97 ml ddH₂O then autoclave
- After autoclaving
 - Add 1000 μ l 2M Mg⁺² stock solution (1M MgCl₂·6H₂O and 1M MgSO₄·7H₂O) (previously filter sterilized)
 - Add 1000 μ l 2M Glucose (previously filter sterilized)

RIPA Buffer (5 ml):

- 750 μ l NaCl from 1M stock (final concentration 150 mM)
- 50 μ l Triton-X (final concentration 1%)
- 50 μ l from 10% Sodium DOC (final concentration 0.5%)
- 25 μ l from 20 %SDS (final concentration 0.1%)
- 250 μ l from 1M Tris-HCl at pH:8.0 (final concentration 50mM)
- Protease cocktail from 100X to 1X
- ddH₂O up to 5 ml

2.2.2 Cell Culture Solutions

Complete DMEM and RPMI

- 10 % FBS
- 1 % L-Glutamine
- 1 % Penicillin/Streptomycin
- 500ml Medium

Complete EMEM

- 20 % FBS
- 1 % L-Glutamine
- 1 % Penicillin/Streptomycin
- 1 % Non-essential amino acid solution
- 1 % Sodiumbicarbonate
- 1 % Sodiumpyruvate
- 500ml Medium

Blasticidin

- 10mg/ml of stock Blasticidin solution was prepared in sterile water, aliquoted then stored at -20°C .

Tetracycline

- 5 mg/ml stock solution of tetracycline was prepared in 70% ethanol

Freezing mix

- 90% FBS
- 10% DMSO

2.3 METHODS

2.3.1 Cancer cell culture techniques

Human colorectal cancer cell lines; HCT116, SW620, LoVo and human small cell lung cancer cell line; SK-LC-17 were grown in RPMI medium supplemented with 10% (v/v) heat-inactivated FBS, 1% L-glutamine and 1% penicillin/streptomycin. MCF-7 cells were grown in high glucose DMEM medium supplemented with 10% (v/v) heat-inactivated FBS, 1% L-glutamine, 1% penicillin/streptomycin, 1% insulin, 1% sodium pyruvate and MDA-MB-157 cells were cultured in DMEM medium supplemented with 10% (v/v) heat-inactivated FBS, 1% L-glutamine and 1% penicillin/streptomycin. HCT116.6TR and SK-LC-17.6TR clones were cultivated in complete RPMI medium containing 2 µg/ml and 1.2 µg/ml Blastidicin respectively. All cell lines were maintained in a 5 % CO₂ atmosphere at 37⁰C.

All cells were cultured by renewing the medium for every 2-3 days. When cells reached confluency, they were washed 1X PBS then harvested with trypsin-EDTA incubation and reseeded with complete medium. Stocks were prepared with 90% DMSO and 10% FBS containing freezing mix by freezing at -20 and -80⁰C respectively. Then stocks were maintained at liquid nitrogen.

2.3.2 RNA isolation with TRIzol

One confluent T-75 flask of cells was used for RNA isolation. Cells were washed with 1X PBS, and then scraped with 1X PBS. After centrifugation, supernatant was removed and 1ml TRIzol was added. Cells were pipetted and homogenized in TRIzol by 5 minutes incubation at room temperature. 200 µl of chloroform was added. The mixture was mixed vigorously, incubated at 10 minutes at room temperature then centrifuged at 13000 rpm 15 minutes at 4⁰C. Upper phase was removed, 500 µl isopropanol was added. The mixture was inverted gently and incubated at 10 minutes at room temperature then centrifuged at 13000 rpm 15 minutes 4⁰C. The precipitate was washed with 75 % ethanol, ethanol was removed with centrifugation. The pellet was air dried

and then resuspended in nuclease free water. RNA was incubated at 55⁰C for 15 minutes to complete dissolution. RNAs were stored at -80 ⁰C for longer storage.

2.3.3 DNA Isolation with Phenol-Chloroform-Isoamylalcohol Extraction

One confluent T-75 flask of cells was used for DNA isolation. Cells were washed with 1X PBS, and then scraped with 1X PBS. After centrifugation, supernatant was removed and pellet was dissolved in 300 µl lysis buffer by pipetting up and down. The mixture was incubated at 50⁰C for overnight. 300 µl phenol-chloroform-isoamyl alcohol was added, mixture was vortexed and centrifuged at 5000 rpm 10 minutes at room temperature. The upper phase was removed, 250 µl phenol-chloroform-isoamyl alcohol was added, mixture was vortexed and centrifuged at 5000 rpm 10 minutes at room temperature. Upper phase was removed, 200 µl chloroform was added, mixture was vortexed and centrifuged at 5000 rpm 10 minutes at room temperature. The upper phase was transferred into a new tube, 50 µl 3 M NaOAC then 375 µl % 100 ice cold EtOH were added onto it. The mixture was inverted gently until the precipitate appeared. The precipitate was removed by a pipette tip and transferred to a tube containing 70% ethanol. Then the mixture was centrifuged at 13000 rpm 3 minutes at room temperature. Supernatant was removed, the pellet was air dried and resuspended in nuclease free water. To dissolve DNA, DNA was incubated at 65⁰C for 2 hours then stored at -20⁰C.

2.3.4 Identification of CT-proximal down-regulated genes in cancer compared to healthy counterparts by Cancer Genome Anatomy Project

X-chromosome genes that were downregulated, with respect to their normal counterparts, in any human cancerous tissues except from embryonic and germ line origin were identified by analyzing SAGE Digital Gene Expression Displayer and cDNA Digital Gene Expression Displayer databases of the Cancer Genome. Anatomy Project based on SAGE and EST libraries. Among existing EST libraries, 269 libraries of cancerous tissues versus 339 libraries of healthy tissues were screened. Among existing SAGE libraries, 78 libraries of cancerous tissues versus 182 libraries of healthy

tissues were screened. Significance filter was adjusted to $p < 0.05$. 59 genes were obtained based on the above criteria. Extracted data were checked by using Monochromatic SAGE/cDNA Virtual Northern. Among the 59 genes, 8 genes that have a neighboring cancer-testis (CT) gene were chosen and expression analyses were made to verify the database data. These 8 genes were located at least 30kb and at most 560kb from a CT gene.

2.3.5 Q RT-PCR Experiments with Taqman Probe Chemistry

Nuclear and cytoplasmic RNA species were prepared with guanidium thiocyanate phenol-chloroform extraction method using TRIzol reagent. 500 ng of RNA was reverse transcribed using Revert-Aid first strand cDNA synthesis kit from Fermentas with random hexamer primer and RNase inhibitor. All PCR reactions were carried out in triplicates in ABI 7500 RT-PCR machine by using Taqman predesigned probes and Taqman gene expression mix of Applied Biosystems. The assay IDs of probes used in the experiments were: Hs00163601_m1* for ALAS2, Hs00601346_s1* for CDR1, 4352934E for GAPDH, Hs02387419_gH for SPANX-B family genes and Hs03805505_mH for PAGE-2 and PAGE-2B genes. Thermal cycle conditions were as follows: 50⁰C for 2 min, 95⁰C for 10 min followed by 45 cycles of 94⁰C for 15 sec, 60⁰C for 1 min.

2.3.6 Sequencing of sodium bisulphite treated tumor cell lines' and normal tissues' DNAs

Genomic DNAs from cell lines were isolated by Proteinase K treatment, following phenol-chloroform extraction protocol. Control human female and male genomic colon DNAs were purchased from Biochain. Human HCT116 DNMT1 (-/-) & DNMT3b (-/-) double knockout cell line DNA and Human HCT116 DNMT1 (-/-) & DNMT3b (-/-) double knockout cell line SssI treated DNA were used as non-methylated and methylated DNA controls and were purchased from Zymo Research. Bisulphite treatment of 200 ng genomic DNA was performed with Zymo DNA Methylation Gold Kit according to the instructions. The bisulphite modified DNA was stored at -20⁰C and

used for PCR up to 2 months. For PCR amplification, 1 µl of DNA was added in a final volume of 20 µl, containing 1X PCR buffer, dNTP (200 µM final concentration), primers (final concentration 0.5 µM of each) and 0.03 unit/ µl of DyNAzyme II Hot Start DNA polymerase. PCR product was 1: 10 diluted and 1 µl of this dilution was used in nested PCR reaction with primers designed specific to initial PCR product. The primers were designed to recognize bisulphite converted DNA only. PCR reactions were carried out in a Perkin Elmer cycler using the following protocol: 94⁰C for 10 min, 35 cycles of 94⁰C for 15 sec, 55⁰C for 30 sec, and 72⁰C for 30 sec, followed by a final extension at 72⁰C for 10 min and soaking at 4⁰C. After electrophoresis on 1.5 % agarose gel, products were gel extracted with QIAgen gel extraction kit and cloned in pCR2.1 linearized vector using TA cloning kit Invitrogen. Clones were picked according to blue-white colony screening. Plasmid DNA from white colony was EcoRI digested to release the insert as a further confirmation. Plasmid DNAs from at least ten clones were picked and sequenced by IONTEK, Istanbul.

Ligation reaction was performed such as:

PCR product (10ng)	... µl
10X Ligation Buffer.....	1 µl
pCR 2.1 vector.....	1 µl
ddH ₂ O.....	... µl
T4 DNA Ligase.....	1 µl
Final volume.....	10 µl

2.3.7 Plasmid constructions

PCR for cloning experiment was carried out under the conditions of 98⁰C for 30 sec followed by 40 cycles of 98⁰C for 30 sec, appropriate melting temperature (68⁰C for ALAS2 and 72⁰C for CDR1) for 30 sec, 72⁰C for 1 min with a final extension at 72⁰C for 10 min in Perkin Elmer PCR machine. For ALAS2 placenta cDNA and for CDR1 brain cDNA were used in the PCR. Phusion High Fidelity DNA polymerase, 5X GC Buffer, dNTP mix, forward and reverse primers at final concentrations of 0.02 unit/µl, 1X, 200 µM, 0.5 µM of each respectively were used. PCR products at correct band size were run on % 1.5 agarose gel at 100V for 40 minutes and then gel extracted. For

ALAS2 BamHI and NotI double digestion, for CDR1 XbaI and HindIII double digestion were performed. pcDNA 4/TO vector was also double digested with either BamHI and NotI or XbaI and HindIII. All of the digested products were purified from enzymes and buffers with gel extraction and digested inserts were ligated with cut pcDNA 4/TO. After ligation and transformation, colonies having the vector were selected with ampicillin resistance and plasmid DNA purification was performed with QIAprep Spin Miniprep kit. Plasmid DNA was cut with appropriate digestion enzymes and clones having the appropriate insert were grown for plasmid DNA purification and plasmid DNA was sent to sequencing with CMV forward and BGH reverse primers.

Both pcDNA6/TR and insert containing pcDNA4/TO plasmid DNAs were transformed in DH5 α Ecoli strain and plasmid DNAs for transfection experiments were prepared with QIAGEN Plasmid MidiPrep Kit.

2.3.8 Generation of stable cell lines

Before stable transfection with pcDNA.6TR vector, 7×10^4 untransfected HCT116 and SK-LC-17 were plated on six-well culture dishes. The next day, culture medium was substituted with medium containing Blasticidin at different concentrations (0.5, 1, 1.5, 2, 2.5 and 3 $\mu\text{g}/\text{ml}$ for HCT116; 1, 1.2, 1.4, 1.6, and 1.8 $\mu\text{g}/\text{ml}$ for SK-LC-17). The selective medium was replenished for every 3 days and the Blasticidin dose leading to cell death within 10-14 days after the addition of antibiotic was chosen as the selection dose in pcDNA6TR transfection experiments.

For stable transfection 2×10^5 HCT116 cells and 5×10^5 SK-LC-17 cells were plated on six-well culture dishes and transfected after 48 hours with 4 μg of FspI cut pcDNA.6TR plasmid DNA using Lipofectamine in a 1:2 ratio in OPTI-MEM medium. 4 hours later the transfection medium was removed and cells were cultured in complete RPMI medium for overnight. Next day, cells were splitted at 1:10, 1:5 and 1:2 ratios and Blasticidin at pre-determined concentration required each cell line was introduced into the medium 24 hours later. Cells were feeded with the selection medium every 3 days

for 14 days. Then, cells were plated in a 96-well plate by serial dilution to obtain single cell colonies. Colonies were picked during 2 weeks period and cultured.

2.3.9 β -Galactosidase Staining Assay

1.5×10^5 HCT116.6TR cells and SK-LC-17.6TR cells were plated on twelve-well culture dishes and later 24 hours transfected with 1 μ g of pcDNA.4TO/lacZ plasmid DNA using Mirus Trans-IT LT1 transfection reagent at a 1:3 ratio (DNA:Transfection reagent) in OPTI-MEM medium. 1 day later the transfection medium was removed and cells were cultured in complete RPMI medium (Prepared with tetracycline reduced FBS) containing either 1 μ g/ml Tetracycline or not. pcDNA3.1/His/lacZ transfection was also performed as a positive control. 24 and 48 hours after tetracycline induction, transfected cells were fixed with fixation solution composed of formaldehyde and gluteraldehyde for 10 minutes at room temperature. After fixation, cells were stained with staining solution containing X-gal for 30 minutes to 2 hours. Stained cells were covered with 70 % glycerol and images were taken at 50X, 100X and 200X total magnification.

2.3.10 MTT Cell Viability Assay

7.5×10^4 HCT116.6TR_clone 4 and HCT116.6TR_clone 9, 1.0×10^4 SK-LC-17.6TR clone_5 cells were plated on 96-well plate without Blasticidin. 24 hours later, transfection was carried with mixing 1 μ g plasmid DNA (pcDNA 4/TO-ALAS2-A3 and pcDNA 4/TO-ALAS2-A4) and 3 μ l Mirus in 100 μ l OPTI-MEM and pipetting 10 μ l of this mixture onto cells that were supplemented with 100 μ l OPTI-MEM. After 24 hours incubation transfection medium was replaced with complete RPMI medium (Prepared with tetracycline reduced FBS) containing either 1 μ g/ml Tetracycline or not. 48 hours after induction, viability was measured by MTT cell proliferation kit from Roche. Untransfected cells were accepted as 100 % alive in order to calculate percent viability.

2.3.11 Spontaneous differentiation and dedifferentiation of Caco-2 cell line

Caco-2 cells (ŞAP Enstitüsü, Ankara, Turkey) were grown in EMEM supplemented with % 20FBS, 2mM L-glutamine, 0.1 mM non-essential amino acids, 1.5 g.L⁻¹ sodium bicarbonate and 1 mM sodium pyruvate. Cells were grown until confluency and the % 100confluent cells were considered to be at day 0 for differentiation. The cells were collected at various intervals (day 0, 10, 20 and 30) until day 30 after reaching confluency. The differentiation monitored with sucrose isomaltose expression and alkaline phosphatase staining. Parallel cultures were carried on to obtain replicated differentiation sets. For the dedifferentiation, cells at day 20 were detached by trypsinizing and pipetting then reseeded at 50 % confluency. Cells were cultured following 5 days for RNA and DNA isolation.

2.3.12 In silico analysis of CT gene expression during Caco-2 spontaneous differentiation

GSE1614 was a microarray experiment performed at 3 time points; day 2 (% 50 confluent cells), day 8 (4 days post-confluent, non-differentiated cells) and day 15 (differentiated cells) during Caco-2 cell line spontaneous differentiation by using Affymetrix Human Genome U95A GeneChip. The raw data of GSE1614 was imported from GEO database and analyzed with GeneSpring GX11 software of Agilent technologies. The data was normalized with GC-RMA normalization method. Experimental grouping was done according to three time points in the experiment (2 days, 8 days and 15 days). An interpretation was generated with entity list composed of CT genes and at three different time points. The list was not further processed with statistical analysis to have a general picture of CT gene expression during Caco-2 differentiation.

2.3.13 Total RNA isolation and DNaseI treatment

Nuclear and cytoplasmic RNA species of Caco-2 cells were isolated with TRIzol reagent from different time points during spontaneous differentiation process. DNase I

treatment was performed with DNA free kit with incubation of RNAs at 37⁰C 30 minutes with DNase I and 1X DNase I Buffer in 50µl solution. DNase I was further inactivated with inactivation buffer and RNAs were precipitated with ammonium acetate, linear acrylamide and ice cold ethanol. The precipitated RNAs were washed with 75% ethanol and resuspended in nuclease free water.

2.3.14 cDNA synthesis

200 ng of RNA was reverse transcribed using Revert-Aid first strand cDNA synthesis kit with random hexamer primer and RNase inhibitor.

2.3.15 Q RT-PCR of CT genes

All PCR reactions were carried out in triplicates in ABI 7500 RT-PCR machine. The assay IDs of ABI probes used in the experiments were: 4352934E for GAPDH, Hs02387419_gH for SPANX-B gene, Hs03805505_mH for PAGE-2 and PAGE-2B genes, Hs00275620_m1 for GAGE family genes, Hs023441531_m1 for SSX4,-4B genes, Hs00265824_m1 for NY-ESO-1 gene, Hs00366532_m1 for MAGEA3 gene. Thermal cycle conditions were as follows: 50⁰C for 2 min, 95⁰C for 10 min followed by 45 cycles of 94⁰C for 15 sec, 60⁰C for 1 min. The relative expression values were calculated with $\Delta\Delta C_t$ method.

2.3.16 *In silico* identification of differentially expressed mesenchymal and epithelial genes during Caco-2 spontaneous differentiation

The raw data of GSE1614 was imported from GEO database and analyzed with GeneSpring GX11 software of Agilent technologies. The data was normalized with GC-RMA normalization method. Experimental grouping was done according to three time points in the experiment (2 days, 8 days and 15 days). An interpretation was generated with entity list composed of EMT related gene list in colorectal cancer generated by Loboda et al and at three different time points. The list was further processed with

statistical analysis by using one way ANOVA test and Bonferroni FWER correction method. Genes having a p value smaller than 0.05 were ranked according to biggest expression value difference between day 2 and day 15 values.

2.3.17 Q RT-PCR of mesenchymal and epithelial marker genes

All PCR reactions were carried out in triplicates in ABI 7500 RT-PCR machine. 2X SYBR Green master mix with ROX reference dye was used. Thermal cycle conditions were as follows: 50⁰C for 2 min, 95⁰C for 10 min followed by 40 cycles of 94⁰C for 15 sec, 60-65⁰C for 1 min. In all experiments, melt curve was also ran. The relative expression values were calculated with $\Delta\Delta C_t$ method.

2.3.18 Promoter methylation analysis

Genomic DNA from Caco-2 cell line at different time points of differentiation was isolated by Proteinase K treatment, following phenol-chloroform extraction protocol. Bisulphite treatment of 200 ng genomic DNA was performed with Zymo DNA Methylation Gold Kit. The bisulphite modified DNA was stored at -20⁰C and used for PCR up to 2 months. For PCR amplification, 1 μ l of DNA was added in a final volume of 25 μ l, containing 1X PCR buffer, dNTP (200 μ M final concentration), primers (final concentration 0.2 μ M of each) and 0.025 unit/ μ l of One Taq Hot Start DNA polymerase. PCR product was 1: 10 diluted and 1 μ l of this dilution was used in another PCR reaction with primers designed specific to initial PCR product. The primers were designed to recognize bisulphite converted DNA only. PCR reactions were carried out in a Perkin Elmer cycler using the following protocol: 94⁰C for 30 sec., 35 cycles of 94⁰C for 15 sec, 55-58⁰C for 30 sec, and 68⁰C for 30-45 sec, followed by a final extension at 68⁰C for 5 min and soak at 4⁰C. After gel electrophoresis on % 1.5 agarose gel, products were gel extracted with QIAgen gel extraction kit and cloned in pCR2.1 linearized vector using TA cloning kit. Clones were picked according to blue-white colony screening. Plasmid DNA from white colony was EcoRI digested to release the insert as a

further confirmation. Plasmid DNAs from at least ten clones were picked and sequenced by IONTEK, Istanbul.

2.3.19 Hydroxymethylated DNA Immunoprecipitation

gDNAs of the cell lines were sheared by probe by sonication (30 sec on, 30 sec off 5 cycles) to obtain 200-600 bp fragments. The size of the fragmented DNA was controlled by % 1 agarose gel electrophoresis analysis. Immunoprecipitation was carried out by hMEDIP kit according to the instructions. 5 pg of control DNA was spiked into 500 ng of gDNA to use as an internal control. Positive and negative controls of the kit were also included in all experiments. 2 µl from the eluted DNA was used as template in Q RT-PCR. The efficiencies of primers were controlled. 2 X SYBR Green master mix with ROX reference dye was used. Thermal cycle conditions were as follows: 50⁰C for 2 min, 95⁰C for 10 min followed by 40 cycles of 94⁰C for 15 sec, 60⁰C for 1 min. In order to calculate with input % method, unshered gDNA were included in Q RT-PCR and the calculations were done with input % method.

2.3.20 Immunofluorescence microscopy

Caco-2 cells at different time points during differentiation were scraped with PBS and attached to the lam by cytopspin instrument (800 rpm for 3 min). The attached cells were immediately fixed with 2% formaldehyde in PBS incubation at room temperature for 15 min. Fixed cells were further permeabilized with 0.2% Triton X-PBS for 10 min. The blocking was performed with 1% BSA mixture in 0.1% PBS-Tween for 1 hour. The primary antibody incubations were performed 1:50 dilution for overnight at 4⁰C. The secondary antibody incubations were performed at 1:200 dilution for 45 minutes at room temperature. Washing steps were done with 0.1% PBS-Tween for 5 minutes and 3 times. Slides were finally closed with Santa Cruz Mounting medium containing DAPI solution. Proper positive controls (For PAGE-2,-2B and SPANX-B; Mahlavu cell lines, for VIM; MDA-MB 231 cell line, for TAGLN MCF-7 cell line, for CDX2 and FB1 SW620 cell line) and negative controls (Primary antibody#1+Secondary

antibody#2, Primary antibody#2+Secondary antibody#1, Secondary antibody #1 and #2) were also included in the experiments. Images were taken at fixed instrument settings.

2.3.21 Protein Isolation

The pelleted cells (stored at -80°C) were resuspended in 200-300 μl RIPA depending on the amount of pellet. Then the sample was incubated on ice for 30 min. with vortexing every 5 min. The sample was sonicated for 5 sec for 4 rounds then incubated on ice for 5 min. The sample was boiled at 90°C for 3 min and centrifuged at 14000rpm for 75 min. $+4^{\circ}\text{C}$. Finally supernatant was taken and stored at -80°C .

2.3.22 Western Blotting

Isolated proteins were run on 4-12% Novex Bis-Tris SDS gels at 120 V for 2 hours. Gels were transferred to PVDF membrane with the wet transfer at 30 V for 2 hours. Blots were blocked with 5% milk powder in 0.02% PBS-T. The primary antibody incubations were performed at the indicated dilutions; 1:1000 for CDX2, fibronectin, vimentin and transgelin, 1:2500 for β -actin, 1:100 for SPANX-B and PAGE-2,-2B antibodies, for overnight at 4°C . Secondary antibody incubations were performed at dilution ratio 1:5000 at room temperature for 1 hour with the suitable HRP conjugated secondary antibodies. The detection was performed with ECL based method.

2.3.23 Chromatin Immunoprecipitation (ChIP)

Caco-2 cells were grown in 10cm dishes. On the 0th, 10th and 20th days after reaching 100% confluency, the culture medium was refreshed and 0.8% formaldehyde was added to initiate the crosslinking, incubated at room temperature for 7 min and stopped by adding glycine to a final concentration of 125mM. Cells were washed with PBS twice, scraped into 1.5ml eppendorf tubes and centrifuged at $13000 \times g$ for 1min at 4°C . The pellets were then frozen in liquid nitrogen and then thawed in buffer A (200M HEPES-KOH pH7.5, 420mM NaCl, 0.2mM EDTA pH8.0, 1.5mM MgCl_2 , 25% glycerol,

1X protease inhibitor). Thawed cells were incubated on ice for 20 min and centrifuged after which they were resuspended in breaking buffer (50mM Tris-Cl pH8.0, 1mM EDTA pH8.0, 150mM NaCl, 1% SDS, 2% Triton X-100, 1X protease inhibitor) and sonicated with a probe sonicator for 12 cycles in 30sec intervals of sonication and incubation on ice. Then, 50 µl inputs were taken and subjected to de-crosslinking (1hr RNaseA at 37°C, 1hr Proteinase K at 50°C and o/n incubation at 60°C) in buffer C (50mM Tris-Cl pH8.0, 1mM EDTA pH8.0, 150mM NaCl, 0.1% Triton X-100). The inputs were ran on 1% agarose gel to confirm the size of the sonicated fragments (200-1000 bp) and DNA amount was measured. The samples in buffer B were separated so that each contained 25µg DNA and were centrifuged at 13000 rpm for 10 min. The pellets were resuspended in Buffer C and 2µg of antibody or isotype specific control IgG was added incubated at 4°C with constant agitation o/n. The samples were then incubated with pre-blocked proteinA/G agarose beads for 2hr at 4°C with constant agitation and washed three times with wash buffer 1 (0.1% SDS, 1% Triton X-100, 2mM EDTA pH8.0, 150mM NaCl, 20mM Tris-Cl pH8.0) and then with wash buffer 2 (0.1% SDS, 1% Triton X-100, 2mM EDTA pH8.0, 500mM NaCl, 20mM Tris-Cl pH8.0). Samples were then eluted with elution buffer (1% SDS, 100mM NaHCO₃) and subjected to de-crosslinking as mentioned before. DNA were isolated with high pure PCR product purification kit. Q-PCR was carried out with both immunoprecipitated and input samples using hMEDIP primers designed for the CpG regions of promoters of PAGE-2, PAGE-2B and SPANX-B. The analyzes were performed by normalizing the Ct values to their isotype IgG values.

2.3.24 *In vitro* treatment of tumor cell lines with 5-aza-2-deoxycytidine

5x10⁵ HCT116, 10x10⁵ SK-LC-17, LoVo, SW620, HT29, Colo205, WiDR, MCF7, CAMA-1 cells were seeded in 100mm cell culture dishes. 24 hours later, the medium was renewed with 1 µM 5-Aza-2-deoxycytidine containing medium. RNAs from 5-Aza-2-deoxycytidine treated cells and DMSO treated control cells were isolated at 24 hours, 48 hours and 72 hours' time points.

2.3.23 Q RT-PCR Experiments with SYBR Green chemistry for noncoding RNA expression in NY-ESO-1 repeat region

Nuclear and cytoplasmic RNA species were prepared with guanidium thiocyanate phenol-chloroform extraction method using TRI-reagent. To eliminate genomic DNA contamination, all samples were treated with RNAase and DNA free DNase. 500 ng of RNA was reverse transcribed using Revert-Aid first strand cDNA synthesis kit from Fermentas with random hexamer primer and RNase inhibitor. All PCR reactions were carried out in triplicates in ABI 7500 RT-PCR machine. 2X SYBR Green master mix with ROX reference dye from Applied Biosystem was used. Thermal cycle conditions were as follows: 50⁰C for 2 min, 95⁰C for 10 min followed by 40 cycles of 94⁰C for 15 sec, 61⁰C for 30 sec, 72⁰C for 45 sec and 72⁰C for 10 min for final extension. In all experiments, melt curve was ran.

3 RESULTS:

3.1 EPIGENETIC MECHANISMS LEADING CANCER TESTIS GENE EXPRESSION IN CACO-2 SPONTANEOUS DIFFERENTIATION MODEL

3.1.1 Cancer Testis gene expression in Caco-2 spontaneous differentiation model:

To investigate whether Caco-2 spontaneous differentiation was a suitable model to study CT gene expression, we used a microarray study performed by Fleet et al. (GSE1614) [64]. When we searched for various CT genes annotated in the U95A platform, we observed that many CT genes were up-regulated in the differentiation process from 2 to 15 days (**Error! Reference source not found.**). We, therefore, decided to validate this data *in vitro*.

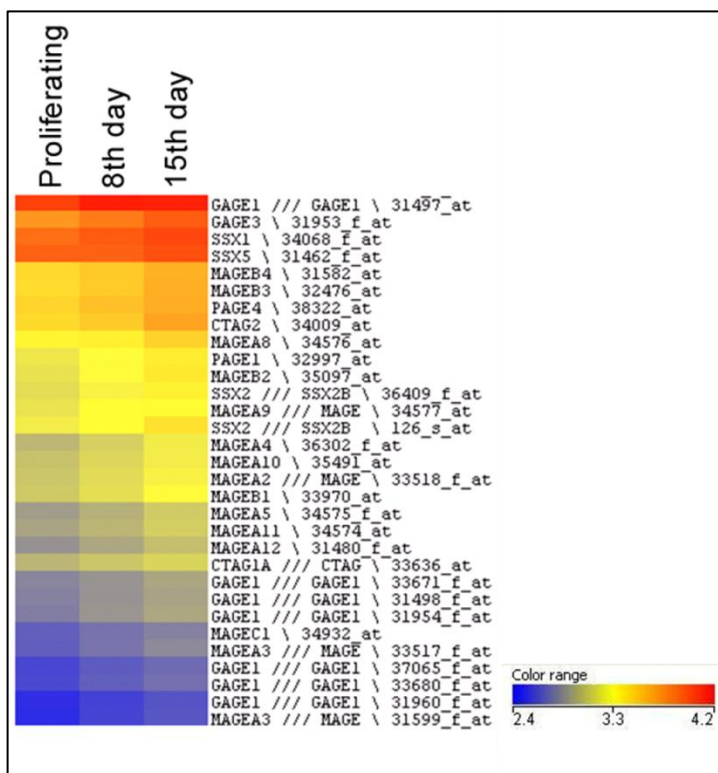


Figure 3.1.1 1: CT gene expression increases during Caco-2 spontaneous differentiation.

Heat map of CT-X gene expression in Caco-2 spontaneous differentiation generated from GSE1614 dataset. Experimental grouping was done according to three time points in the experiment (2 days, 8 days and 15 days). An interpretation was generated with entity list composed of CT genes and at three different time points.

Caco-2 spontaneous differentiation model is a well-established enterocytic differentiation model. Functional and absorptive intestinal epithelial cells developed from Caco-2 colon adenocarcinoma cell line upon contact inhibition after confluency [39,65]. Increase in *sucrose isomaltose* mRNA level, alkaline phosphatase staining and carcinoembryonic antigen protein level showed that differentiation had taken place successfully in our experimental set up.

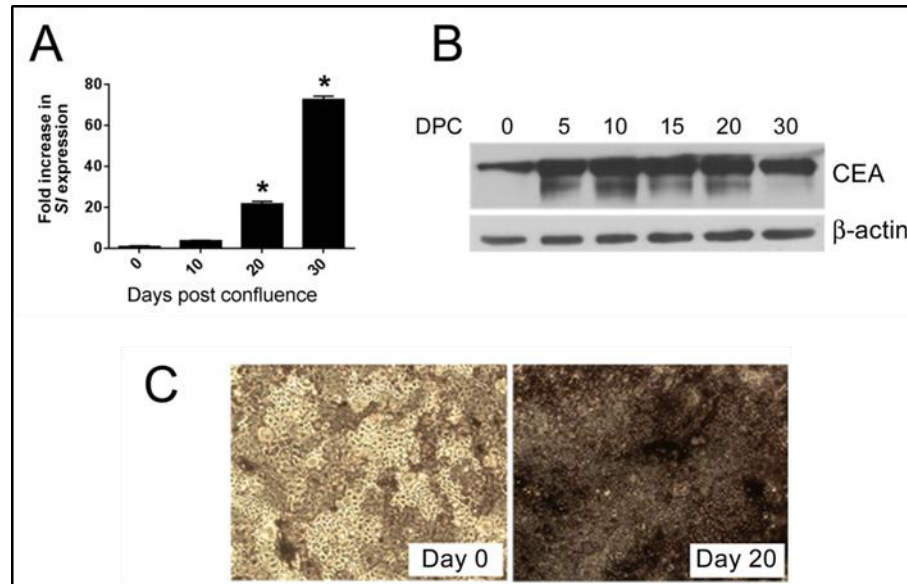


Figure 3.1.1 2: Caco-2 cells differentiate during 30 days post confluence culturing. Caco-2 cells differentiated upon 30 days post confluence culture. (A) Differentiation was confirmed with the increase in mRNA level of sucrose isomaltose expression and (B) protein level of carcinoembryonic antigen. (C) The up-regulation in alkaline phosphatase level was also showed with immunohistochemistry. The difference in sucrose isomaltose expression was statistically significant with ANOVA with Tukey's post hoc test (* $P < 0.001$). (These experiments were performed by Dr. Aslı Sade Memişoğlu from METU)

When we analyzed CT gene expression in the Caco-2 spontaneous differentiation model, we observed that 3 CT genes; *PAGE-2*, *PAGE-2B* and *SPANX-B* were up-regulated dramatically. We were unable to observe a change in gene expression for *MAGE-A3*, *NY-ESO-1*, *SSX4* and *GAGE* family genes. Up-regulation of *PAGE-2*, *-2B* and *SPANX-B* genes was further confirmed at 4 different time points in two different differentiation experiments.

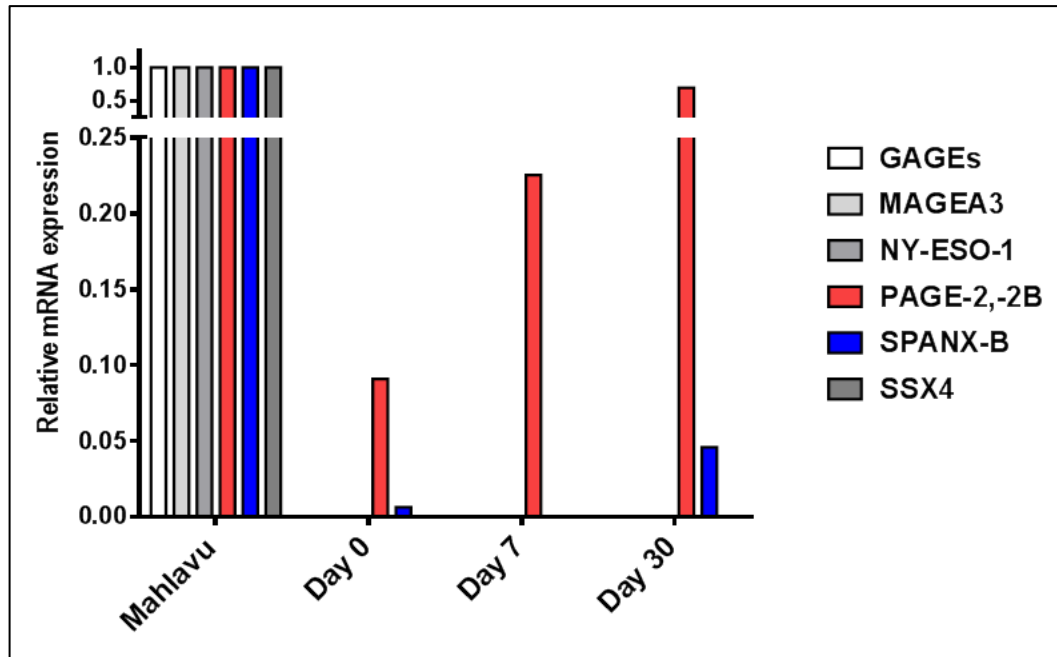


Figure 3.1.1 3: Among 6 CT gene families; the gene expressions of *PAGE-2,-2B* and *SPANX-B* increase in Caco-2 spontaneous differentiation.

The relative mRNA expressions of various CT genes were shown during Caco-2 spontaneous differentiation at 3 different time points by Taqman probe q RT-PCR. *GAPDH* gene was used as endogenous control. Mahlavu cell line RNA was used as reference sample in $\Delta\Delta C_t$ calculations due to the well-known CT gene expression levels.

3.1.2 Characterization of Caco-2 spontaneous differentiation in association with MET and CT gene expression:

The gene expression profile of Caco-2 cells during differentiation was thoroughly analyzed by Sääf and Halbleib et al. [40,41]. By analyzing microarray gene expression data, these authors identified two distinct clusters named prepolarization (samples from 0 to 4 days) and polarization (samples from 4 to 26 days) which were formed by a switch in gene regulation at day 4. When the gene expression pattern of Caco-2 cells during differentiation was compared with normal colon and colorectal cancer samples, there were two clusters; tumor and normal epithelial cluster. While prepolarized cells remained in tumor clusters, polarized cells remained in normal epithelial cluster. Finally, they established that differentiated Caco-2 cells were more similar to normal epithelial cells compared to tumor cells [40,41]. In light of this data we

asked if the differentiation observed in Caco2 cells was similar to what would be expected in a mesenchymal to epithelial transition. We, therefore, studied alterations in gene expression in candidate epithelial and mesenchymal marker genes in this model by analyzing the GSE1614 dataset and using the EMT related gene list in colon cancer of Loboda et al [64,66]. We identified 3 mesenchymal marker genes; *fibronectin*, *vimentin* and *transgelin* and 3 epithelial marker genes; *E-cadherin*, *claudin-4* and *CDX-2* that were differentially expressed in Caco-2 differentiation. To validate these *in silico* findings, we performed qRT-PCR to show the gene expression differences of marker genes in the model at 4 time points; day 0 (100% confluency), 10, 20 and 30 (fully differentiated). As the cells differentiated, epithelial marker genes (*CDH1*, *CLDN4*, *CDX2*) increased and mesenchymal marker genes (*FNI*, *VIM*, *TAGLN*) decreased in mRNA level in the analyzed two different differentiation sets (Figure 3.1.2 1). For both epithelial and mesenchymal marker genes, differential expressions were time dependent. mRNA expression study confirmed that cells were in a differentiation from mesenchymal to epithelial phenotype. Changes in mRNA expression levels of both CT and EMT genes were statistically significant according to one way ANOVA test. The increase in CT gene expression was in concordance with the increase in epithelial marker gene expression and the decrease in mesenchymal marker gene expression.

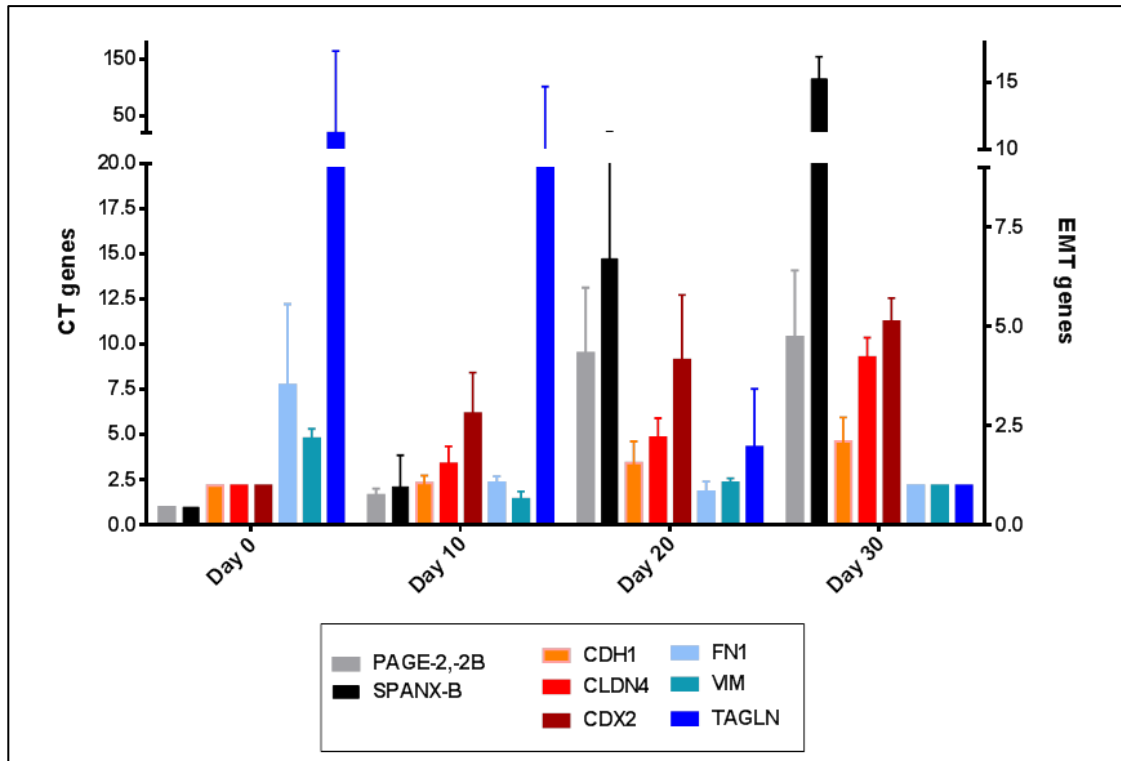


Figure 3.1.2 1: CT gene mRNA levels increase concomitant with mesenchymal to epithelial transition.

The relative mRNA expressions of mesenchymal marker genes (*Fibronectin 1*, *Vimentin* and *Transgelin*), epithelial marker genes (*E-Cadherin*, *Claudin4* and *Cdx2*) and 3 CT genes (*PAGE-2,-2B* & *SPANX-B*) were shown during Caco-2 spontaneous differentiation at 2 different differentiation sets by q RT-PCR. *GAPDH* gene was used as endogenous control. Caco-2 cell line RNA at day 0 was used as reference sample in $\Delta\Delta Ct$ calculations. In two independent sets of differentiation, the increase in CT gene expression was related with the increase in epithelial marker gene expression and the decrease in mesenchymal marker gene expression. The changes in gene expression levels were statistically significant and the p values were smaller than 0.0001 according to one way ANOVA test for all studied genes.

In addition to the difference we observed in mRNA expression levels, we found down-regulation of fibronectin, transgelin and vimentin and up-regulation of SPANX-B and CDX-2 proteins as well, in three different differentiation experiments by western blotting technique (Figure 3.1.2 2).

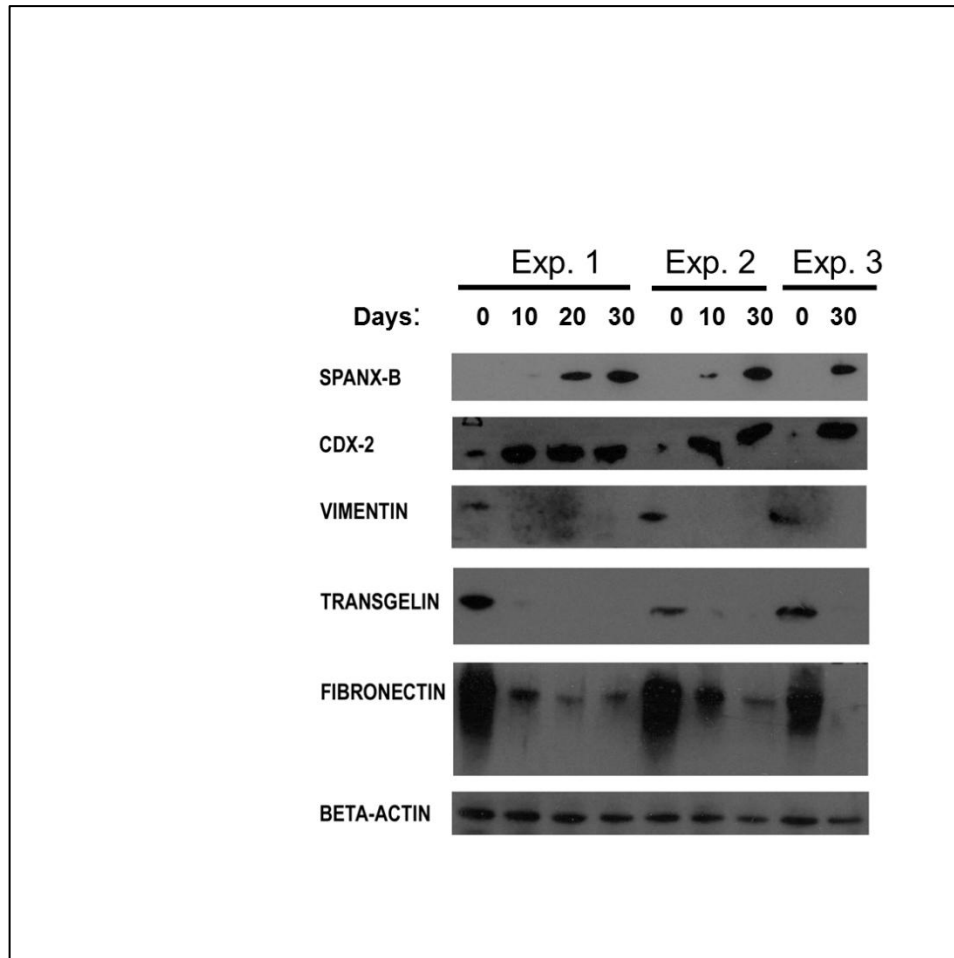


Figure 3.1.2 2: Increase in CDX-2 (34 kDa, epithelial protein) and SPANX-B (12 kDa, CT protein), the decrease in Transgelin (23 kDa), Fibronectin (263 kDa) and Vimentin (54 kDa) (mesenchymal proteins) at the protein level by western blot experiment in 3 different differentiation sets.

Since the antibody of PAGE-2,-2B did not work in western blotting, immunofluorescence (IF) experiment was also performed. Although IF experiment was not for protein level determination, we achieved it as an alternative technique to western blotting. We performed IF experiments with all settings fixed throughout the experiment to be able to compare different time points. Confirming the western blots, mesenchymal proteins declined and epithelial protein inclined in the differentiation process (Figure 3.1.2 3). CT proteins SPANX-B and PAGE-2,-2B accumulated in the cells as the cells differentiated (Figure 3.1.2 4). PAGE-2,-2B and SPANX-B proteins were localized at the nucleus, upon increase in protein levels cytoplasmic staining was also observed for

SPANX-B at day 30. Vimentin antibody stained the cells at the beginning of differentiation but, due to decrease in mRNA levels, staining completely disappeared at day 10 and 20. Fibronectin staining was also attenuated as cells differentiated. CDX2, an essential transcription factor for intestine epithelial cells, had nuclear staining pattern and increased in time dependent manner. Interestingly, heterogeneous staining patterns for both CT and EMT proteins were observed showing the heterogeneous population in Caco-2 cells during differentiation.

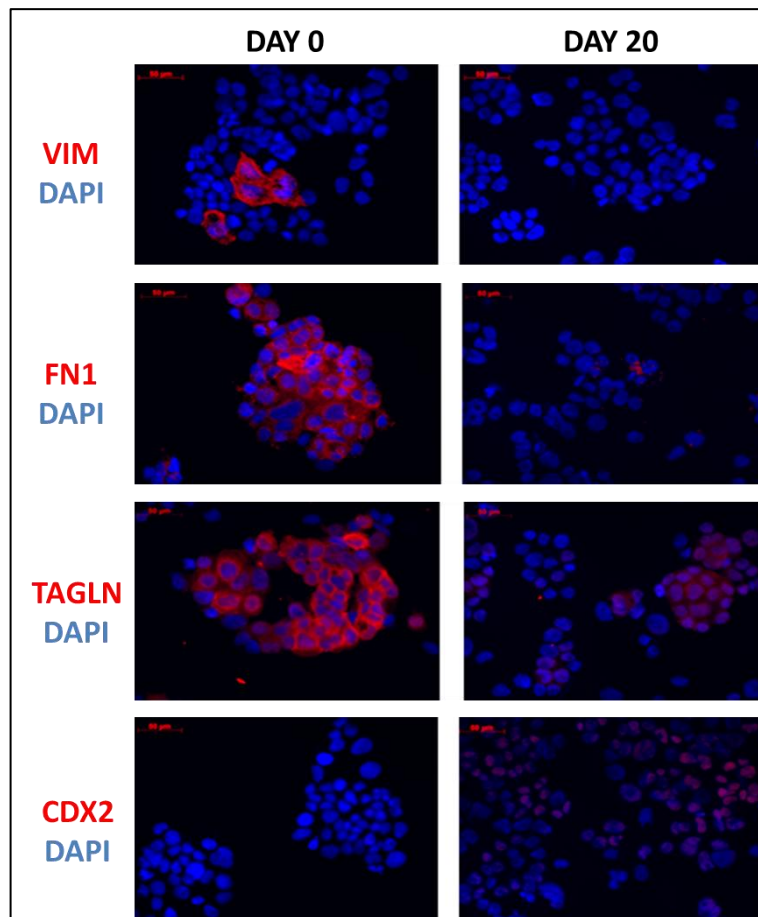


Figure 3.1.2 3: Decrease in mRNA levels of mesenchymal marker genes (VIM, FN1 and TAGLN) and increase in mRNA level of epithelial marker gene (CDX2) exist in protein level as well.

Immunofluorescence staining results of MET marker proteins (red-Alexa 568) during Caco-2 spontaneous differentiation at day 0 and 20 were shown (40X). Cell nuclei were stained with DAPI. The decrease in Transgelin, Vimentin and Fibronectin protein levels and the increase in CDX2 protein level were observed from day 0 to day 20.

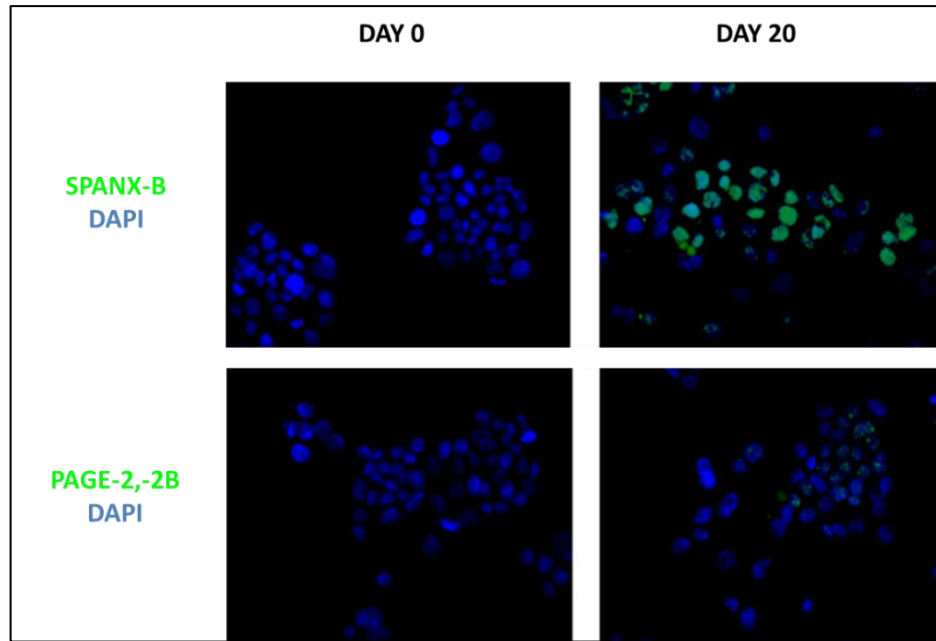


Figure 3.1.2 4: Increase in mRNA levels of CT genes (SPANX-B and PAGE-2,-2B) exists in protein level as well.

Immunofluorescence staining results of CT proteins (green-Alexa 488) during Caco-2 spontaneous differentiation at day 0 and 20 were shown (40X). Cell nuclei were stained with DAPI. The increase in CT protein levels were observed from day 0 to day 20 and the increase in SPANX-B protein level was more evident than the increase in PAGE-2,-2B protein level.

In order to show further evidence to this connection existing in mRNA and protein levels, we performed double staining in immunofluorescence (IF) experiment. One of the remarkable result that we obtained from IF staining, was divergent staining pattern of CT proteins with mesenchymal proteins and convergent staining pattern of CT proteins with epithelial proteins. CT protein positive cells were mostly negative for mesenchymal marker proteins (Vimentin and fibronectin). This observation was highly dramatic at day 0 images due to the abundance of mesenchymal proteins at the beginning of differentiation. The co-existence of CT proteins with epithelial marker protein (CDX-2) in the corresponding cells was detected in day 0, 10 and 30 images (Figure 3.1.2 5, Figure 3.1.2 6, Figure 3.1.2 7, Figure 3.1.2 8, Figure 3.1.2 9, Figure 3.1.2 10).

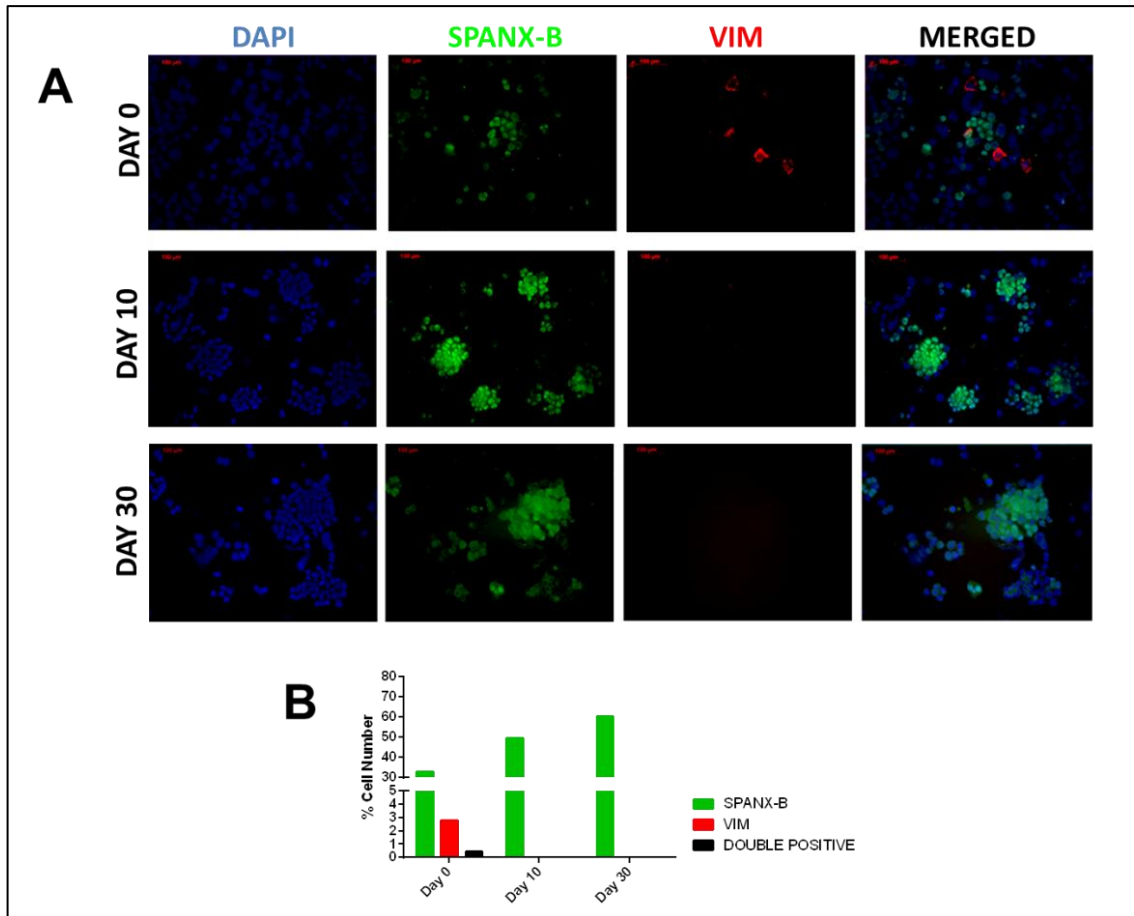


Figure 3.1.2 5: Double immunofluorescence staining at day 0 shows that vimentin positive cells are negative for SPANX-B protein and SPANX-B positive cells are negative for vimentin protein.

(A) Cells were stained with α -SPANX-B antibody (green-Alex 488) and α -vimentin antibody (red-Alexa568) and DAPI was used to stain the nuclei. Representative images for day 0, day 10 and day 30 were shown (20X). SPANX-B protein localized in nucleus and vimentin protein had cytoskeletal staining pattern. At day 10, vimentin staining disappeared and vimentin and SPANX-B staining did not overlap due to the decrease of vimentin during differentiation. (B) The percent number of SPANX-B positive, vimentin positive and double positive cells were shown as bar graphs as a result of counting the cells in 3 independent IF images.

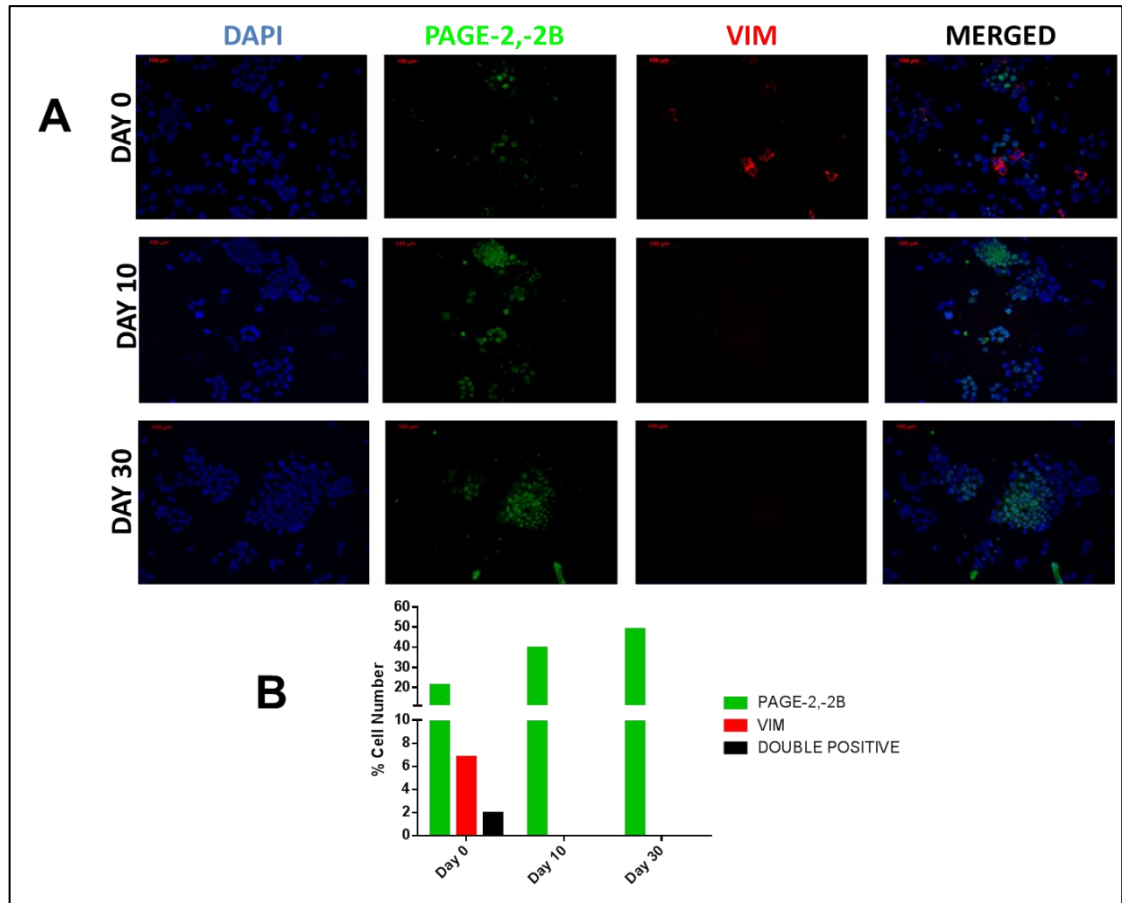


Figure 3.1.2 6: Double immunofluorescence staining at day 0 shows that vimentin positive cells are negative for PAGE-2,-2B protein and PAGE-2,-2B positive cells are negative for vimentin protein.

(A) Cells were stained with α -PAGE-2,-2B antibody (green-Alexa 488) and α -vimentin antibody (red-Alexa 568) and DAPI was used to stain the nuclei. Representative images for day 0, day 10 and day 30 were shown (20X). PAGE-2,-2B protein localized in nucleus and vimentin protein had cytoskeletal staining pattern. At day 10, vimentin staining disappeared and vimentin and PAGE-2,-2B staining did not overlap due to the decrease of vimentin during differentiation. **(B)** The percent number of PAGE-2,-2B positive, vimentin positive and double positive cells were shown as bar graphs as a result of counting the cells in 3 independent IF images.

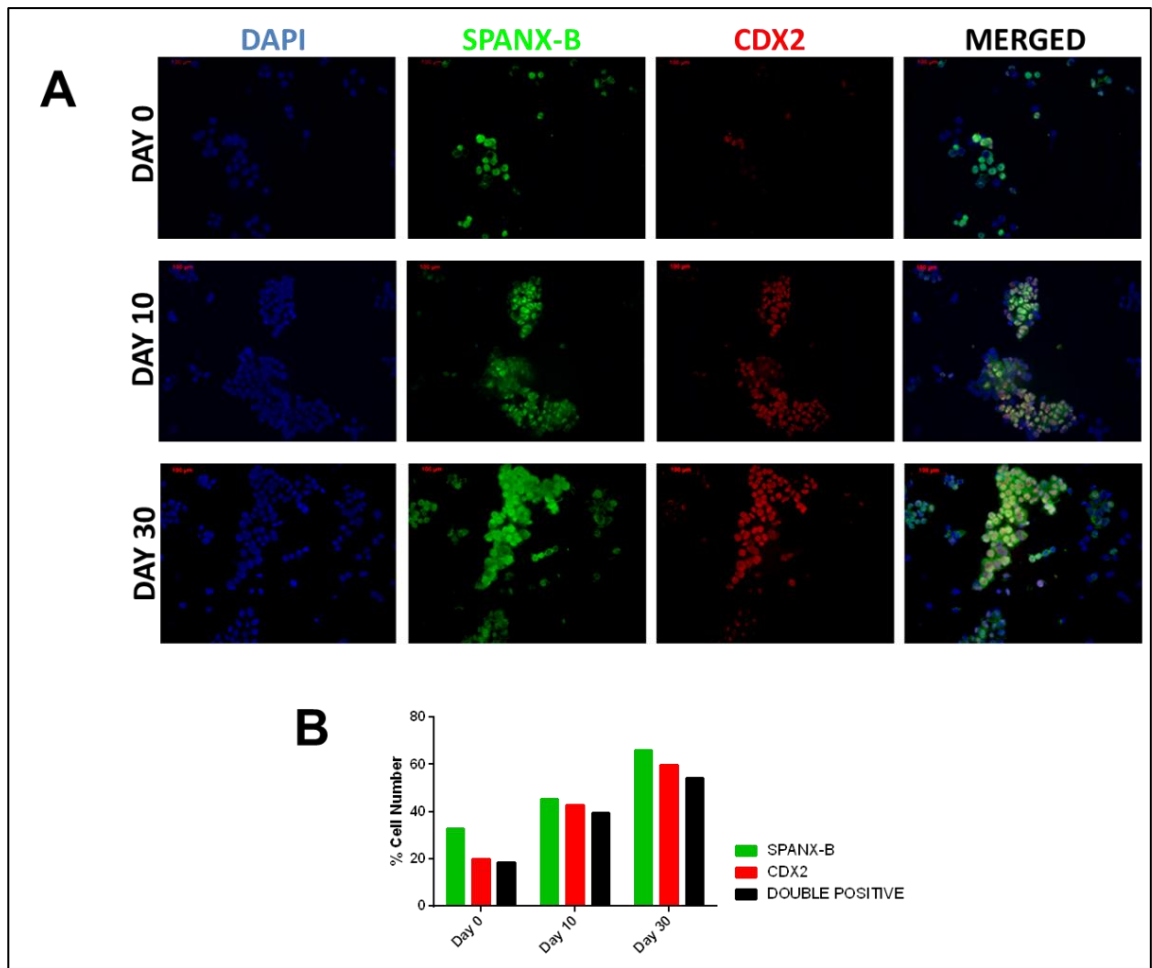


Figure 3.1.2 7: Double immunofluorescence staining shows that CDX2 protein co-localizes with SPANX-B protein in the corresponding cells during differentiation. (A) Cells were stained with α -SPANX-B antibody (green-Alexa488) and α -CDX2 antibody (red-Alexa568) and DAPI was used to stain the nuclei. Representative images for day 0, day 10 and day 30 were shown (20X). SPANX-B and CDX2 proteins co-localized in the same cells. Both proteins had nuclear localizations. The co-localization was more pronounced at day 10 and at day 30 since levels of both proteins increased throughout the differentiation. (B) The percent number of SPANX-B positive, CDX2 positive and double positive cells were shown as bar graphs as a result of counting the cells in 3 independent IF images.

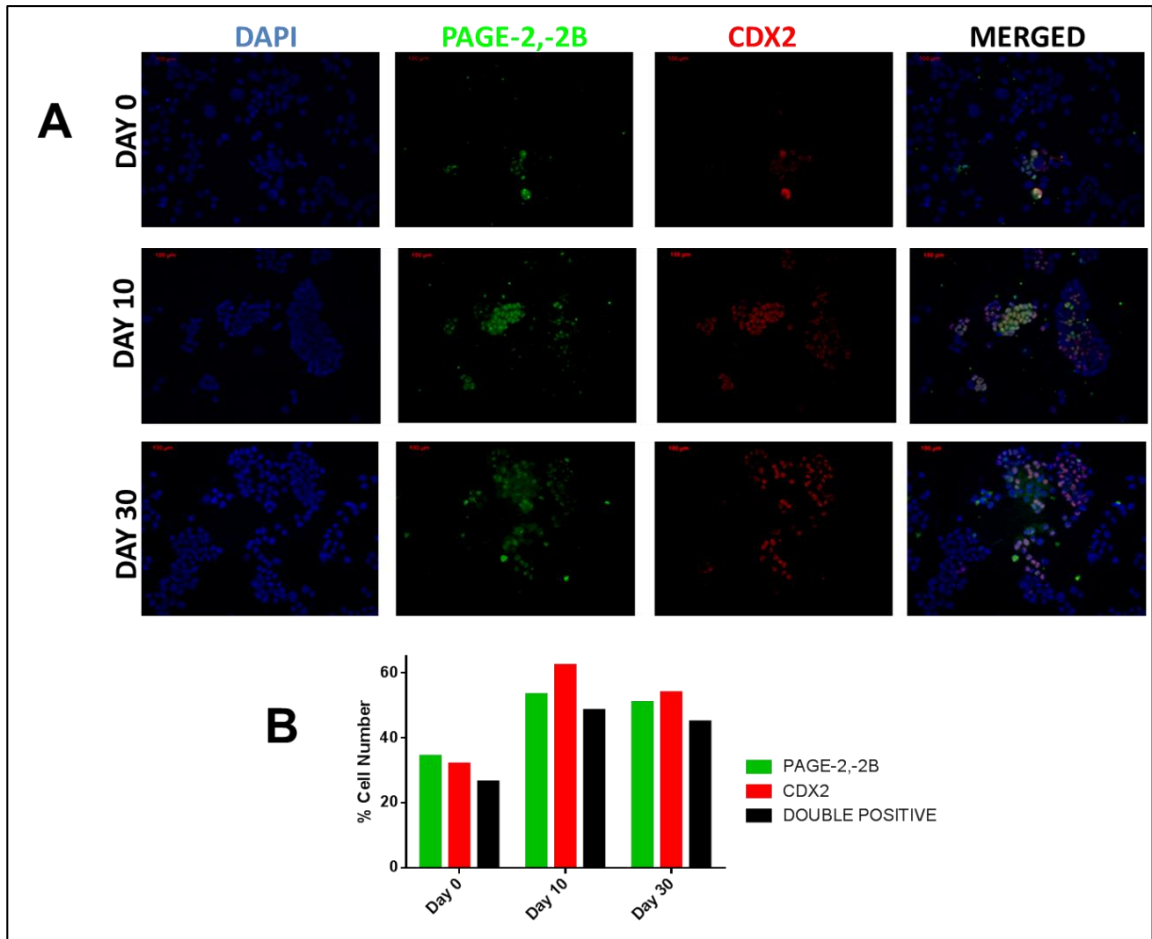


Figure 3.1.2 8: Double immunofluorescence staining shows that CDX2 protein co-localizes with PAGE-2,-2B protein in the corresponding cells during differentiation. (A) Cells were stained with α -PAGE-2,-2B antibody (green-Alexa488) and α -CDX2 antibody (red-Alexa568) and DAPI was used to stain the nuclei. Representative images for day 0, day 10 and day 30 were shown (20X). PAGE-2,-2B and CDX2 proteins co-localized in the same cells. Both proteins have nuclear localizations. The co-localization was more pronounced at day 10 since levels of both proteins increased at day 10. **(B)** The percent number of PAGE-2,-2B positive, CDX2 positive and double positive cells were shown as bar graphs as a result of counting the cells in 3 independent IF images.

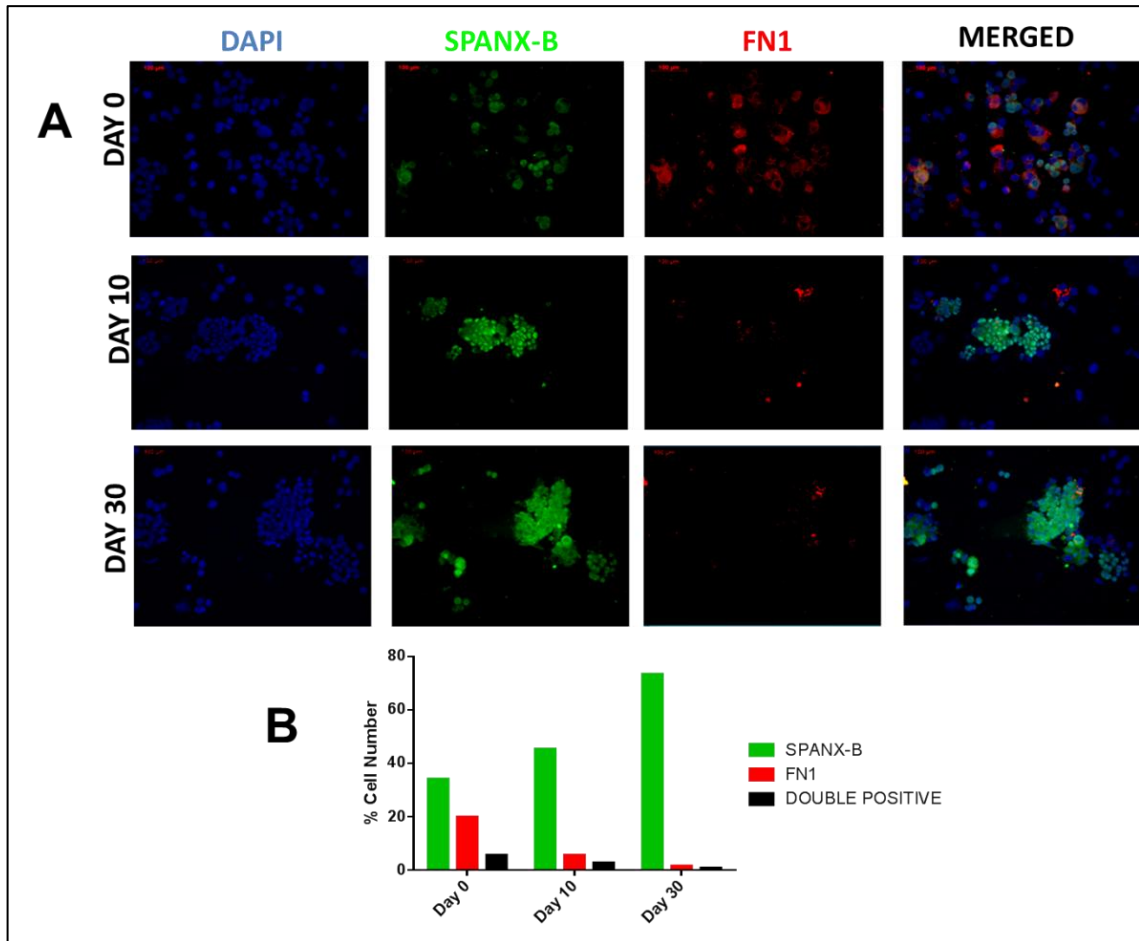


Figure 3.1.2 9: Double immunofluorescence staining at day 0 shows that fibronectin positive cells are negative for SPANX-B protein and SPANX-B positive cells are negative for fibronectin protein.

(A) Cells were stained with α -SPANX-B antibody (green-Alexa488) and α -fibronectin antibody (red-Alexa568) and DAPI was used to stain the nuclei. Representative images for day 0, day 10 and day 30 were shown (20X). SPANX-B protein localized in nucleus and fibronectin protein had cytoplasmic staining pattern. At day 10, fibronectin staining decreased. (B) The percent number of SPANX-B positive, fibronectin positive and double positive cells were shown as bar graphs as a result of counting the cells in 3 independent IF images.

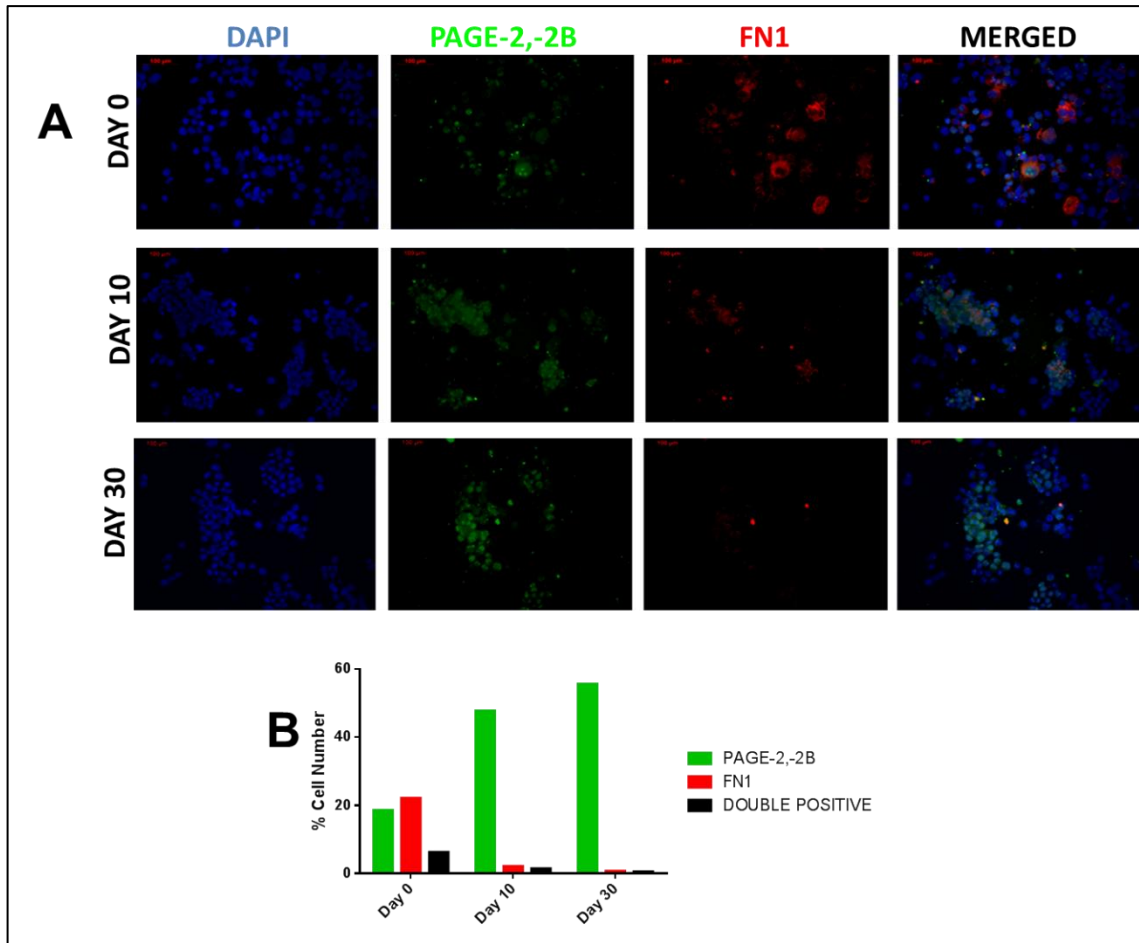


Figure 3.1.2 10: Double immunofluorescence staining at day 0 shows that fibronectin positive cells are negative for PAGE-2,-2B protein and PAGE-2,-2B positive cells are negative for fibronectin protein.

(A) Cells were stained with α -PAGE-2,-2B antibody (green-Alexa488) and α -fibronectin antibody (red-Alexa568), DAPI was used to stain the nuclei. Representative images for day 0, day 10 and day 30 were shown (20X). PAGE-2,-2B protein localized in nucleus and fibronectin protein had cytoplasmic staining pattern. At day 10, fibronectin staining decreased. (B) The percent number of PAGE-2,-2B positive, fibronectin positive and double positive cells were shown as bar graphs as a result of counting the cells in 3 independent IF images.

3.1.3 Epigenetic mechanisms underlying CT gene expression in Caco-2 spontaneous differentiation:

A generally accepted epigenetic mechanism for CT gene expression regulation is promoter DNA methylation [1,5,11,21]. In order to understand whether promoter proximal DNA alterations correlated with CT gene upregulation during differentiation we carried out bisulphite sequencing of CpG islands for *PAGE-2* and *PAGE-2B* genes identified by searching 5500 bp length regions up to from -1500 bp from transcription start site (*CpG Island Finder Software* (<http://cpgislands.usc.edu/>)). For *PAGE-2* and *PAGE-2B* genes, 8 and 10 CpG residues respectively were analyzed in the identified CpG islands. In all time points analyzed (day 0, 10 and 30), we identified that more than 90% of the CpGs were methylated. According to one way ANOVA test, the difference in methylation levels for *PAGE-2* and *PAGE-2B* genes was not statistically significant. For *SPANX-B* gene, a promoter region that was previously analyzed was chosen for the bisulphite analysis. Demethylation of this region with critical specific 4 CpGs (CpG # 5, 6, 7, 9) had previously been shown to be related with the gene expression [67,68]. And, of the 11 CpG residues analyzed within the *SPANX-B* promoter, no change in methylation was observed during the course of differentiation. Those CpGs previously reported as being critical for expression [67,68] were heavily methylated in our differentiation model at all-time points of differentiation. As a result, we conclude that for *PAGE-2*, *-2B* and *SPANX-B* genes, DNA hypomethylation is not the underlying epigenetic mechanism resulting in CT gene expression throughout the differentiation of Caco-2 cells (Figure 3.1.3 1).

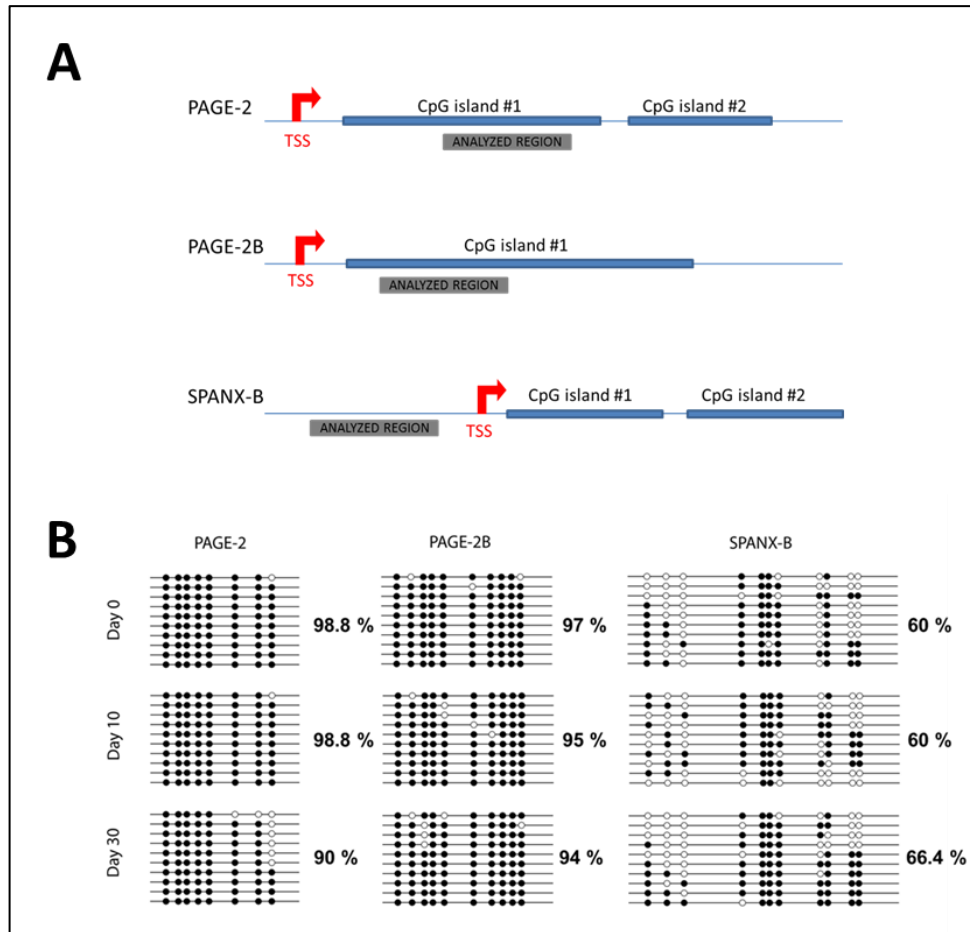


Figure 3.1.3 1: The promoter proximal DNA regions of 3 CT genes are heavily hypermethylated.

(A) Bisulphite sequencing within the promoter proximal regions of *PAGE-2*, *PAGE-2B*, and *SPANX-B* genes were shown. 8, 10, 11 CpG residues were analyzed for *PAGE-2*, *PAGE-2B* and *SPANX-B* genes, respectively, during Caco-2 differentiation at day 0, 10 and 30 by bisulphite sequencing. (B) The methylated CpG residues were designated as black circles, and the unmethylated ones were designated as unfilled circles. The difference in DNA methylation was not significant for all genes and the p values were; for *PAGE-2* $p=0.1938$, for *PAGE-2B* $p=0.6110$ and for *SPANX-B* $p=0.7495$ according to one way ANOVA test.

Although bisulphite sequencing results seemed uninformative, as 5hmC residues are observed as 5mC residues with this method, we decided to analyze 5hmC residue in the promoters. The previously analyzed regions for CT genes were investigated for the occupancy of 5-hydroxymethylcytosine residue by hydroxymethylated DNA immunoprecipitation experiment. Besides detecting hydroxymethylated DNA in the beginning of differentiation (day 0), we observed an increase in hydroxymethylation

levels in the following days of differentiation for both *PAGE-2* and *SPANX-B* genes. The change in 5-hydroxymethylcytosine occupied DNA was statistically significant for *PAGE-2* (Figure 3.1.3 2).

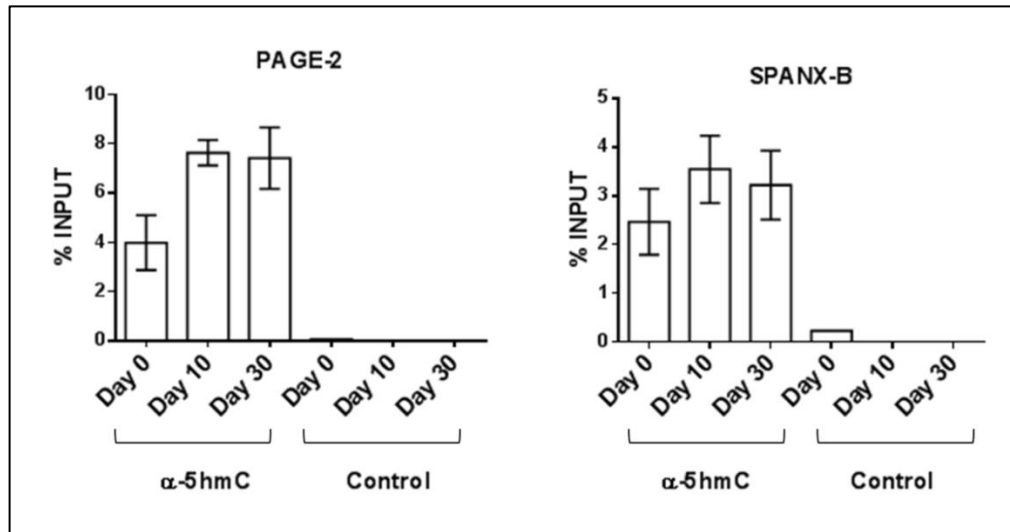


Figure 3.1.3 2: The amount hydroxymethylated DNA increases in the promoter proximal regions of *PAGE-2* and *SPANX-B* genes during Caco-2 spontaneous differentiation.

The genomic DNAs isolated at day 0, 10 and 30 were sonicated and immunoprecipitated with α -5hmC antibody. The immunoprecipitated DNA was amplified by the primers spanning the promoter proximal regions of *PAGE-2* and *SPANX-B* genes by SYBR based q RT-PCR. Preimmune serum was used as the negative control in the experiment. PCR result was analyzed by percent input method. The change in hydroxymethylation level for *PAGE-2* was statistically significant ($p=0.001$). Although a similar trend was observed for *SPANX-B* hydroxymethylation levels, it was not significant ($p=0.0773$).

Increases in 5-hydroxymethylcytosine levels have been previously associated with increased *TET1,-2,-3* expression levels [56,69]. We, therefore, analyzed mRNA expression levels of those enzymes responsible for 5hmC DNA generation during Caco2 spontaneous differentiation, and observed that both *TET1,-2,-3* genes were induced (Figure 3.1.3 3).

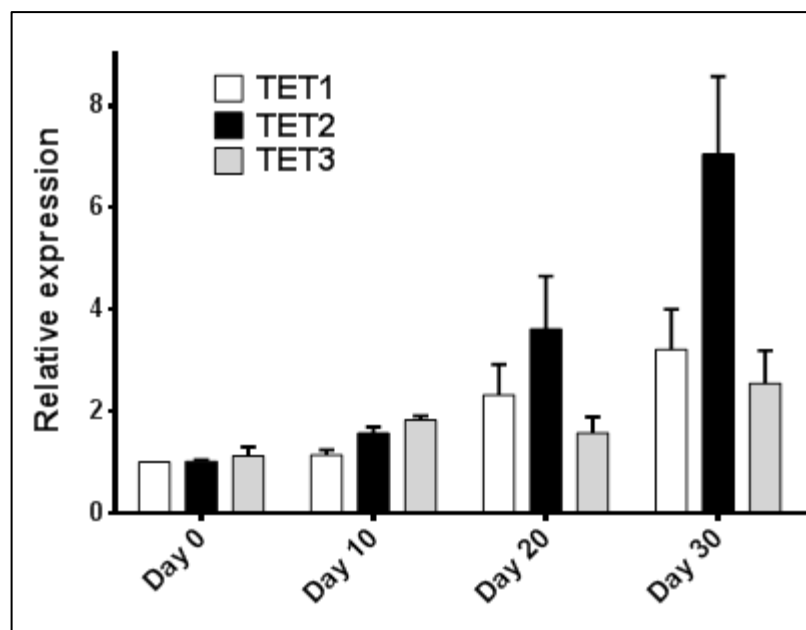


Figure 3.1.3 3: mRNA levels of *TET* genes (*TET1*, *TET2*, *TET3*), responsible for 5hmC residue generation, increase during Caco-2 spontaneous differentiation. Relative mRNA expressions of various CT genes were shown during Caco-2 spontaneous differentiation at 4 different time points by SYBR based q RT-PCR. *GAPDH* gene was used as endogenous control. The change in mRNA levels of *TET1* and *TET2* genes was statistically significant and the p values were; for *TET1* p=0.0304, for *TET2* p=0.0093. (For *TET3* p value was 0.0720 and was not statistically significant)

Among three *TET* enzymes, *TET2* showed the most dramatic change. When we investigated the change in protein level by Western blotting, we did not find a difference in the amount of the full length *TET2* protein (220 kDa) using one commercial antibody. However, with a second antibody generated by Abcam, we detected a 25kDa band whose quantity increased through the differentiation process, as observed in 3 different differentiation sets consistently (Figure 3.1.3 4). To ensure the specificity of the band, we incubated *TET2* antibody with its specific blocking peptide during the western blot experiment. Since the band disappeared with blocking with the specific peptide we were certain about the 25kDa band belonging to *TET2* (Figure 3.1.3 4). To explain the 25kDa band, we performed bioinformatic analyses but were unable to identify an alternatively spliced *TET2* mRNA that could translate a 25kDa peptide. Since we knew from the literature that *TET* proteins could be post translationally modified by calpains, we performed western blotting with Caco-2 lysates treated with a general Ca^{+2} chelator

(BAPTA-AM) which is expected to inhibit most calpains, as they are Ca^{+2} .dependent. Although BAPTA-AM treatment did not result in the loss of the 25kDa band, a TET2 peptide with a higher molecular weight appeared, which is likely to be an incompletely processed version of TET2 (Figure 3.1.3 5). Thus we conclude that TET2 might be cleaved with a Ca^{+2} dependent calpain.

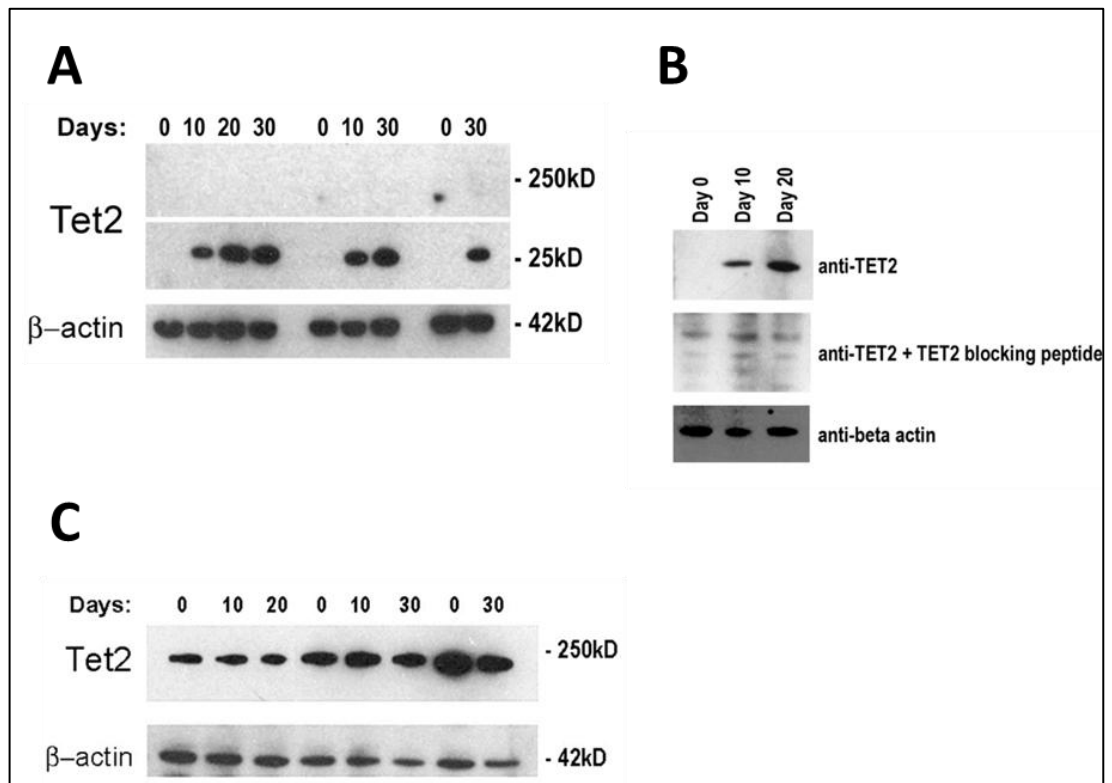


Figure 3.1.3 4: A possible small variant of TET2 protein is found to be increased in Caco-2 differentiation consistently in 3 different differentiation sets.

(A) The predicted band at 220 kDa could not be detected by Abcam (UK) anti-Tet2 antibody (ab94580) but a band close to 25 kDa was detected consistently increased during the differentiation in 3 different sets. **(B)** The band was specific to TET2 protein since it disappeared when TET2 peptide was introduced in the antibody incubation step. **The protein level of full length TET2 does not increase in Caco-2 differentiation.** **(C)** The predicted band at 220 kDa was identified by Active Motif anti-TET2 antibody (61389) and the level did not increase as expected similar to the small variant. The small variant could not be detected with this antibody.

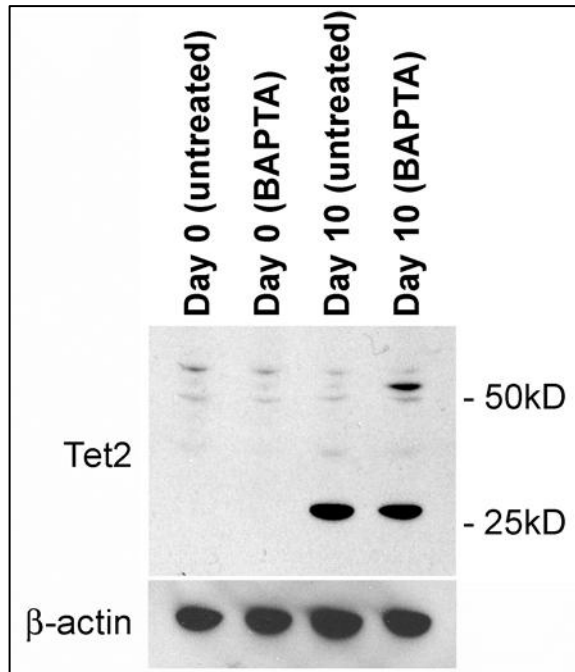


Figure 3.1.3 5: A possible truncated form of TET2 is generated with Ca^{+2} dependent calpains.

Caco-2 cells at day 0 and day10 time points were incubated with Ca^{+2} chelator BAPTA-AM which inhibited calpains` activity. Though 25kDa band did not disappear significantly, a larger molecular weight band appeared showing the cleavage by calpains.

When we double stained Caco-2 cells with TET2 and CT antibodies, surprisingly we observed that cells having PAGE-2,-2B or SPANX-B proteins had TET2 protein at the same time and vice versa (Figure 3.1.3 6). Based on this data, we think the truncated TET2 form we identified might be functional.

In summary, as we could show an accumulation in 5hmC levels at promoter proximal regions of the CT genes, an increase in the expression levels of TET genes, and the colocalization of TET2 protein with CT proteins, we hereby demonstrate - to our knowledge - for the first time the involvement of 5-hydroxymethylcytosine in CT gene expression.

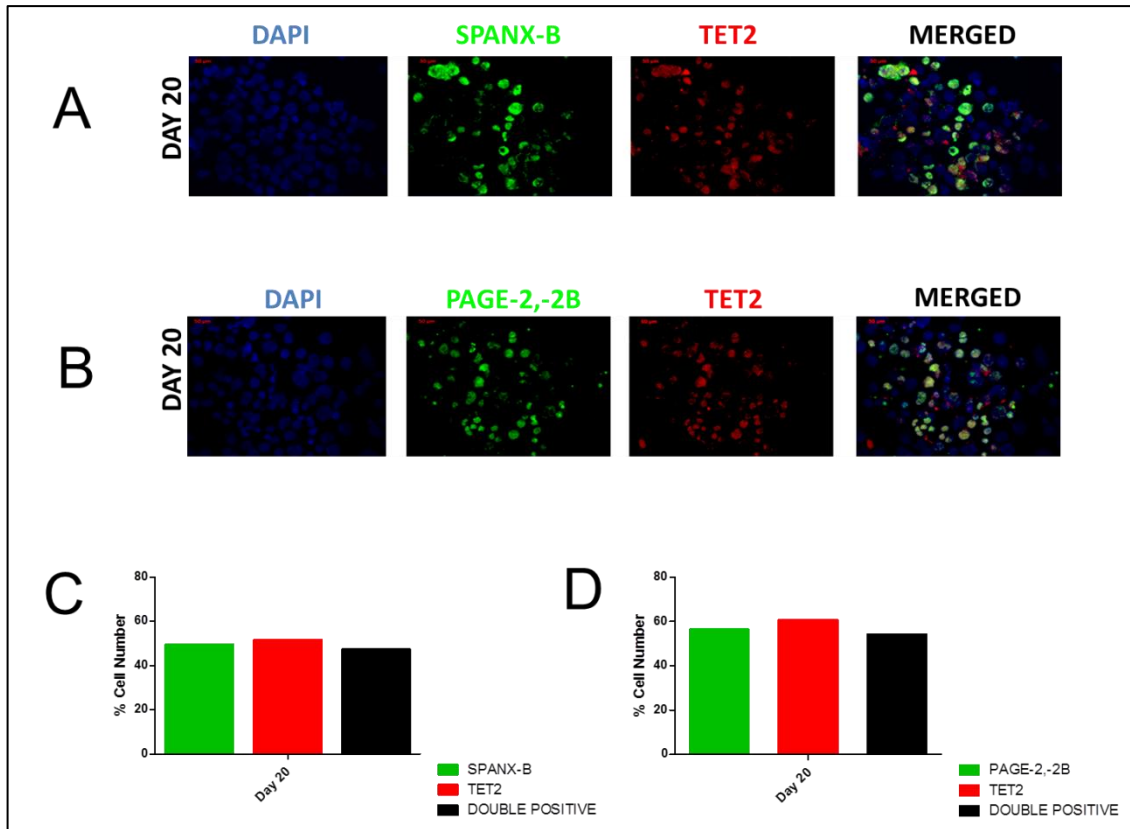


Figure 3.1.3 6: Double immunofluorescence staining shows that TET2 protein co-localizes with SPANX-B and PAGE-2,-2B proteins in Caco-2 cells during differentiation.

(A) Cells were stained with α -SPANX-B antibody (green-Alexa488) and (B) α -TET2 antibody (red-Alexa568) or α -PAGE-2,-2B antibody (green-Alexa488) and α -TET2 antibody (red-Alexa568) and DAPI was used to stain the nuclei. Representative images for day 20 were shown (40X). Both proteins had nuclear localizations. In both of the staining experiments, TET2 positive cells were positive for SPANX-B and PAGE-2,-2B. The percent number of (C) SPANX-B positive or (D) PAGE-2,-2B positive, TET2 positive and double positive cells were shown as bar graphs as a result of counting the cells in 3 independent IF images.

Since the role of histone modifications is known to have a role in CT gene expression, we analyzed inhibitory chromatin marks on the promoters of CT genes as well. Interestingly, as the cells differentiated and expressed CT genes, repressive chromatin marks such as HP1, EZH2 and H3K27me3 diminished (Figure 3.1.3 7). The increase in 5hmC levels on DNA might relate to the loss of HP1, EZH2 and H3K27me3 marks from chromatin and led to CT gene expression.

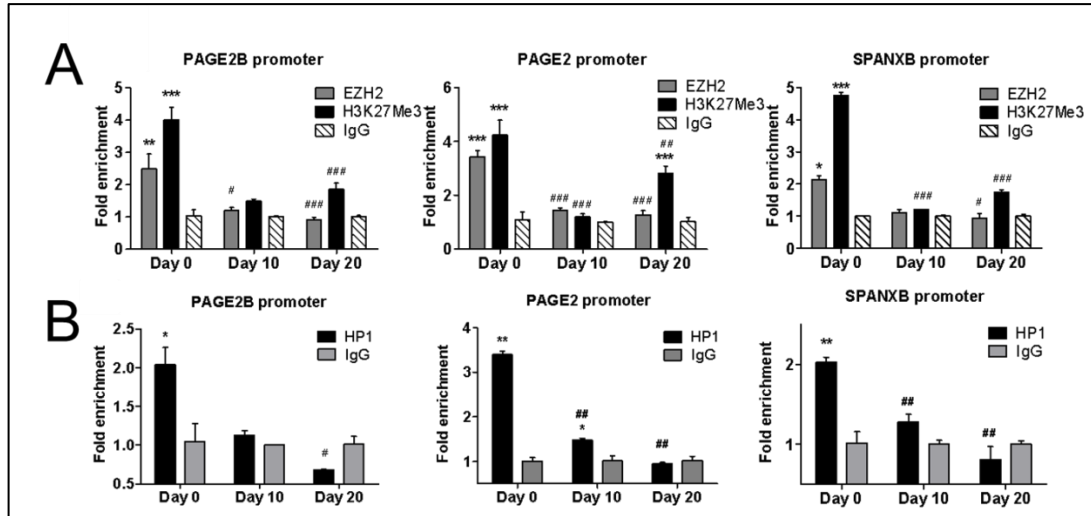


Figure 3.1.3 7: Binding of (A) EZH2, H3K27Me3 and (B) HP1 to the promoters of *PAGE-2B*, *PAGE-2* and *SPANX-B* decreases during differentiation shown by ChIP with the indicated antibodies or control IgG.

Figures are representative of three independent biological replicates. * $p < 0.05$, ** $p < 0.01$, *** $p < 0.001$ compared to IgG. # $p < 0.05$, ## $p < 0.01$, ### $p < 0.001$ compared to Day 0. (These experiments were performed by Dr. Aslı Sade Memişoğlu from METU)

Up to this point, we showed that CT genes were expressed concomitant with an increase in 5hmC levels on DNA and the dissociation of repressive chromatin marks, as the Caco-2 cells gained epithelial properties during differentiation. We next asked if these events could be reversed upon dedifferentiating Caco-2 cells. Indeed, when Caco-2 cells were dedifferentiated (as evidenced by the decrease in sucrose isomaltase expression) by detaching and reseeding differentiated cells at low seeding density, CT genes were down-regulated and epithelial to mesenchymal transition took place together with a decrease in TET gene expression (Figure 3.1.3 8).

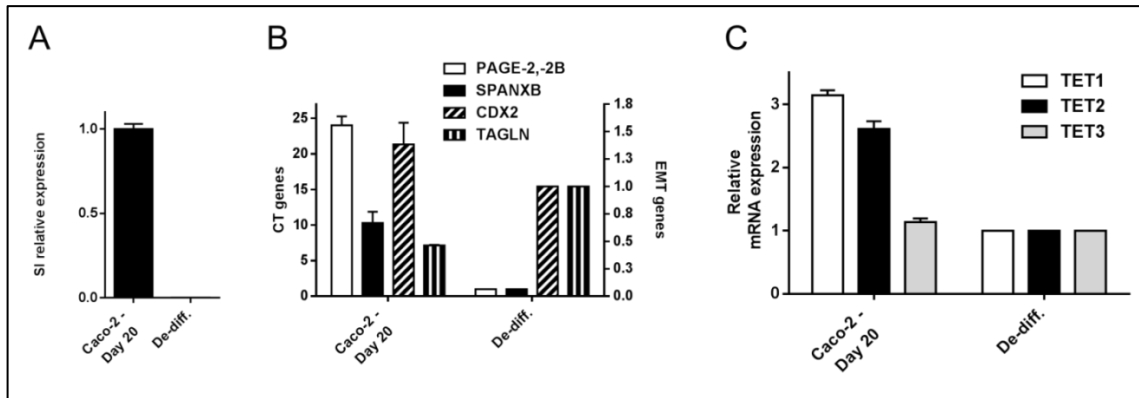


Figure 3.1.3 8: As the dedifferentiation occurs, cells gain mesenchymal character, down-regulate CTs and TET enzymes at the same time.

(A) Caco-2 cells were dedifferentiated according to decrease in *sucrose isomaltase* mRNA expression. (B) Relative mRNA expressions of CT genes, *CDX2* (epithelial marker), *TAGLN* (mesenchymal marker) and (C) *TET* genes were shown during Caco-2 dedifferentiation at 5 days later the reseeding by SYBR based q RT-PCR. *GAPDH* gene was used as endogenous control.

3.2 REGION SPECIFIC EPIGENETIC MECHANISMS OF CANCER TESTIS (CT) AND CT PROXIMAL GENE EXPRESSION

3.2.1 Analysis of CT proximal genes down-regulated in cancer by CGAP:

If epigenetic changes that relate to CT gene expression are contained within a region in the genome that includes CT genes but excludes others, then there should be clear boundaries between such regions if they are in close proximity. To identify such regions we hypothesized that we could study CT-proximal “non-CT genes”. To identify such genes previously in our lab, by using SAGE and EST databases of Cancer Genome Anatomy Project (CGAP) and analyzing libraries of cancerous versus healthy tissues, 59 genes on chromosome X were found to be down-regulated in cancer by Aydan Bulut. Among 59 genes, 8 of them were in close proximity of a CT gene. Since the down-regulation of 2 genes were verified in lung and colon cancer panels by RT-PCR, we conducted our further experiments with these 2 CT proximal genes down-regulated in cancer; *ALAS2* (*aminolevulinate, delta-, synthase 2*) and *CDR1* (*cerebellar degeneration-related protein 1*). In Figure 3.2.1 1, genomic alignments of *ALAS2* and *CDR1* genes on chromosome X and their proximities to the CT genes are shown.

ALAS2 is about 50 kb away from *PAGE-2,-2B* genes. *CDR1* is about 200 kb away from *SPANX-B* genes. *SPANX-B1,-B2* genes are allelic variant of *SPANX-B* gene that result with one amino acid substitution in the encoded protein [70]. *PAGE-2,-2B* and *SPANX-B* genes form a repeat region on chromosome X.

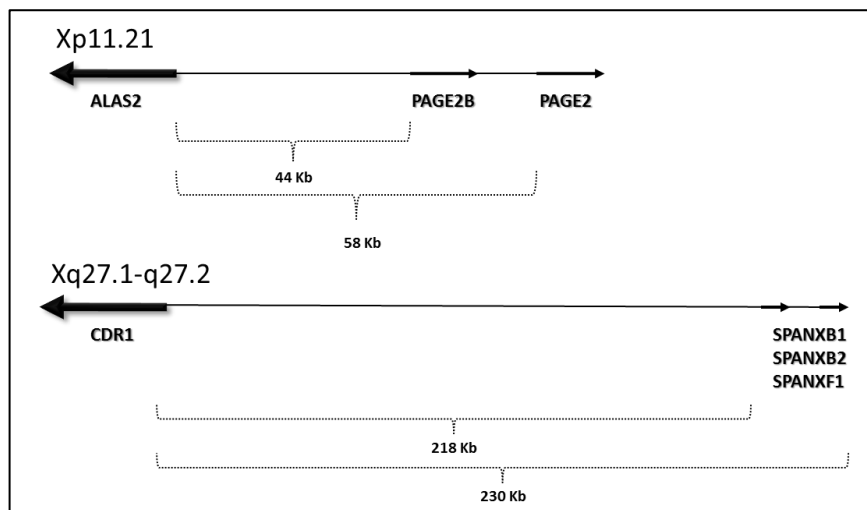


Figure 3.2.1 1: The genomic location of *ALAS2* and *CDRI* genes with respect to proximal cancer-testis antigens; *PAGE-2,-2B* and *SPANX-B* respectively.

3.2.2 The down-regulation in mRNA expression of CT proximal genes; *ALAS2* and *CDRI* and CT gene expression in cancer:

Expression analyses of *ALAS2* and *CDRI* genes were performed by predesigned Taqman probes based q RT-PCR technique. As shown in Figure 3.2.2 1 and Figure 3.2.2 3, *ALAS2* and *CDRI* were found to be down-regulated in a panel of colon and lung cancer cell lines compared to normal healthy tissues. *ALAS2* was expressed most at placenta and least at colon but, including the colon tissue it was expressed in all of the tested healthy tissues. *CDRI* was also expressed in all normal tissues at different levels. To sum up, *ALAS2* and *CDRI* genes were found to be expressed constitutively by all of healthy tissues that were analyzed. The significant down-regulation of *ALAS2* and *CDRI* genes in cancer cell lines compared to healthy tissues was demonstrated as seen in Figure 3.2.2 1 and Figure 3.2.2 3. Except NCI-H69 which still dramatically down-regulated *ALAS2* gene, none of the tested cancer cell lines had *ALAS2* mRNA expression. The significant down-regulation in *CDRI* gene was also shown in colon and lung cancer cell lines compared to normal counterparts.

When mRNA expressions of CT genes were analyzed in this panel, they were mainly detected in testis and placenta among normal healthy tissues as expected. *PAGE-2* and *2B* were also found to be weakly expressed in some normal tissues since some CT genes were classified as testis selective. *PAGE-2,-2B* and *SPANX-B* were expressed in cancer cell lines at comparable or higher levels than the expression levels in testis (Figure 3.2.2 2 and Figure 3.2.2 4). Finally these extensive expression analyses confirmed the opposite expression patterns of CT and CT proximal genes in normal tissues versus cancer cell lines that were previously identified by CGAP analysis.

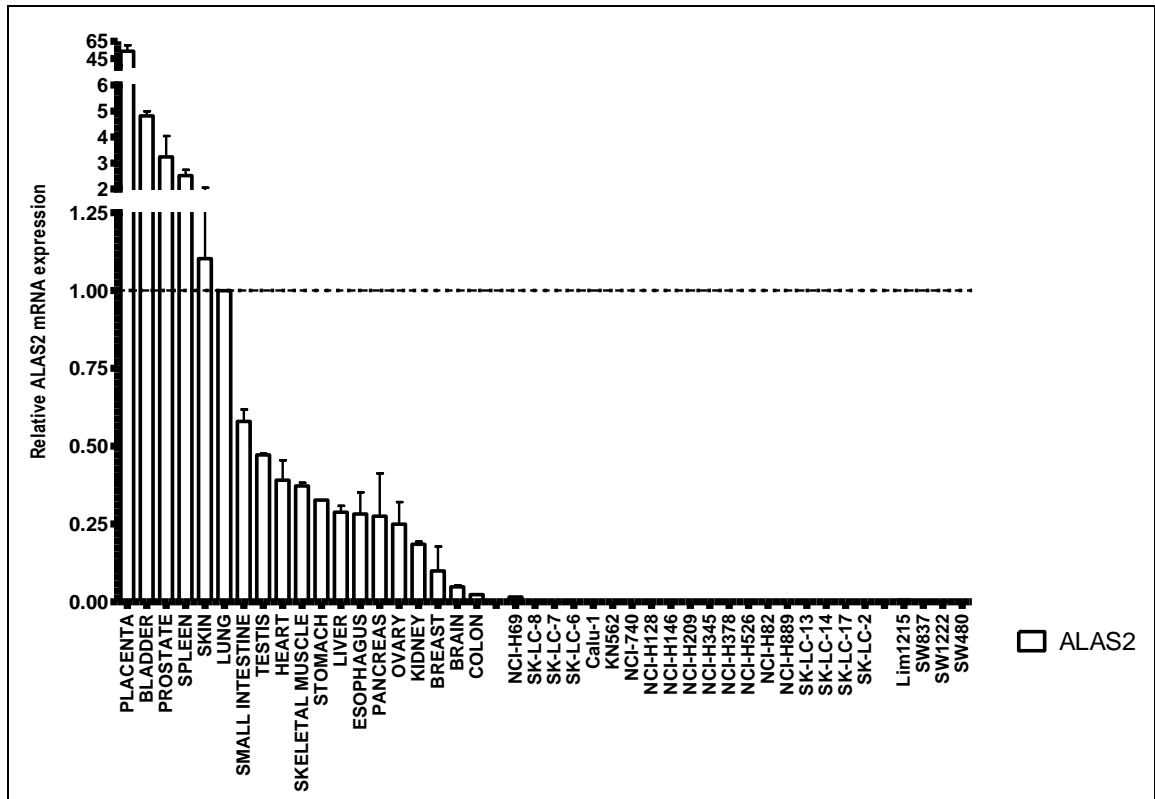


Figure 3.2.2 1: The mRNA expression of *ALAS2* gene is shown in normal tissues and a panel of colon and lung cancer cell lines by Taqman probe based q RT-PCR. *GAPDH* gene was used as endogenous control. Although *ALAS2* expression was detected in variable amounts in all healthy tissues, in none of the tested lung and colon cancer cell lines *ALAS2* mRNA expression existed.

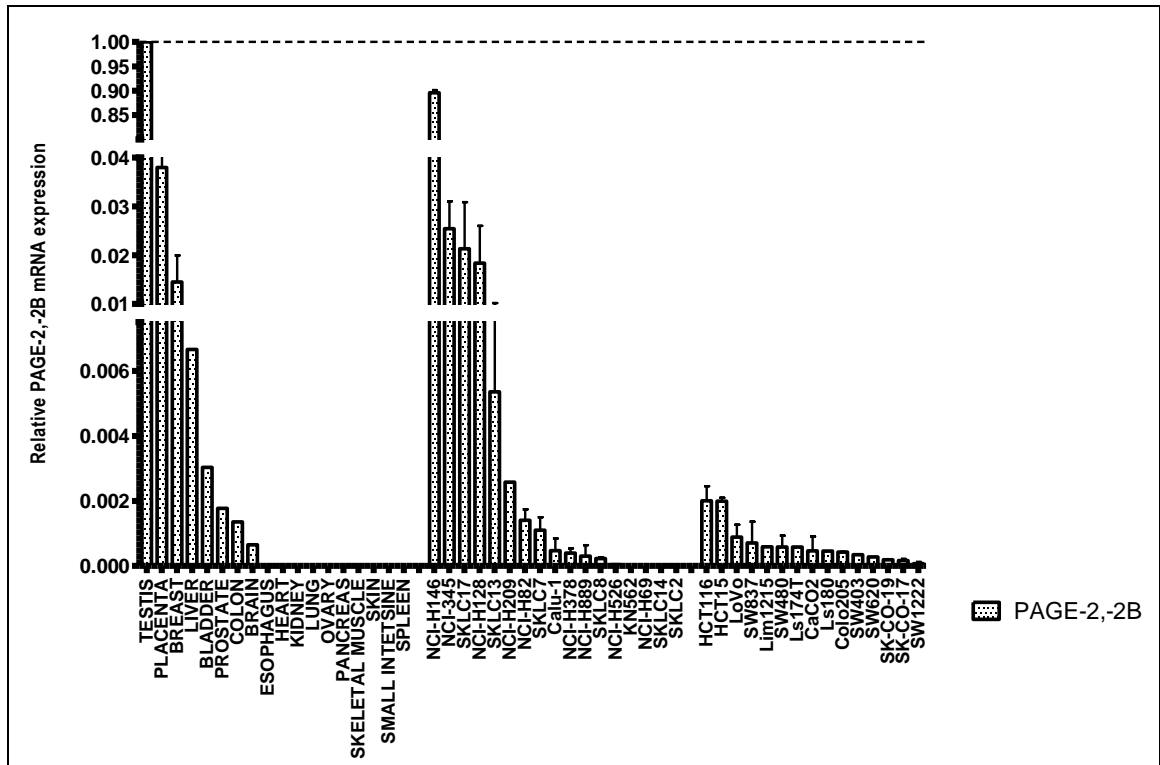


Figure 3.2.2 2: The mRNA expressions of *PAGE-2,-2B* genes proximal to *ALAS2* are shown in normal tissues and a panel of colon and lung cancer cell lines by Taqman probe q RT-PCR.

GAPDH gene was used as endogenous control. In addition to testis and placenta, *PAGE-2,-2B* expression was detected in some of the normal tissues. Most of the cancer cell lines were positive for *PAGE-2,-2B* expression.

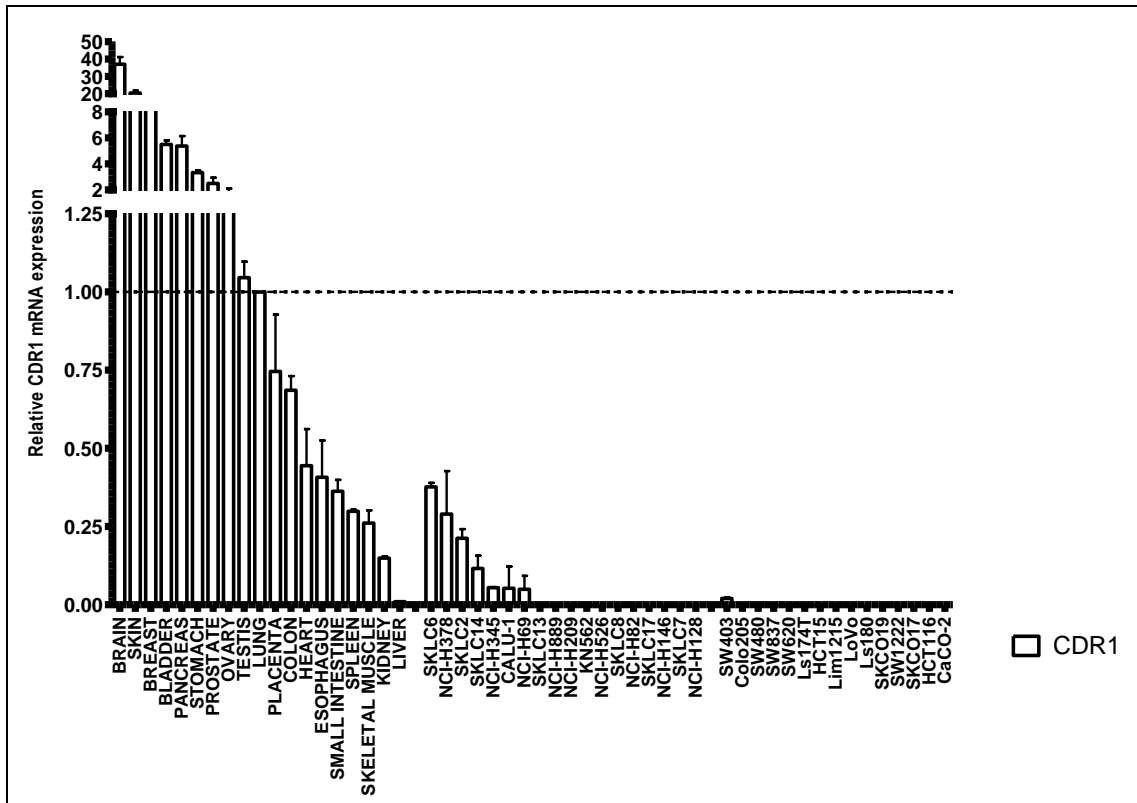


Figure 3.2.2 3: The mRNA expression of *CDR1* gene is shown in normal tissues and a panel of colon and lung cancer cell lines by Taqman probe q RT-PCR. *GAPDH* gene was used as endogenous control. The significant down-regulation in *CDR1* mRNA expression was detected in a large panel of lung and colon cancer cell lines compared to normal tissues.

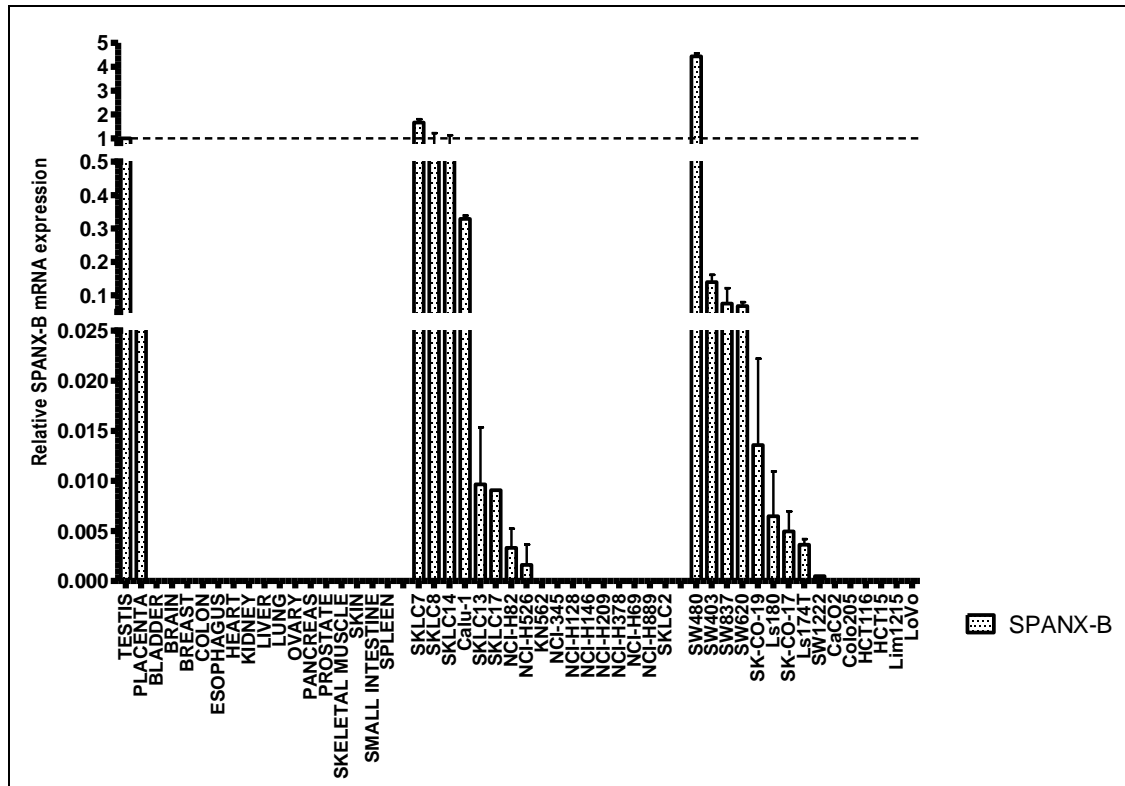


Figure 3.2.2 4: The mRNA expression of *SPANX-B* gene proximal to *CDR1* is shown in normal tissues and a panel of colon and lung cancer cell lines by Taqman probe q RT-PCR.

GAPDH gene was used as endogenous control. *SPANX-B* expression was observed in testis and placenta as a classical CT gene among normal tissues. Some of the cancer cell lines expressed *SPANX-B* at levels even higher than testis tissue.

3.2.3 The promoter proximal DNA methylation of *ALAS2* and *CDR1* genes in normal tissues and colon and lung cancer cell lines:

In order to identify the promoter methylation status of *ALAS2* and *CDR1*, a region between -2500 to +2500 bp from transcription start site was analyzed to find a CpG island for each gene. However, none of the tested CpG island prediction programs; *CpG Island Search Software* (<http://cpgislands.usc.edu/>) and *EMBOSS CpG Plot Software* (http://www.ebi.ac.uk/Tools/seqstats/emboss_cpgplot/), could predict a CpG island in 5000 bp length region for both *ALAS2* and *CDR1* genes. Due to the absence of CpG islands, we focused on individual CpG residues that were covered in this 5000 bp length region. The primers were designed to span maximum number of CpGs and not to hit methylated or unmethylated CpGs in order to eliminate bias in PCR reaction. Due to

the limitation of bisulphite sequencing technique; in 3 different regions, totally 10 and 9 CpG residues respectively for *ALAS2* and *CDRI* genes could be analyzed as shown in Figure 3.2.3 1 and Figure 3.2.3 2.

The bisulphite sequencing experiment was performed with genomic DNAs of cell lines that did not have *ALAS2* and *CDRI* expression and the genomic DNAs of normal male colon, female colon and lung tissues. The sum of sequencing results are shown as percent methylation in Table 3.2.3 1 and Table 3.2.3 2. According to these results, the promoter of *ALAS2* gene was highly methylated in normal colon tissues. The results of q RT-PCR experiment showed that colon was one of the tissues having low *ALAS2* mRNA expression. Thus, we suggested that promoter methylation of *ALAS2* in colon tissue might be related with this low level of expression. The promoter region of *ALAS2* in SK-LC-17 and HCT116 cancer cell lines was hypermethylated. However in LoVo and SW620, the region was hypomethylated even though none of the cell lines had *ALAS2* mRNA expression. *CDRI* promoter in normal colon tissues was hypermethylated although colon had *CDRI* expression in significant amounts. *CDRI* promoter was highly hypomethylated in all of the cancer cell lines lacking *CDRI* expression. For both *ALAS2* and *CDRI* gene, normal healthy tissues expressing the genes had methylated promoters whereas cancer cell lines lacking the gene expression had low levels of promoter methylation. In conclusion, the promoter methylation status of *ALAS2* and *CDRI* genes did not correlate with the gene expression levels.

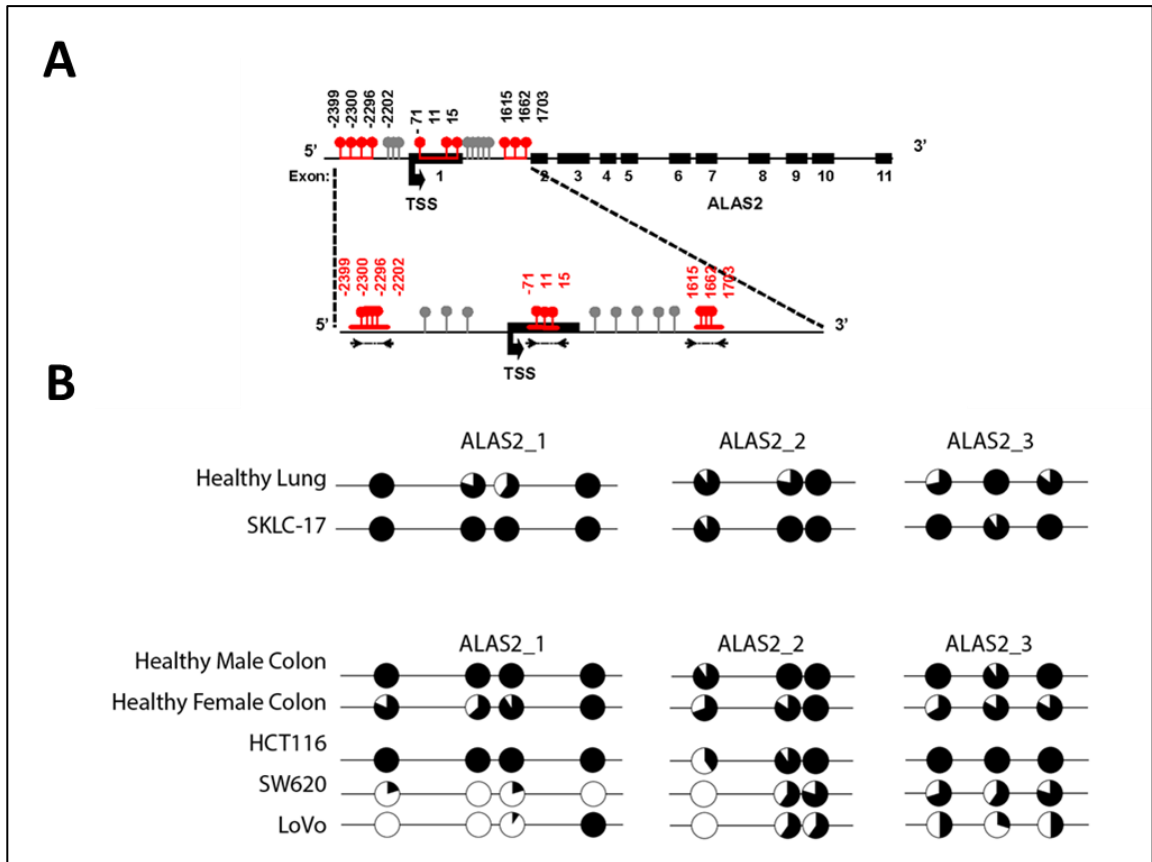


Figure 3.2.3 1: The organization of *ALAS2* gene; promoter, exon-intron structure and bisulphite sequencing result of the analyzed CpG residues are shown. (A) Dark black boxes denote exons, lines between them denote introns, red and grey lollipops denote CpG residues that are analyzed and not analyzed respectively. The CpG residues of *ALAS2* gene were analyzed in three regions, one in the promoter, one in the first exon and one in the first intron. (B) The bisulphite sequencing results were shown in circle designation for normal healthy lung and colon tissues versus SKLC-17 lung cancer cell line and HCT116, SW620, LoVo colon cancer cell lines. The degree of methylation was revealed with the darkness of the circle.

Table 3.2.3 1: The methylation status of *ALAS2* promoter in analyzed normal tissues and cancer cell lines shown as percent methylation

<u>% METHYLATION</u>	<u>ALAS2.1</u>	<u>ALAS2.2</u>	<u>ALAS2.3</u>
<i>NORMAL LUNG</i>	85.00%	88.90%	85.70%
SK-LC-17	100.00%	96.67%	97.22%

<u>% METHYLATION</u>	<u>ALAS2.1</u>	<u>ALAS2.2</u>	<u>ALAS2.3</u>
<i>NORMAL COLON_MALE</i>	100.00%	80.00%	96.97%
<i>NORMAL COLON_FEMALE</i>	84.09%	84.62%	77.78%
HCT116	100.00%	78.79%	100.00%
LOVO	27.27%	33.33%	48.48%
SW620	10.00%	48.72%	71.79%

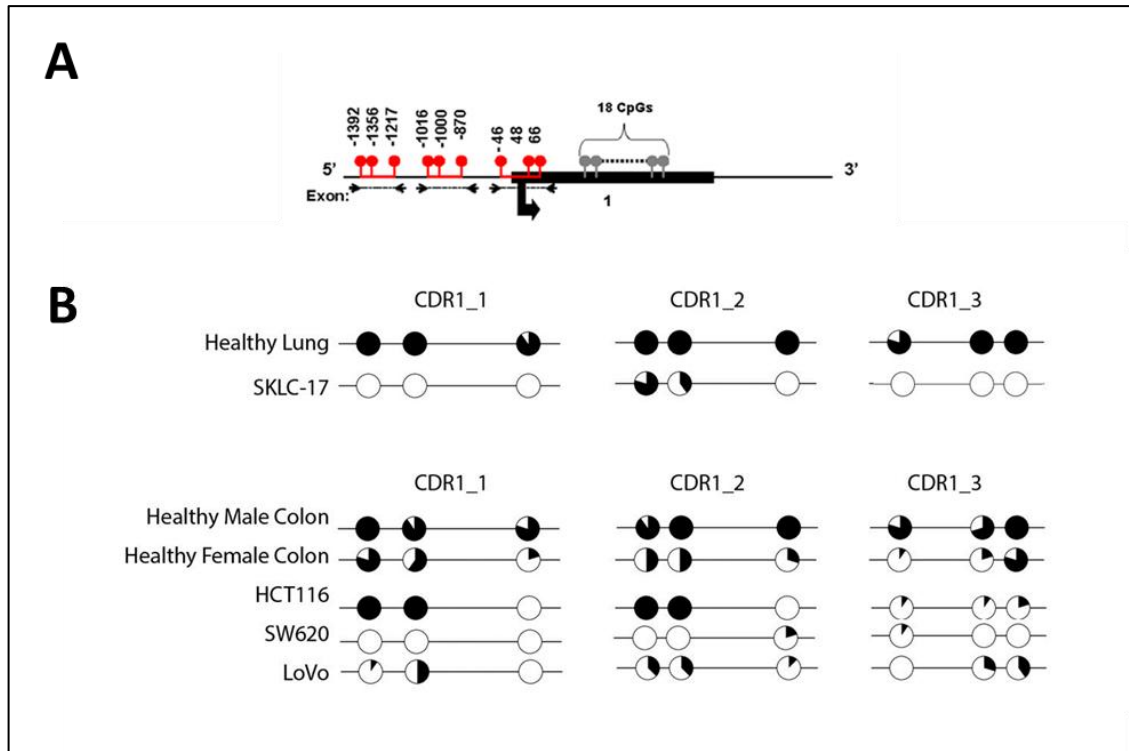


Figure 3.2.3 2: The organization of CDR1 gene; promoter, exon-intron structure and bisulphite sequencing result of the analyzed CpG residues are shown.

(A) Dark black boxes denote exons, lines between them denote introns, red and grey lollipops denote CpG residues that are analyzed and not analyzed respectively. The CpG residues of CDR1 gene were analyzed in three regions, first two in the promoter, and the last one in the first exon. (B) The bisulphite sequencing results were shown in circle designation for normal healthy lung and colon tissues versus SKLC-17 lung cancer cell line and HCT116, SW620, LoVo colon cancer cell lines. The degree of methylation was revealed with the darkness of the circle.

Table 3.2.3 2: The methylation status of *CDR1* promoter in analyzed normal tissues and cancer cell lines shown as percent methylation

<u>% METHYLATION</u>	<u>CDR1.1</u>	<u>CDR1.2</u>	<u>CDR1.3</u>
<i>NORMAL LUNG</i>	97.20%	100.00%	93.30%
SK-LC-17	0.00%	40.00%	0.00%

<u>% METHYLATION</u>	<u>CDR1.1</u>	<u>CDR1.2</u>	<u>CDR1.3</u>
<i>NORMAL COLON_MALE</i>	90.91%	97.92%	82.05%
<i>NORMAL COLON_FEMALE</i>	48.72%	42.22%	31.11%
HCT116	66.67%	66.67%	16.67%
LOVO	20.00%	29.17%	23.33%
SW620	0.00%	6.06%	2.56%

3.2.4 The response of CT proximal genes; *ALAS2*, *CDR1* and CT genes; *PAGE-2,-2B*, *SPANX-B* to 5-aza-2'-deoxycytidine treatment in cancer cell lines:

To have a complete understanding in epigenetic mechanisms resulting up-regulation of CT gene expression and down-regulation of CT proximal gene expression in cancer, we treated cancer cell lines with DNMTi, 5-aza-2'-deoxycytidine, for 72 hours. As seen in Figure 3.2.4 1; upon 5-aza-2'-deoxycytidine treatment, *PAGE-2,-2B* and *SPANX-B* genes were up-regulated in significant amounts compared to untreated controls in HCT116 and SK-LC-17 cell lines. On the other hand, the expressions of *ALAS2* and *CDR1* genes did not differ in any of the analyzed cell lines.

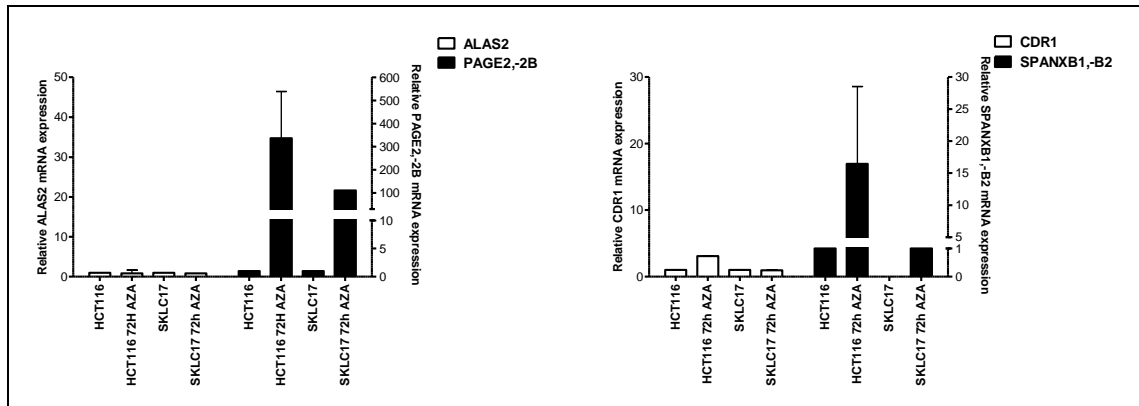


Figure 3.2.4 1: The response of CT genes and CT proximal genes to 5-aza-2'-deoxycytidine treatment is showed by q RT-PCR.

PAGE-2,-2B and *SPANX-B* genes were induced by 5-aza-2'-deoxycytidine treatment in cancer cell lines whereas *ALAS2* and *CDR1* did not respond 5-aza-2'-deoxycytidine treatment.

3.2.5 The promoter proximal DNA hydroxymethylation of *ALAS2* and *CDR1* genes in normal tissues, colon and lung cancer cell lines:

The bisulphite sequencing results were unable to clarify the difference in epigenetic basis of expression of CT and CT proximal genes in healthy versus cancerous condition, so we searched for other DNA modifications having effect on gene expression. 5hmC, a newly identified epigenetic mark on DNA, might be identified as methylated CpG in bisulphite sequencing experiment. Although the hypomethylated promoters of cancer cell lines could not be explained with this new residue, we believed the identified hypermethylated promoters in normal tissues having *ALAS2* and *CDR1* expression might contain 5hmC instead of 5mC. To detect 5hmC residue on the promoters, we performed q RT-PCR following hydroxymethylated DNA immunoprecipitation specific to the analyzed region in bisulphite experiment. PCR primers for *ALAS2* gene hit 3rd region and for *CDR1* gene hit 2nd region. As predicted, normal lung and colon tissues had high amount of 5hmC containing DNA compared to cancer cell lines. Interestingly, when the promoters of CT genes were examined for 5hmC residue, cancer cell lines had higher amounts of 5hmC compared to normal tissues (Figure 3.2.5 1).

Even though, DNA methylation was insufficient to explain the gene expression pattern of *ALAS2* and *CDR1*, CT proximal gene expression in normal tissues and CT expression in cancer cell lines might be described with the abundance of 5hmC residue on promoter proximal regions.

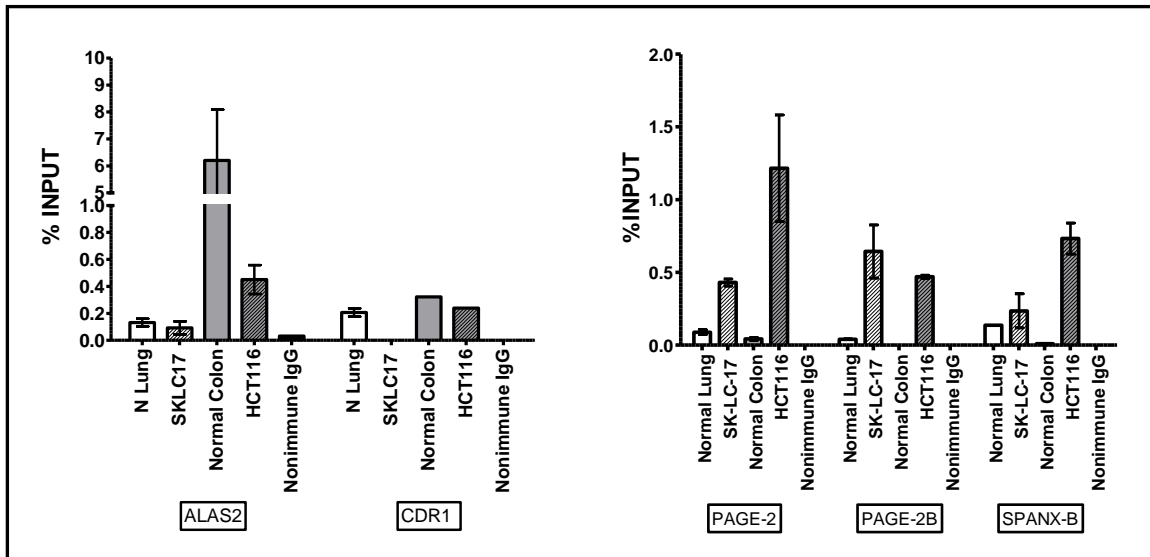


Figure 3.2.5 1: The amount hydroxymethylated DNA in the promoter proximal regions of CT genes and CT-proximal genes are shown.

The genomic DNAs were sonicated and immunoprecipitated with α -5hmC antibody. The immunoprecipitated DNA was amplified by the primers spanning the promoters of CT and CT proximal genes by SYBR based q RT-PCR. Preimmune serum was used as the negative control in the experiment. q RT-PCR result was analyzed by percent input method. The immunoprecipitated DNA amount was high in normal tissues for CT proximal genes and in cancer cell lines for CT genes in consistency with the expression patterns.

3.2.6 The gene expression of *TET* enzymes in normal tissues and colon and lung cancer cell lines:

Hydroxymethylated DNA immunoprecipitation results showed that the hydroxymethylation was gene specific event since we detected hydroxymethylated DNA at different abundance in the same sample for different genes. Even though this observation, we wondered the expressions of *TET*, 5hmC generating, enzymes. For colon cancer cell lines, *TET* enzymes were down-regulated according to normal colon tissue except *TET1* enzyme in SW620 cell line. For lung cancer cell lines, all enzymes

were up-regulated in SK-LC-17 (Figure 3.2.6 1). Thus we concluded that instead of *TET* enzymes` expression levels, the position of hydroxymethylcytosine residue was relevant with the gene expression.

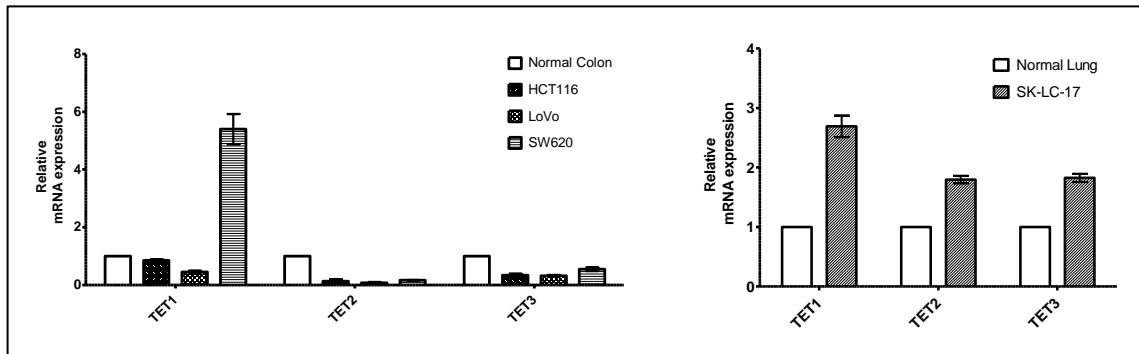


Figure 3.2.6 1: The mRNA levels of *TET* genes (*TET1*, *TET2*, *TET3*) in colon cancer and lung cancer cell lines with respect to normal counterparts.

The relative mRNA expressions of three *TET* enzymes were shown by SYBR based q RT-PCR. *GAPDH* gene was used as endogenous control.

3.2.7 The result of ectopic expressions of *ALAS2* and *CDR1* genes in cancer cell lines in cell viability manner:

Previously we showed that *ALAS2* and *CDR1* genes were notably down regulated in cancer. Due to the apparent down-regulation in cancer, we asked whether these genes had tumor suppressor abilities. To answer this question, we ectopically expressed these genes by using tetracycline (Tet) inducible expression system in HCT116 and SK-LC-17 cell lines. Before transfection experiments, we generated Tet repressor expressing stable clones and selected the clones expressing Tet repressor in highest amount and continued our experiments with them (Figure 3.2.7 1). After transient transfection, we verified that *ALAS2* gene was overexpressed in tetracycline induced clones, as shown in Figure 3.2.7 2. We could not eliminate the leaky expression in non-induced cells although we used tetracycline reduced serum for this experiment. We conducted MTT cell viability experiment after transient transfection in clones either transfected with *ALAS2* or *CDR1* transgenes or with empty vector both in the presence or absence tetracycline. In results of ectopic expression of *ALAS2* and *CDR1* genes, no significant difference in cell viability compared to control cells transfected with empty vector was observed, as seen in Figure 3.2.7 3.

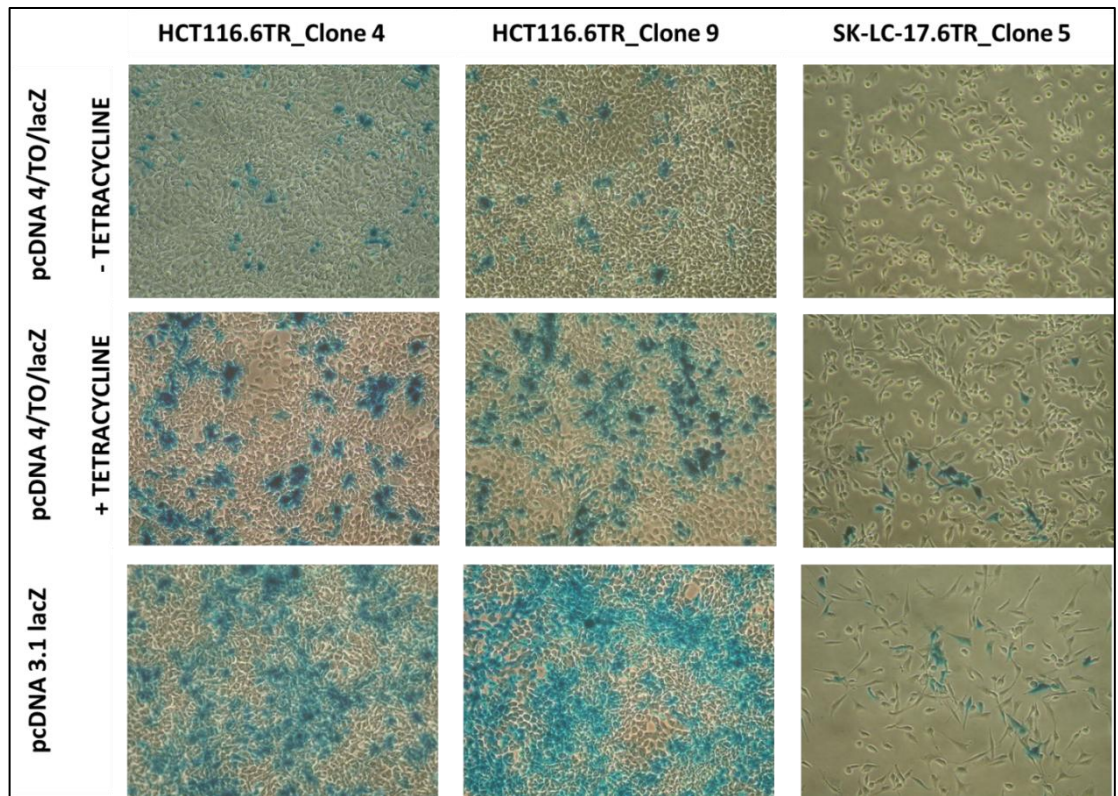


Figure 3.2.7 1: 3 candidate clones are identified as a result of β -Galactosidase staining experiment performed after pcDNA4/TO/lacZ transfection to stable clones expressing Tet repressor.

pcDNA3.1lacZ was used as positive control to determine transfection efficiency.

Although the leaky expression was seen in the absence of tetracycline,

HCT116.6TR_Clone4, HCT116.6TR_Clone9 and SKLC17.6TR_Clone5 were the three clones having the highest induction of lacZ gene with tetracycline addition.

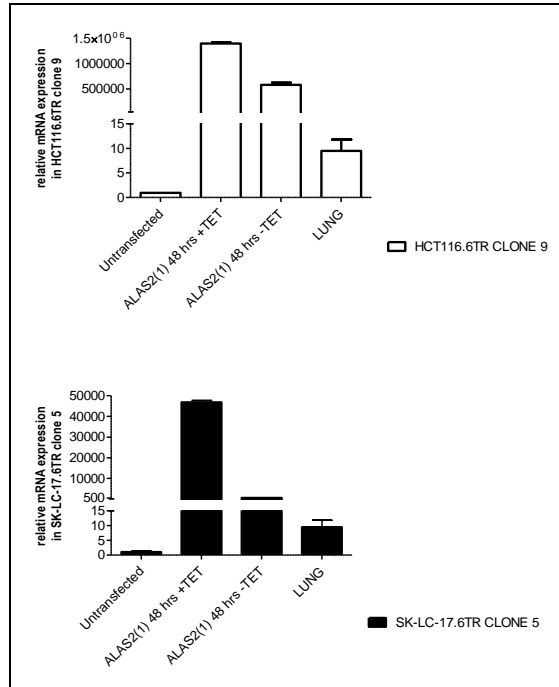


Figure 3.2.7 2: *ALAS2* gene expression in tetracycline treated clones compared to untreated and untransfected clones.

ALAS2 gene was cloned in pcDNA/4TO vector. The transfection was performed to two stable clones expressing tet repressor via Mirus TransIT-LT1 transfection reagent transiently. The transfection efficiency in this experiment is 45% for HCT116.6TR clone 9 and 13% for SK-LC-17.6TR clone 5. Although the leaky expression existed in the absence of tetracycline, the induction of *ALAS2* was evident with the addition of tetracycline. *ALAS2* expression was much more than the physiological levels.

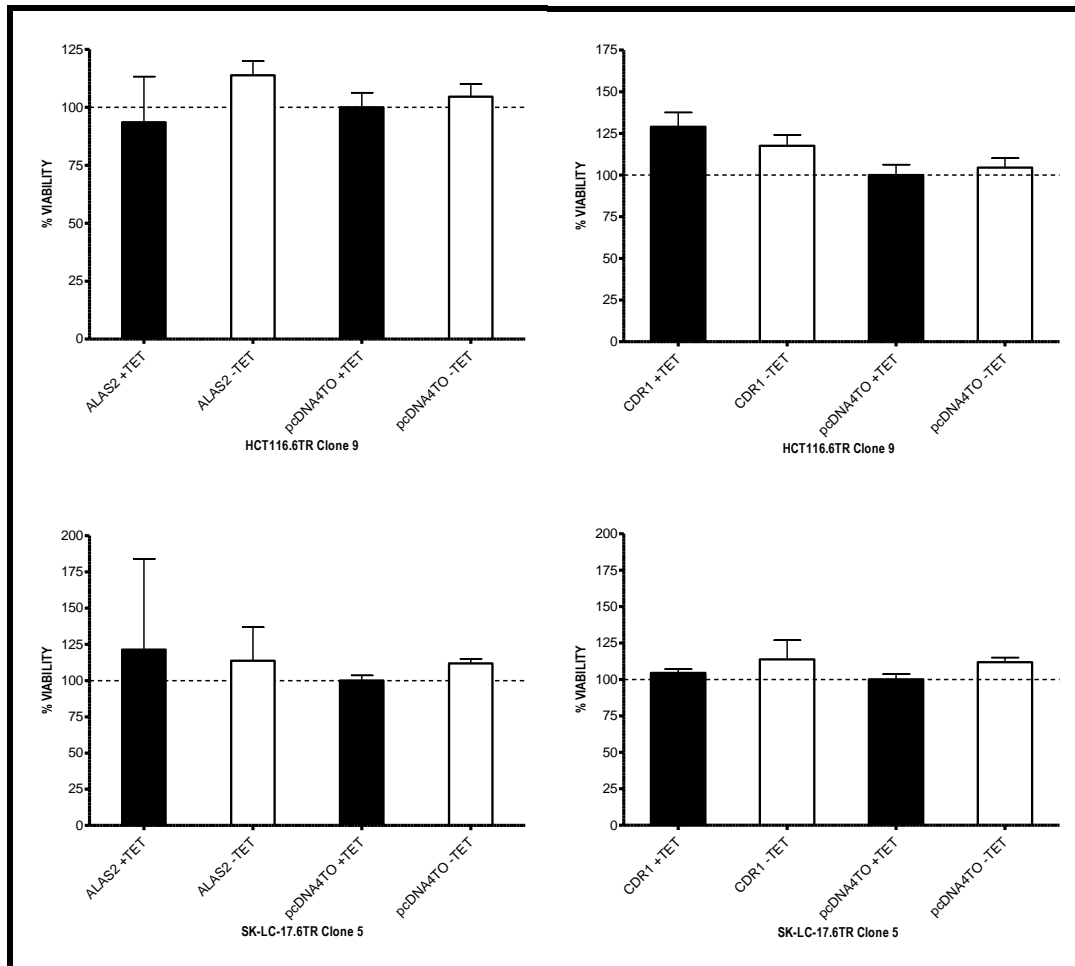


Figure 3.2.7 3: The cell viability results are measured by MTT assay after ectopic expression of *ALAS2* and *CDR1* gene.

ALAS2 and *CDR1* genes were cloned in pcDNA/4TO vector. The transfections were performed to two stable clones expressing tet repressor via Mirus TransIT-LT1 transfection reagent transiently. With the addition of tetracycline and the induction of transgenes, the cell viability values did not change.

3.2.8 *ALAS2* and *CDR1* expression in Caco-2 spontaneous differentiation model

Previously, we showed that *PAGE-2,-2B* and *SPANX-B* genes were dynamically expressed in Caco-2 spontaneous differentiation. Since we analyzed CT proximal gene expression (*ALAS2* and *CDR1*) in association with CT gene expression (*PAGE-2,-2B* and *SPANX-B*) in cancer cell lines, we examined *ALAS2* and *CDR1* gene expression in Caco-2 spontaneous model as well. We determined that in addition to the up-regulation of CT genes, proximal genes were also up-regulated in the model contrary to the situation in cancer cell lines. We speculated that Caco-2 spontaneous differentiation

model established a window of MET where both CT and CT proximal genes were simultaneously expressed.

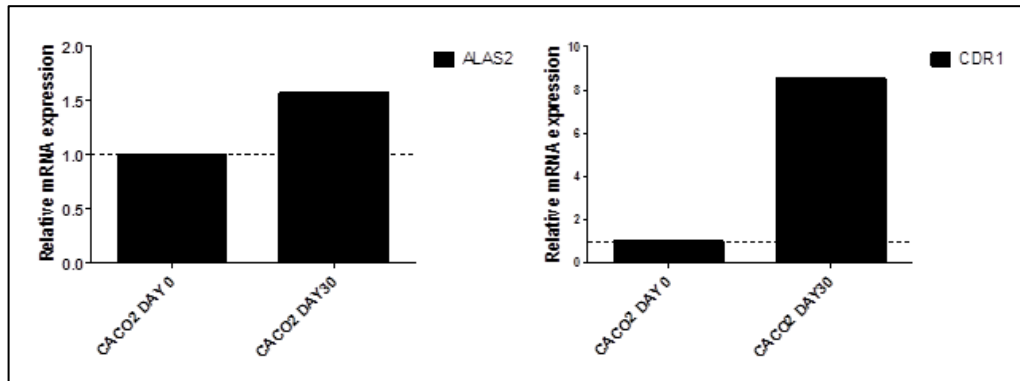


Figure 3.2.8 1: *ALAS2* and *CDR1* gene expression in Caco-2 spontaneous differentiation

3.3 GENE EXPRESSION INSIDE AND OUTSIDE OF A CANCER TESTIS GENE-CONTAINING REPEAT REGION

3.3.1 Uncoordinated expression of *NY-ESO-1*, *IκBG* and the noncoding RNAs in *NY-ESO-1* containing repeat region:

To test whether the repeat regions that were composed of CT genes were boundaries of region specific epigenetic mechanisms and forming a 3 dimensional loop structure to control coordinate CT gene expression, we focused on *NY-ESO-1* containing repeat region. We chose *NY-ESO-1* region due to the simplicity of the region. In addition to *IκBG* and *NY-ESO-1* genes, we identified various noncoding RNAs coded within the repeat region and one noncoding RNA coded outside the repeat region (Figure 3.3.1 1). By analyzing expressions of genes within the repeat region and outside the repeat region, a similar expression pattern of noncoding RNAs with *NY-ESO-1* expressions was investigated. For q RT-PCR experiments, in addition to *NY-ESO-1* positive (Mahlavu, SK-LC-17 and MDA-MB157) and negative cell lines (HCT116, SW20 and MCF-7), 5-aza-2'-deoxycytidine treated *NY-ESO-1* negative cell lines were used. No significant difference in noncoding RNA expression between *NY-ESO-1* positive and negative cell lines was observed. The only gene induced with 5-aza-2'-deoxycytidine was *NY-ESO-1* in the repeat region (Figure 3.3.1 2). Thus, we concluded that there was not a clear association in gene expression within the repeat region. *NY-ESO-1* was controlled in an exclusive manner according to DNA methylation. This information led us to think that the proposed 3 dimensional structure formed by repeat regions may not be critical as an epigenetic regulation mechanism in CT gene expression.

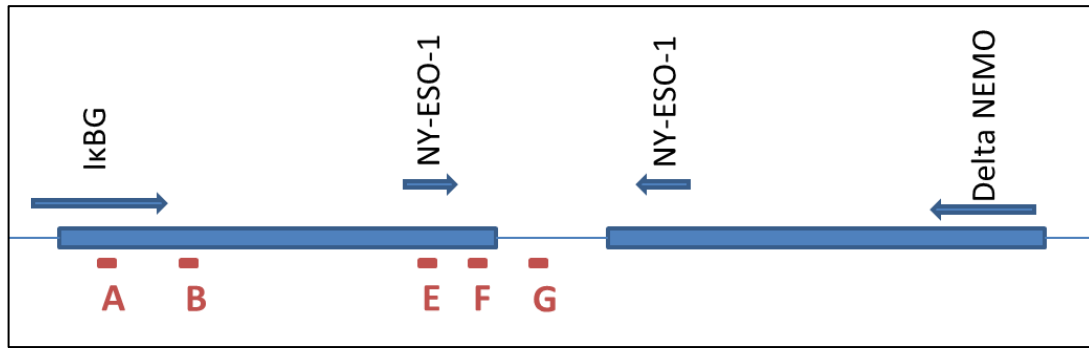


Figure 3.3.1 1: The localization of primers hitting *IκBG*, *NY-ESO-1* and 3 noncoding RNA genes in *NY-ESO-1* repeat region.

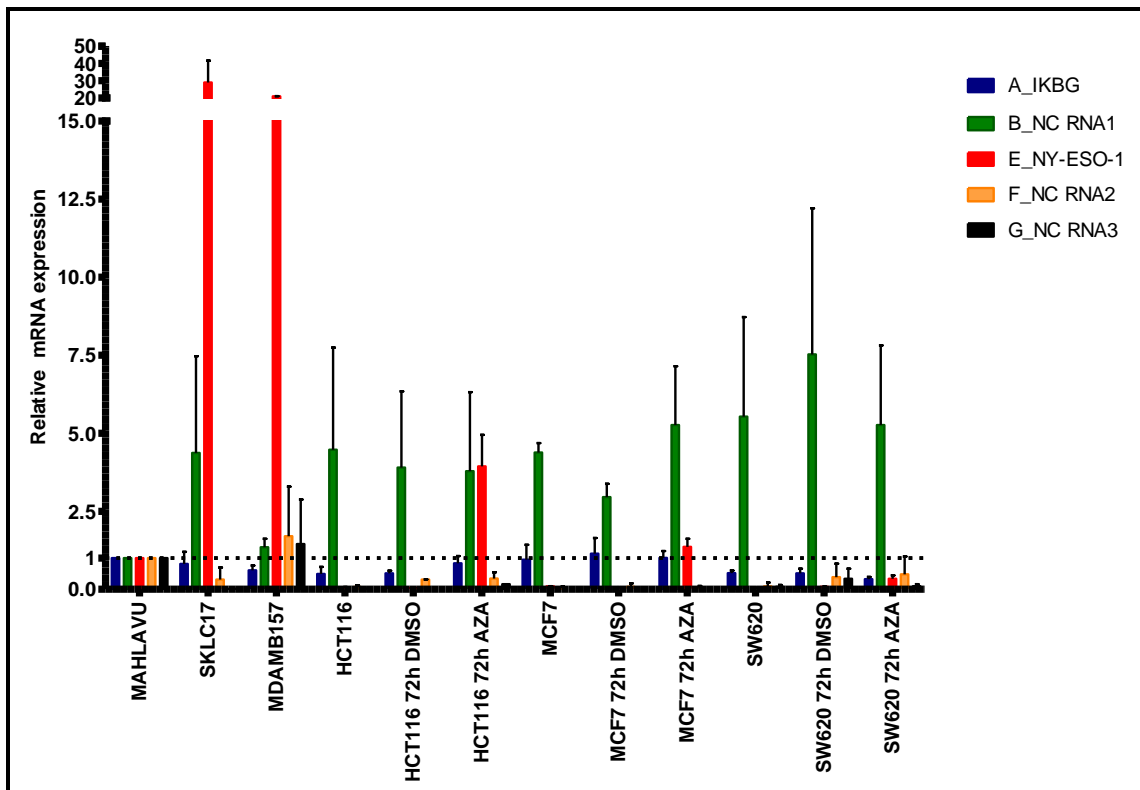


Figure 3.3.1 2: The expressions of noncoding RNAs in repeat region, *IκBG* and *NY-ESO-1* in *NY-ESO-1* positive (Mahlavu, SK-LC-17 and MDA-MB157) and negative cell lines (HCT116, SW20 and MCF-7) are analyzed by q RT-PCR.

The expression of genes within the repeat region did not correlate with *NY-ESO-1* expression. 5-aza-2-deoxycytidine treatment of *NY-ESO-1* negative cell lines induced only *NY-ESO-1* in repeat region.

4 DISCUSSION AND CONCLUSION

In our Caco-2 spontaneous differentiation model, we detected dynamic and reversible expressions of 3 CT genes (*PAGE-2,-2B* and *SPANX-B*). Up to now, the only mechanism to induce CT gene expression was treating the cells with either DNA hypomethylating agents or histone deacetylase inhibitors. For the first time, we showed the induction of 3 CT genes in a differentiation model without treatment. Expression levels of *PAGE-2,-2B* and *SPANX-B* were far beyond the expression levels in colorectal cancer tumors (unpublished data). The overexpression of CT genes in various tumors is aimed in order use them in immunotherapeutic approaches in cancer treatments for many years [5]. Because of CT immunotherapy attempts, the induction of these CT genes without chemical treatment might be critical, if an in vivo process mimicking this differentiation can be generated. The reason of detecting CT genes among the rest of the other CT genes might be the existence of basal expressions of *PAGE-2,-2B* and *SPANX-B* genes at the beginning of differentiation. Also, *SPANX-B* gene was previously characterized as being expressed in later stages of spermatogenesis such as late spermatids and spermatozoa whereas many other CT genes were detected in spermatogonia or primary spermatocytes [8]. Although the expression patterns of *PAGE-2,-2B* genes were not considered in that study, we believe that *PAGE-2,-2B* may differ from the other CT genes according to gene expression pattern in the light of our existing data.

We showed and verified that Caco-2 spontaneous differentiation model was a mesenchymal to epithelial model where the mesenchymal cancer cells differentiated and resembled to normal intestinal epithelial cells. Our result supported previously performed micro array studies [41,64,71].

CT gene expression in relation to either mesenchymal or epithelial phenotype of the cell is a controversial issue for the literature. Some studies claim that CT gene expression mainly associates with the mesenchymal and migratory phenotype of the cells [26,28,29,72-75]. The information comes from the analysis of CT gene expression in cancer stem cells and either knockdown or overexpression studies of CT genes. On

the other hand various studies argue as CT gene expression being a part of epithelial phenotype of the cells [35,36,76,77]. In the study conducted by Gupta et al., the gene expression in transformed HMLE in response of either salinomycin (shown to be effective on mesenchymal type of cells in tumor) or paclitaxel (shown to be effective on epithelial type of cells in tumor) was analyzed. *MAGE-A1* gene was up-regulated in salinomycin treatment which eliminated the mesenchymal cells and down-regulated in paclitaxel treatment which eliminated the epithelial cells [35]. Similarly, the result of another study done by Thomson et al. claimed that CT (*SPANXA1,-A2, SPANX-B1,-B2, SPANXC, MAGEA8*) gene expression was diminished in two EMT models generated by stable transfection of Snail gene and TGF- β exposure [36]. In addition to up-regulation of *MAGE-A1* gene in epithelial enriched population and down-regulation of various CT genes in two important EMT models, CT gene expression identified in our MET model proved that CT gene expression might be related with epithelial phenotype during the EMT process.

Although promoter DNA hypomethylation is a well-established epigenetic event leading expressions of most CT genes, we could not identified difference in DNA demethylation in promoter proximal regions of analyzed 3 CT genes. We knew from our previous data, DNA hypomethylating agent and histone deacetylase inhibitor treatments resulted with the induction of various CT genes not only *PAGE-2,-2B* and *SPANX-B* in many cancer cell lines as well as in Caco-2 cells. The observed over-expression of *PAGE-2,-2B* and *SPANX-B* genes in the model had to be somewhat different than simple DNA hypomethylation or histone modification in that manner.

When we analyzed CT promoter proximal regions for DNA hydroxymethylation, not only we observed that the highly methylated promoter proximal DNA was in fact hydroxymethylated since we immunoprecipitated it, but also we showed hydroxymethylation levels for the promoters of *PAGE-2* and *SPANX-B* genes increased at day 10 after the differentiation started. For the first time, we identified hydroxymethylation as a new epigenetic mechanism in CT gene expression in addition to DNA hypomethylation and histone modifications. Effect of 5hmC containing DNA on gene expression was shown in previous studies [43,69] . 5hmC can be converted

further to 5-formylcytosine (5-fC) and 5-carboxycytosine (5-caC) and both residues are recognized as unmethylated cytosine in bisulphite sequencing [56]. Therefore, we are sure that 5hmC that we detected is not DNA demethylation intermediate or any other residues. Related with the increase in 5hmC levels on the promoter proximal regions, we also detected an increase in mRNA levels of *TET* enzymes that generate 5hmC residues from existing 5mC residues. Interestingly, there was a clear co-localization of TET2 protein with CT proteins in the heterogeneous Caco-2 cell population during differentiation. Studies trying to map 5hmC residue in the genome suggested that 5hmC mainly localized at euchromatin, at gene bodies of actively transcribed genes and promoters of polycomb repressed development related genes in pluripotent stem cells showing the function of 5hmC on gene expression [43,78]. 5hmC residue was detected in various differentiated human tissues and its levels were diminished in cancerous tissues [51,52]. Those results claimed that 5hmC not only have an effect on gene expression in pluripotent stem cells but also in somatic tissues and in carcinogenesis. The association of CT gene expression to 5hmC occupancy on promoter proximal regions of CT genes was in concordance with the literature in this manner. Decrease in 5hmC levels and reduction in expression of *TET* enzymes in cancer tissues compared to normal counterparts supported our data while cancer like Caco-2 cells were resembling to normal epithelial cells during differentiation [52]. Previously, role of TET2 and 5hmC residue on CpG dense region of HOXA cluster was shown in retinoic acid induced NTERA2 D1 differentiation. They not only showed activation of HOXA cluster with 5hmC enrichment on the region upon differentiation but also established the important function of TET2 on HOXA activation by using siRNA mediated depletion of *TET2* and *TET2* knockout mouse model. [69] Here in our Caco-2 spontaneous differentiation model, we showed the expression of CT genes with respect to 5hmC abundance on the promoter proximal regions and the clear colocalization of TET2 protein with CT proteins in CT expressing cells in a similar way. Vitamin C supplementation to ESCs also resulted with TET activity, an increase in the level hmC on DNA and activation of germline genes. Those observations were also very consistent with our results [79].

For the first time, we claimed that the presence of a short form of TET2 protein. This small peptide was recognized with Abcam (ab94580) antibody but not Active motif

(61389) antibody. Abcam antibody was generated by using 18aa long peptide inside 1-50 aa length region of TET2. Active motif antibody was generated against a recombinant peptide corresponding to 1-300 aa of the full length peptide. We concluded that somehow active motif antibody was recognizing TET2 protein between 50-300 aa and the identified short form was not recognized because of this reason. Our results stated that the truncated form of TET2 might be generated with Ca^{+2} dependent calpains and was even functional, though previously performed data argued that calpain mediated cleavage generated protein turnover instead of a truncated functional form of TET proteins [80]. To be certain about calpain cleavage, additional specific calpain inhibitors can be used in further experiments. Transfection experiments can be performed with tag containing TET2 vectors (such as HA-TET2 or Flag-TET2) and the cleaved TET2 products can be analyzed with anti-tag antibodies. In addition to calpain cleavage, it might be possible that the identified short form of TET2 product might be a newly identified alternative spliced form. Since the short form is recognized with Abcam antibody, first 50 aa coding region can be cloned and transfection experiments can be performed to understand whether it is an alternative spliced form.

In a study to show the DNA methylation events taking place in mouse neuronal differentiation, increase in 5hmC levels was together with loss of H3K27me3 and EZH2. For the first time the epigenetic connection between 5hmC with histone marks and polycomb proteins was established [60]. We also showed in a similar way, increase in 5hmC and gene expression levels were accompanied by decrease in EZH2 and H3K27me3 occupancies on the promoters of CT genes.

We looked into two different regions both containing a CT gene and a proximal non-CT gene which have differential gene expression in healthy and cancerous situations. Though they have different expression pattern, we identified that CT genes were controlled with DNA methylation whereas the proximal genes were not. Moreover the significant down-regulation of CT proximal genes in cancer was independent from promoter DNA methylation. From the literature, there were many examples that the gene expression may not associate with the DNA methylation status of the gene [81-83].

Since we identified that *ALAS2* and *CDRI* mRNA expressions existed in normal healthy colon and lung tissues, it is remarkable that promoters of 2 CT proximal gene were highly methylated in these tissues. Recently a new epigenetic mark, 5-hydroxymethylcytosine (5hmC) was discovered (Kriaucionis and Heintz 2009; Tahiliani, Koh et al. 2009). 5hmC not only performs in DNA demethylation process but also is accepted as a unique epigenetic mark since it has its unique distribution pattern in the genome, inhibits the binding of 5mC binding proteins to DNA and has its own binding proteins (Shen and Zhang 2013). Because bisulphite sequencing method is insufficient to discriminate 5hmC from 5mC, we suggested that the identified methylated cytosines might be hydroxymethylated indeed. The results of hydroxymethylated DNA immunoprecipitation showed that promoters of *ALAS2* and *CDRI* had higher 5hmC contents compared to cancer cell lines. Though 5hmC presence was shown in healthy human tissues [51], for the first time we claimed that the gene expression was related with DNA hydroxymethylation in colon and lung tissues. The abundance of hydroxymethylated CT promoter proximal DNA in cancer cell lines and hydroxymethylated DNA of CT proximal genes in normal tissues stated that the function of TET enzymes was position specific. The expressions of *TET* enzymes justified this fact. Locus specific role of TET enzymes were shown previously in concordance with our data [84].

To identify whether the highly homologous repeat regions covering CT genes have a role in concordant CT gene expression by forming a loop structure, we analyzed the gene expression in NY-ESO-1 repeat region. We included noncoding RNAs in the region in addition to protein coding genes *IκBG* and *NY-ESO-1* and to showed gene expression pattern inside and outside the repeat region was not coordinate. Even though Bredenbeck and her colleagues established the coordinate CT gene expression in MAGEA containing repeat [10], we believe the analysis of noncoding RNAs and genes other than CTs might be responsible from discrepancy between two studies. Other repeat regions coding CT genes might be further investigated with a similar approach. In case of identification of a coordinate gene expression in repeat regions, additional experiments such as chromosome conformation capture can be performed to show the 3 dimensional structure affecting the gene expression.

Finally, with the help of Caco-2 spontaneous differentiation model, we identified a window during EMT process and showed the dynamic expression of *PAGE-2*, *-2B* and *SPANX-B* genes by explaining the epigenetic mechanism behind it. (Figure 4 1).

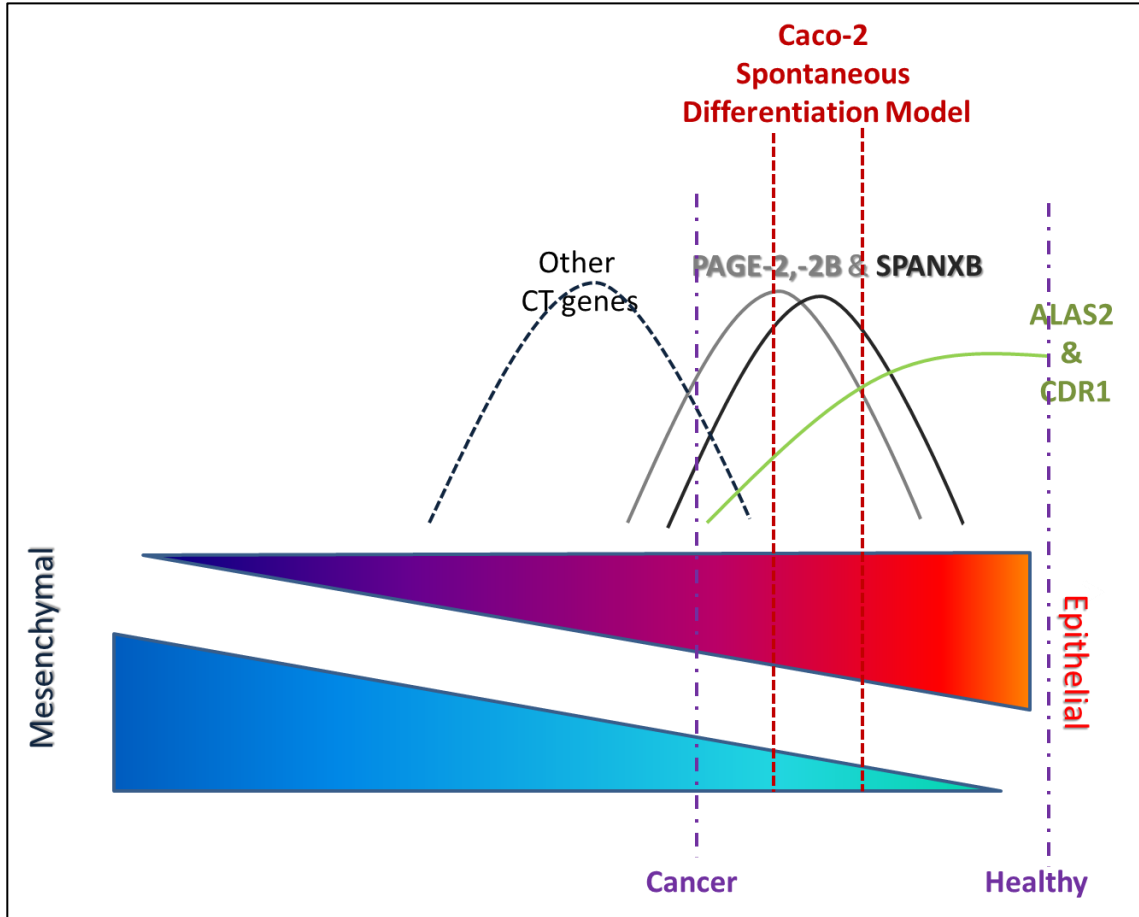


Figure 4 1: The proposed window of EMT and the suggested expression patterns of CT genes in EMT.

5 FUTURE PERSPECTIVES

The detection of 5hmC in CT promoters and the association of hydroxymethylation with CT gene expression created new era for CT epigenetics. The information in relation to epigenetic of CT genes should be revised in this manner.

Since the dynamic and reversible expression identified in the model was important for CT immunotherapy field, it is essential to mimic this differentiation in vivo as well. As an alternative approach, other hydroxymethylation agents such as Vitamin C or any differentiation agents could be analyzed to find out the induction of CT genes.

Following functional studies about the truncated form of TET2 in order to identify the mechanism that it act or find out whether there are any other examples of this truncated form, is a necessity.

Performing analysis about miR-22 and miR-200 during Caco-2 spontaneous differentiation would be an interesting expansion of the project because the associations of EMT with miR-22, miR-200 and TET proteins were recently shown [85]

In a very recent study colorectal cancer was classified in different subtypes representing to where the tumors belong in crypt villus axis and their responses to specific chemotherapeutic agents [86]. In parallel to this approach, Caco-2 differentiation can be analyzed to find out whether this differentiation window matches with this classification. In addition to that, CT expression as a biomarker in different subtypes of colon cancer can also be investigated.

6 REFERENCES

1. Scanlan MJ, Gure AO, Jungbluth AA, Old LJ, Chen YT (2002) Cancer/testis antigens: an expanding family of targets for cancer immunotherapy. *Immunological Reviews* 188: 22-32.
2. Vanderbruggen P, Traversari C, Chomez P, Lurquin C, Deplaen E, et al. (1991) A Gene Encoding an Antigen Recognized by Cytolytic Lymphocytes-T on a Human-Melanoma. *Science* 254: 1643-1647.
3. Sahin U, Tureci O, Pfreundschuh M (1997) Serological identification of human tumor antigens. *Current Opinion in Immunology* 9: 709-716.
4. Fratta E, Coral S, Covre A, Parisi G, Colizzi F, et al. (2011) The biology of cancer testis antigens: Putative function, regulation and therapeutic potential. *Molecular Oncology* 5: 164-182.
5. Caballero OL, Chen YT (2009) Cancer/testis (CT) antigens: Potential targets for immunotherapy. *Cancer Science* 100: 2014-2021.
6. Hofmann O, Caballero OL, Stevenson BJ, Chen YT, Cohen T, et al. (2008) Genome-wide analysis of cancer/testis gene expression. *Proceedings of the National Academy of Sciences of the United States of America* 105: 20422-20427.
7. Gure AO, Chua R, Williamson B, Gonen M, Ferreira CA, et al. (2005) Cancer-testis genes are coordinately expressed and are markers of poor outcome in non-small cell lung cancer. *Clinical Cancer Research* 11: 8055-8062.
8. Chen YT, Chiu RT, Lee P, Beneck D, Jin BQ, et al. (2011) Chromosome X-encoded cancer/testis antigens show distinctive expression patterns in developing gonads and in testicular seminoma. *Human Reproduction* 26: 3232-3243.
9. Warburton PE, Giordano J, Cheung F, Gelfand Y, Benson G (2004) Inverted repeat structure of the human genome: The X-chromosome contains a preponderance of large, highly homologous inverted repeats that contain testes genes. *Genome Research* 14: 1861-1869.
10. Bredenbeck A, Hollstein VM, Trefzer U, Sterry W, Walden P, et al. (2008) Coordinated expression of clustered cancer/testis genes encoded in a large inverted repeat DNA structure. *Gene* 415: 68-73.

11. Fratta E, Coral S, Covre A, Parisi G, Colizzi F, et al. (2011) The biology of cancer testis antigens: putative function, regulation and therapeutic potential. *Mol Oncol* 5: 164-182.
12. De Smet C, Lorient A, Boon T (2004) Promoter-dependent mechanism leading to selective hypomethylation within the 5' region of gene MAGE-A1 in tumor cells. *Mol Cell Biol* 24: 4781-4790.
13. Lim JH, Kim SP, Gabrielson E, Park YB, Park JW, et al. (2005) Activation of human cancer/testis antigen gene, XAGE-1, in tumor cells is correlated with CpG island hypomethylation. *International Journal of Cancer* 116: 200-206.
14. Sigalotti L, Fratta E, Coral S, Tanzarella S, Danielli R, et al. (2004) Intratumor heterogeneity of cancer/testis antigens expression in human cutaneous melanoma is methylation-regulated and functionally reverted by 5-aza-2'-deoxycytidine. *Cancer Res* 64: 9167-9171.
15. Woloszynska-Read A, Mhaweche-Fauceglia P, Yu JH, Odunsi K, Karpf AR (2008) Intertumor and intratumor NY-ESO-1 expression heterogeneity is associated with promoter-specific and global DNA methylation status in ovarian cancer. *Clinical Cancer Research* 14: 3283-3290.
16. James SR, Cedeno CD, Sharma A, Zhang W, Mohler JL, et al. (2013) DNA methylation and nucleosome occupancy regulate the cancer germline antigen gene MAGEA11. *Epigenetics* 8: 849-863.
17. Wischnewski F, Pantel K, Schwarzenbach H (2006) Promoter demethylation and histone acetylation mediate gene expression of MAGE-A1,-A2,-A3, and-A12 in human cancer cells. *Molecular Cancer Research* 4: 339-349.
18. Sun F, Chan E, Wu Z, Yang X, Marquez VE, et al. (2009) Combinatorial pharmacologic approaches target EZH2-mediated gene repression in breast cancer cells. *Mol Cancer Ther* 8: 3191-3202.
19. Rao M, Chinnasamy N, Hong JA, Zhang Y, Zhang M, et al. (2011) Inhibition of histone lysine methylation enhances cancer-testis antigen expression in lung cancer cells: implications for adoptive immunotherapy of cancer. *Cancer Res* 71: 4192-4204.
20. Han H, Yang X, Pandiyan K, Liang G (2013) Synergistic re-activation of epigenetically silenced genes by combinatorial inhibition of DNMTs and LSD1 in cancer cells. *Plos One* 8: e75136.

21. Cannuyer J, Lorient A, Parvizi GK, De Smet C (2013) Epigenetic Hierarchy within the MAGEA1 Cancer-Germline Gene: Promoter DNA Methylation Dictates Local Histone Modifications. *Plos One* 8.
22. Hong JA, Kang Y, Abdullaev Z, Flanagan PT, Pack SD, et al. (2005) Reciprocal binding of CTCF and BORIS to the NY-ESO-1 promoter coincides with derepression of this cancer-testis gene in lung cancer cells. *Cancer Res* 65: 7763-7774.
23. Bhan S, Negi SS, Shao C, Glazer CA, Chuang A, et al. (2011) BORIS binding to the promoters of cancer testis antigens, MAGEA2, MAGEA3, and MAGEA4, is associated with their transcriptional activation in lung cancer. *Clinical Cancer Research* 17: 4267-4276.
24. Vatolin S, Abdullaev Z, Pack SD, Flanagan PT, Custer M, et al. (2005) Conditional expression of the CTCF-paralogous transcriptional factor BORIS in normal cells results in demethylation and derepression of MAGE-A1 and reactivation of other cancer-testis genes. *Cancer Res* 65: 7751-7762.
25. Woloszynska-Read A, James SR, Song C, Jin B, Odunsi K, et al. (2010) BORIS/CTCF expression is insufficient for cancer-germline antigen gene expression and DNA hypomethylation in ovarian cell lines. *Cancer Immunol* 10: 6.
26. Cronwright G, Le Blanc K, Gotherstrom C, Darcy P, Ehnman M, et al. (2005) Cancer/testis antigen expression in human mesenchymal stem cells: down-regulation of SSX impairs cell migration and matrix metalloproteinase 2 expression. *Cancer Res* 65: 2207-2215.
27. Costa FF, Le Blanc K, Brodin B (2007) Concise review: Cancer/testis antigens, stem cells, and cancer. *Stem Cells* 25: 707-711.
28. Sigalotti L, Covre A, Zabierowski S, Himes B, Colizzi F, et al. (2008) Cancer testis antigens in human melanoma stem cells: expression, distribution, and methylation status. *Journal of Cellular Physiology* 215: 287-291.
29. Gedye C, Quirk J, Browning J, Svobodova S, John T, et al. (2009) Cancer/testis antigens can be immunological targets in clonogenic CD133+ melanoma cells. *Cancer Immunol Immunother* 58: 1635-1646.
30. Yawata T, Nakai E, Park KC, Chihara T, Kumazawa A, et al. (2010) Enhanced Expression of Cancer Testis Antigen Genes in Glioma Stem Cells. *Molecular Carcinogenesis* 49: 532-544.
31. Cronwright G, Le Blanc K, Gotherstrom C, Darcy P, Ehnman M, et al. (2005) Cancer/testis antigen expression in human mesenchymal stem cells: Down-regulation of

SSX impairs cell migration and matrix metalloproteinase 2 expression. *Cancer Research* 65: 2207-2215.

32. Lifantseva N, Koltsova A, Krylova T, Yakovlena T, Poljanskaya G, et al. (2011) Expression patterns of cancer-testis antigens in human embryonic stem cells and their cell derivatives indicate lineage tracks. *Stem Cells International*.

33. Lorient A, Reister S, Parvizi GK, Lysy PA, De Smet C (2009) DNA Methylation-Associated Repression of Cancer-Germline Genes in Human Embryonic and Adult Stem Cells. *Stem Cells* 27: 822-824.

34. Mani SA, Guo W, Liao MJ, Eaton EN, Ayyanan A, et al. (2008) The epithelial-mesenchymal transition generates cells with properties of stem cells. *Cell* 133: 704-715.

35. Gupta PB, Onder TT, Jiang GZ, Tao K, Kuperwasser C, et al. (2009) Identification of Selective Inhibitors of Cancer Stem Cells by High-Throughput Screening. *Cell* 138: 645-659.

36. Thomson S, Petti F, Sujka-Kwok I, Mercado P, Bean J, et al. (2011) A systems view of epithelial-mesenchymal transition signaling states. *Clinical & Experimental Metastasis* 28: 137-155.

37. Rousset M (1986) THE HUMAN-COLON CARCINOMA CELL-LINES HT-29 AND CACO-2 - 2 INVITRO MODELS FOR THE STUDY OF INTESTINAL DIFFERENTIATION. *Biochimie* 68: 1035-1040.

38. Yeaman C, Grindstaff KK, Nelson WJ (1999) New perspectives on mechanisms involved in generating epithelial cell polarity. *Physiological Reviews* 79: 73-98.

39. Pinto M, Robineleon S, Appay MD, Kedinger M, Triadou N, et al. (1983) Enterocyte-Like Differentiation and Polarization of the Human-Colon Carcinoma Cell-Line Caco-2 in Culture. *Biology of the Cell* 47: 323-330.

40. Halbleib JM, Saaf AM, Brown PO, Nelson WJ (2007) Transcriptional modulation of genes encoding structural characteristics of differentiating Enterocytes during development of a polarized epithelium in vitro. *Molecular Biology of the Cell* 18: 4261-4278.

41. Saaf AM, Halbleib JM, Chen X, Yuen ST, Leung SY, et al. (2007) Parallels between global transcriptional programs of polarizing caco-2 intestinal epithelial cells in vitro and gene expression programs in normal colon and colon cancer. *Molecular Biology of the Cell* 18: 4245-4260.

42. Kriaucionis S, Heintz N (2009) The nuclear DNA base 5-hydroxymethylcytosine is present in Purkinje neurons and the brain. *Science* 324: 929-930.

43. Ficz G, Branco MR, Seisenberger S, Santos F, Krueger F, et al. (2011) Dynamic regulation of 5-hydroxymethylcytosine in mouse ES cells and during differentiation. *Nature* 473: 398-402.
44. Yildirim O, Li R, Hung JH, Chen PB, Dong X, et al. (2011) Mbd3/NURD complex regulates expression of 5-hydroxymethylcytosine marked genes in embryonic stem cells. *Cell* 147: 1498-1510.
45. Wu H, D'Alessio AC, Ito S, Wang Z, Cui K, et al. (2011) Genome-wide analysis of 5-hydroxymethylcytosine distribution reveals its dual function in transcriptional regulation in mouse embryonic stem cells. *Genes Dev* 25: 679-684.
46. Valinluck V, Tsai HH, Rogstad DK, Burdzy A, Bird A, et al. (2004) Oxidative damage to methyl-CpG sequences inhibits the binding of the methyl-CpG binding domain (MBD) of methyl-CpG binding protein 2 (MeCP2). *Nucleic Acids Res* 32: 4100-4108.
47. Xu Y, Wu F, Tan L, Kong L, Xiong L, et al. (2011) Genome-wide regulation of 5hmC, 5mC, and gene expression by Tet1 hydroxylase in mouse embryonic stem cells. *Mol Cell* 42: 451-464.
48. Choi I, Kim R, Lim HW, Kaestner KH, Won KJ (2014) 5-hydroxymethylcytosine represses the activity of enhancers in embryonic stem cells: a new epigenetic signature for gene regulation. *BMC Genomics* 15: 670.
49. Tahiliani M, Koh KP, Shen Y, Pastor WA, Bandukwala H, et al. (2009) Conversion of 5-methylcytosine to 5-hydroxymethylcytosine in mammalian DNA by MLL partner TET1. *Science* 324: 930-935.
50. Pastor WA, Aravind L, Rao A (2013) TETonic shift: biological roles of TET proteins in DNA demethylation and transcription. *Nat Rev Mol Cell Biol* 14: 341-356.
51. Li W, Liu M (2011) Distribution of 5-hydroxymethylcytosine in different human tissues. *J Nucleic Acids* 2011: 870726.
52. Yang H, Liu Y, Bai F, Zhang JY, Ma SH, et al. (2013) Tumor development is associated with decrease of TET gene expression and 5-methylcytosine hydroxylation. *Oncogene* 32: 663-669.
53. Cimmino L, Abdel-Wahab O, Levine RL, Aifantis I (2011) TET family proteins and their role in stem cell differentiation and transformation. *Cell Stem Cell* 9: 193-204.
54. Valinluck V, Sowers LC (2007) Endogenous cytosine damage products alter the site selectivity of human DNA maintenance methyltransferase DNMT1. *Cancer Res* 67: 946-950.

55. Hackett JA, Zyllicz JJ, Surani MA (2012) Parallel mechanisms of epigenetic reprogramming in the germline. *Trends Genet* 28: 164-174.
56. Shen L, Zhang Y (2013) 5-Hydroxymethylcytosine: generation, fate, and genomic distribution. *Curr Opin Cell Biol* 25: 289-296.
57. Piccolo FM, Bagci H, Brown KE, Landeira D, Soza-Ried J, et al. (2013) Different roles for Tet1 and Tet2 proteins in reprogramming-mediated erasure of imprints induced by EGC fusion. *Mol Cell* 49: 1023-1033.
58. Huang Y, Chavez L, Chang X, Wang X, Pastor WA, et al. (2014) Distinct roles of the methylcytosine oxidases Tet1 and Tet2 in mouse embryonic stem cells. *Proc Natl Acad Sci U S A* 111: 1361-1366.
59. Dawlaty MM, Breiling A, Le T, Raddatz G, Barrasa MI, et al. (2013) Combined deficiency of Tet1 and Tet2 causes epigenetic abnormalities but is compatible with postnatal development. *Dev Cell* 24: 310-323.
60. Hahn MA, Qiu R, Wu X, Li AX, Zhang H, et al. (2013) Dynamics of 5-hydroxymethylcytosine and chromatin marks in Mammalian neurogenesis. *Cell Rep* 3: 291-300.
61. Chen Q, Chen YB, Bian CJ, Fujiki R, Yu XC (2013) TET2 promotes histone O-GlcNAcylation during gene transcription. *Nature* 493: 561-+.
62. Deplus R, Delatte B, Schwinn MK, Defrance M, Mendez J, et al. (2013) TET2 and TET3 regulate GlcNAcylation and H3K4 methylation through OGT and SET1/COMPASS. *EMBO J* 32: 645-655.
63. Zhang Q, Liu X, Gao W, Li P, Hou J, et al. (2014) Differential regulation of the ten-eleven translocation (TET) family of dioxygenases by O-linked beta-N-acetylglucosamine transferase (OGT). *J Biol Chem* 289: 5986-5996.
64. Fleet JC, Wang L, Vitek O, Craig BA, Edenberg HJ (2003) Gene expression profiling of Caco-2 BBe cells suggests a role for specific signaling pathways during intestinal differentiation. *Physiol Genomics* 13: 57-68.
65. Simon-Assman P, Turck N, Sidhoum-Jenny M, Gradwohl G, Kedinger M (2007) In vitro models of intestinal epithelial cell differentiation. *Cell Biology and Toxicology* 23: 241-256.
66. Loboda A, Nebozhyn MV, Watters JW, Buser CA, Shaw PM, et al. (2011) EMT is the dominant program in human colon cancer. *Bmc Medical Genomics* 4.

67. Wang ZQ, Zhang J, Zhang YN, Lim SH (2006) SPAN-Xb expression in myeloma cells is dependent on promoter hypomethylation and can be upregulated pharmacologically. *International Journal of Cancer* 118: 1436-1444.
68. Wang ZQ, Zhang J, Zhang Y, Srivenugopal K, Lim SH (2006) SPAN-XB core promoter sequence is regulated in myeloma cells by specific CpG dinucleotides associated with MeCP2 protein. *Blood* 108: 628a-628a.
69. Bocker MT, Tuorto F, Raddatz G, Musch T, Yang FC, et al. (2012) Hydroxylation of 5-methylcytosine by TET2 maintains the active state of the mammalian HOXA cluster. *Nat Commun* 3: 818.
70. Zendman AJ, Zschocke J, van Kraats AA, de Wit NJ, Kurpisz M, et al. (2003) The human SPANX multigene family: genomic organization, alignment and expression in male germ cells and tumor cell lines. *Gene* 309: 125-133.
71. Tremblay E, Auclair J, Levy E, Menard D, Rivard N, et al. (2006) Gene expression profiles of normal proliferating and differentiating human intestinal epithelial cells: A comparison with the Caco-2 cell model. *Gastroenterology* 130: A539-A539.
72. Sigalotti L, Covre A, Nicolay HJM, Coral S, Maio M (2010) Cancer testis antigens and melanoma stem cells: new promises for therapeutic intervention. *Cancer Immunology Immunotherapy* 59: 487-488.
73. Curioni-Fontecedro A, Nuber N, Mihic-Probst D, Seifert B, Soldini D, et al. (2011) Expression of MAGE-C1/CT7 and MAGE-C2/CT10 Predicts Lymph Node Metastasis in Melanoma Patients. *Plos One* 6.
74. Chen L, Zhou WB, Zhao Y, Liu XA, Ding Q, et al. (2012) Cancer/testis antigen SSX2 enhances invasiveness in MCF-7 cells by repressing ERalpha signaling. *Int J Oncol* 40: 1986-1994.
75. Caballero OL, Cohen T, Gurung S, Chua R, Lee P, et al. (2013) Effects of CT-Xp Gene Knock down in Melanoma Cell Lines. *Oncotarget* 4: 531-541.
76. Wallden B, Emond M, Swift ME, Disis ML, Swisshelm K (2005) Antimetastatic gene expression profiles mediated by retinoic acid receptor beta 2 in MDA-MB-435 breast cancer cells. *Bmc Cancer* 5.
77. Hu Y, Xing J, Wang L, Huang M, Guo X, et al. (2011) RGS22, a novel cancer/testis antigen, inhibits epithelial cell invasion and metastasis. *Clin Exp Metastasis* 28: 541-549.

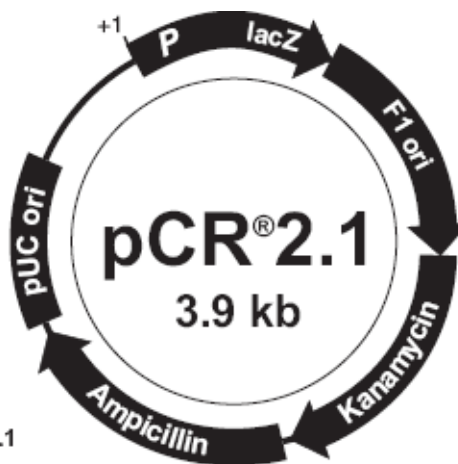
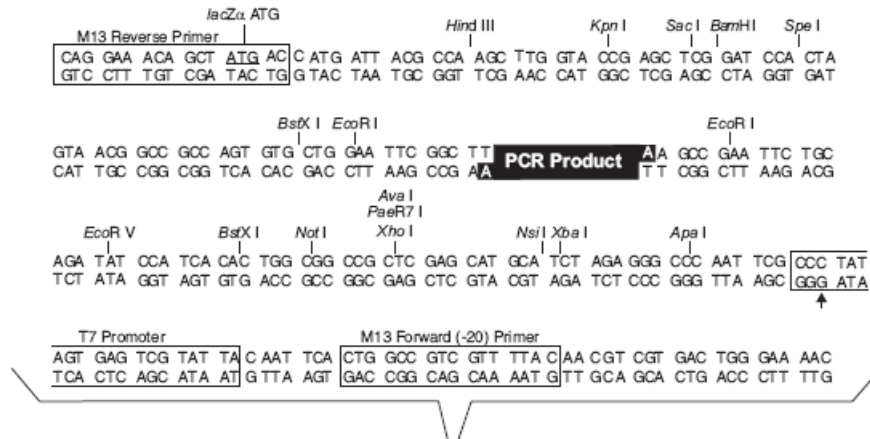
78. Wu H, D'Alessio AC, Ito S, Wang ZB, Cui KR, et al. (2011) Genome-wide analysis of 5-hydroxymethylcytosine distribution reveals its dual function in transcriptional regulation in mouse embryonic stem cells. *Genes & Development* 25: 679-684.
79. Blaschke K, Ebata KT, Karimi MM, Zepeda-Martinez JA, Goyal P, et al. (2013) Vitamin C induces Tet-dependent DNA demethylation and a blastocyst-like state in ES cells. *Nature* 500: 222-226.
80. Wang Y, Zhang Y (2014) Regulation of TET protein stability by calpains. *Cell Rep* 6: 278-284.
81. Glasow A, Barrett A, Petrie K, Gupta R, Boix-Chornet M, et al. (2008) DNA methylation-independent loss of RARA gene expression in acute myeloid leukemia. *Blood* 111: 2374-2377.
82. Milutinovic S, Brown SE, Zhuang Q, Szyf M (2004) DNA methyltransferase 1 knock down induces gene expression by a mechanism independent of DNA methylation and histone deacetylation. *J Biol Chem* 279: 27915-27927.
83. Schmelz K, Sattler N, Wagner M, Lubbert M, Dorken B, et al. (2005) Induction of gene expression by 5-Aza-2'-deoxycytidine in acute myeloid leukemia (AML) and myelodysplastic syndrome (MDS) but not epithelial cells by DNA-methylation-dependent and -independent mechanisms. *Leukemia* 19: 103-111.
84. Vincent JJ, Huang Y, Chen PY, Feng S, Calvopina JH, et al. (2013) Stage-specific roles for tet1 and tet2 in DNA demethylation in primordial germ cells. *Cell Stem Cell* 12: 470-478.
85. Song SJ, Poliseno L, Song MS, Ala U, Webster K, et al. (2013) MicroRNA-antagonism regulates breast cancer stemness and metastasis via TET-family-dependent chromatin remodeling. *Cell* 154: 311-324.
86. Sadanandam A, Lyssiotis CA, Homicsko K, Collisson EA, Gibb WJ, et al. (2013) A colorectal cancer classification system that associates cellular phenotype and responses to therapy. *Nat Med* 19: 619-625.

APPENDIX A

Map and multiple cloning sites of vectors:

pcDNA2.1:

Map of pCR[®]2.1 The map of the linearized vector, pCR[®]2.1, is shown below. The arrow indicates the start of transcription for the T7 RNA polymerase. The complete sequence of pCR[®]2.1 is available from our Web site (www.invitrogen.com) or by contacting Technical Service (page 18).



Comments for pCR[®]2.1
3929 nucleotides

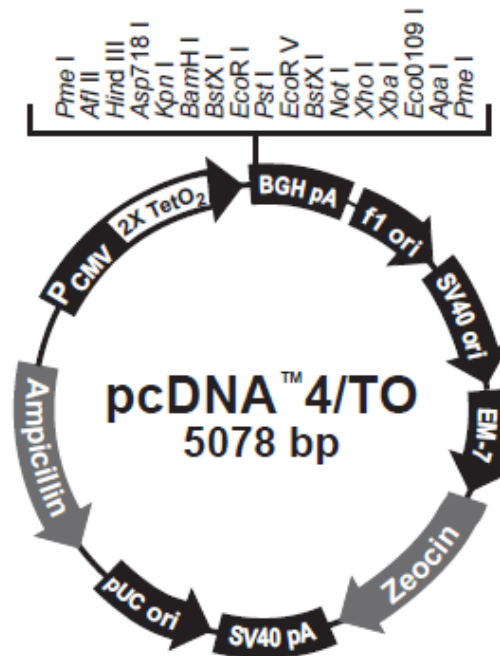
LacZα gene: bases 1-545
M13 Reverse priming site: bases 205-221
T7 promoter: bases 362-381
M13 (-20) Forward priming site: bases 389-404
f1 origin: bases 546-983
Kanamycin resistance ORF: bases 1317-2111
Ampicillin resistance ORF: bases 2129-2989
pUC origin: bases 3134-3807

pcDNA 4/TO:

```

721 AAAATCAACG GGACMV Forward priming siteCTTTCCA AAATGTCGTA ACAACTCCGC CCCATTGACG CAAATGGGCG
781 GTAGGCGTGT ACGGTGGGAG GTCTATATAATATA box GCAGAGCTCTTetracycline operator (TetO2) CCCTATCAGT GATAGAGATC
841 TCCCTATCAGTetracycline operator (TetO2) TGATAGAGAT CGTCGACGAG CTCGTTTAGT GAACCGTCAG ATCGCCTGGA
901 GACGCCATCC ACGCTGTTTT GACCTCCATA GAAGACACCG GGACCGATCC AGCCTCCGGA
961 CTCTAGCGTTPme I* Afl II Hind III Asp718 I Kpn I BamH I BstX I* EcoR I TAAACTTAAG CTTGGTACCG AGCTCGGATC CACTAGTCCA GTGTGGTGGG
1021 ATTCTGCAGAPst I EcoR V BstX I* Not I Xho I Xba I Eco0109 I Apa I Pme I* TATCCAGCAC AGTGGCGGCC GCTCGAGTCT AGAGGGCCCG TTTAAACCCG
1081 CTGATCAGCCBGH Reverse priming site TCGACTGTGC CTTCTAGTTG CCAGCCATCT

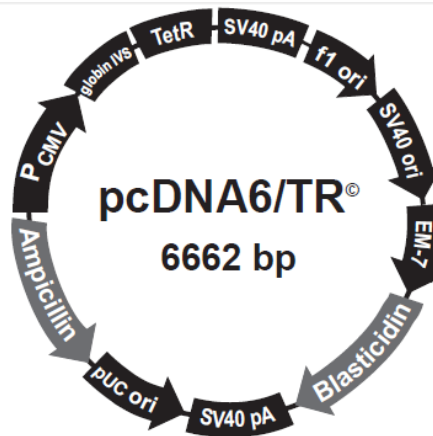
```



Comments for pcDNA™4/TO 5078 nucleotides

CMV promoter: bases 232-958
 TATA box: bases 804-810
 Tetracycline operator (2X TetO₂) sequences: bases 820-859
 CMV forward priming site: bases 769-789
 Multiple cloning site: bases 967-1077
 BGH reverse priming site: bases 1089-1106
 BGH polyadenylation sequence: bases 1095-1319
 f1 origin: bases 1365-1793
 SV40 promoter and origin: bases 1803-2143
 EM-7 promoter: bases 2183-2249
 Zeocin™ resistance gene: bases 2250-2624
 SV40 early polyadenylation sequence: bases 2754-2884
 pUC origin: bases 3267-3937
 bla promoter: bases 4937-5041 (complementary strand)
 Ampicillin (bla) resistance gene: bases 4082-4942 (complementary strand)

pcDNA 6/TR:



Comments for pcDNA6/TR[®] 6662 nucleotides

CMV promoter: bases 232-819

Rabbit β-globin intron II (IVS): bases 1028-1600

TetR gene: bases 1684-2340

SV40 early polyadenylation sequence: bases 2346-2477

f1 origin: bases 2897-3325

SV40 promoter and origin: bases 3335-3675

EM-7 promoter: bases 3715-3781

Blasticidin resistance gene: bases 3782-4180

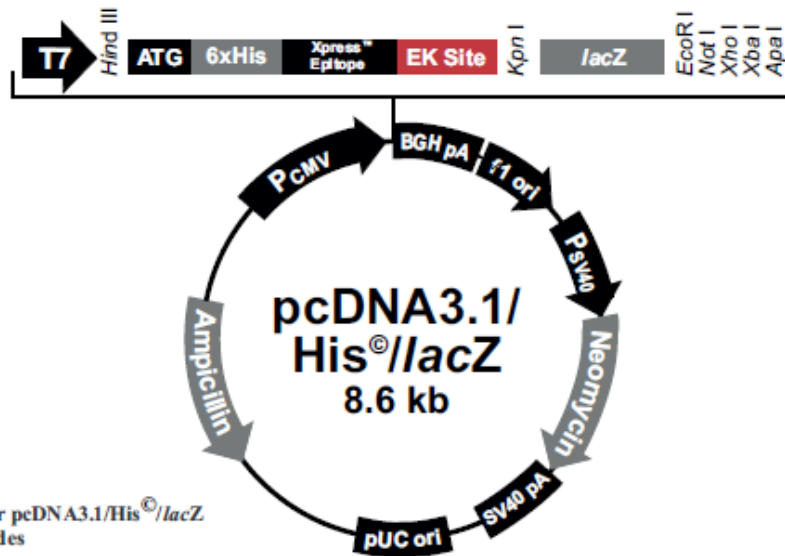
SV40 early polyadenylation sequence: bases 4338-4468

pUC origin: bases 4851-5521

bla promoter: bases 6521-6625 (complementary strand)

Ampicillin (*bla*) resistance gene: bases 5666-6526 (complementary strand)

pcDNA3.1/His/lacZ:



Comments for pcDNA3.1/His[®]/lacZ.
8577 nucleotides

- CMV promoter: bases 209-863
- T7 promoter/priming site: bases 863-882
- ATG initiation codon: bases 920-922
- Polyhistidine region: bases 932-949
- Xpress™ epitope: bases 989-1012
- Enterokinase recognition site: bases 998-1012
- LacZ ORF: bases 1033-4090
- BGH reverse priming site: bases 4168-4185
- BGH polyadenylation signal: bases 4167-4381
- f1 origin: bases 4444-4857
- SV40 promoter and origin: bases 4922-5246
- Neomycin resistance gene: bases 5282-6076
- SV40 polyadenylation signal: bases 6092-6331
- pUC origin: bases 6763-7436 (Complementary strand)
- Ampicillin resistance gene: bases 7581-8442 (Complementary strand)

APPENDIX B

Sequence of pcDNA 4/TO-ALAS2

GACGGATCGGGAGATCTCCCGATCCCCTATGGTGCACCTCTCAGTACAATCTGCTCTGATGCCGCATAGTTA
AGCCAGTATCTGCTCCCTGCTTGTGTGTTGGAGGTCGCTGAGTAGTGCGCGAGCAAAAATTTAAGCTACAAC
AAGGCAAGGCTTGACCGACAATTGCATGAAGAATCTGCTTAGGGTTAGGCGTTTTGCGCTGCTTCGCGATG
TACGGGCCAGATATACGCGTTGACATTGATTATTGACTAGTTATTAATAGTAATCAATTACGGGGTCATTA
GTTTCATAGCCCATATATGGAGTTCGCGTTACATAACTTACGGTAAATGGCCCGCCTGGCTGACCGCCCAA
CGACCCCGCCATTGACGTCAATAATGACGTATGTTCCCATAGTAACGCCAATAGGGACTTTCCATTGAC
GTCAATGGGTGGAGTATTTACGGTAAACTGCCCACTTGGCAGTACATCAAGTGTATCATATGCCAAGTACG
CCCCCTATTGACGTCAATGACGGTAAATGGCCCGCCTGGCATTATGCCCAGTACATGACCTTATGGGACTT
TCCTACTTGGCAGTACATCTACGTATTAGTCATCGCTATTACCATGGTGTATGCGGTTTTGGCAGTACATCA
ATGGGCGTGGATAGCGGTTTTGACTCACGGGGATTTCCAAGTCTCCACCCATTGACGTCAATGGGAGTTTG
TTTTGGAACCAAAATCAACGGGACTTTCCAAAATGTCGTAACAACCTCCGCCCATTTGACGCAAATGGGCGG
TAGGCGTGTACGGTGGGAGGTCTATATAAGCAGAGCTCTCCCTATCAGTGATAGAGATCTCCCTATCAGTG
ATAGAGATCGTCGACGAGCTCGTTTTAGTGAACCGTCAGATCGCCTGGAGACGCCATCCACGCTGTTTTGAC
CTCCATAGAAGACACCGGGACCGATCCAGCCTCCGGACTCTAGCGTTTTAACTTAAGCTTGGTACCGAGCT
CGGATCCACTTTAGGTTCAAGATGGTGACTGCAGCCATGCTGCTACAGTGCTGCCCAGTGCTTGCCCGGGG
CCCCACAAGCCTCCTAGGCAAGGTGGTTAAGACTCACCAAGTTCCCTGTTTTGGTATTGGACGCTGTCCCATCC
TGGCTACCCAAGGACCAAACTGTTCTCAAATCCACCTTAAGGCAACAAAGGCTGGAGGAGATTCTCCATCT
TGGGCGAAGGGCCACTGTCCCTTCATGCTGTGCGAACTCCAGGATGGGAAGAGCAAGATTGTGCAGAAGGC
AGCCCCAGAAGTCCAGGAAGATGTGAAGGCTTTCAAGACAGATCTGCCTAGCTCCCTGGTCTCAGTCAGCC
TAAGGAAGCCATTTTCCGGTCCCCAGGAGCAGGAGCAGATCTCTGGGAAGGTCACACACCTGATTCCAGAAC
AATATGCCTGGAACTATGTCTTCAGTTATGACCAGTTTTTCAGGGACAAGATCATGGAGAAGAAACAGGA
TACACCTACCGTGTGTTCAAGACTGTGAACCGCTGGGCTGATGCATATCCCTTTGGCCCAACATTTCTCTG
AGGCATCTGTGGCCTCAAAGGATGTGTCGTCTGGTGTAGTAATGATTACCTGGGCATGAGCCGACCCCT
CAGGTCTTGCAAGCCACACAGGAGACCCTGCAGCGTCATGGTGCTGGAGCTGGTGGCACCCGCAACATCTC
AGGCACCAGTAAGTTTCATGTGGAGCTTGAGCAGGAGCTGGCTGAGCTGCACCAGAAGGACTCAGCCCTGC
TCTTCTCCTCCTGCTTTGTTGCCAATGACTCTACTCTCTTACCTTGGCCAAGATCCTGCCAGGGTGCAGAG
ATTTACTCAGACGCAGGCAACCATGCTTCCATGATCCAAGGTATCCGTAACAGTGGAGCAGCCAAGTTTTGT
CTTCAGGCACAATGACCCTGACCACCTAAAGAACTTCTAGAGAAGTCTAACCCCTAAGATACCCAAAATTG
TGGCCTTTGAGACTGTCCACTCCATGGATGGTGGCCATCTGTCCCCTCGAGGAGTTGTGTGATGTGTCCCAC
CAGTATGGGGCCCTGACCTTCGTGGATGAGGTCCATGCTGTAGGACTGTATGGGTCCCGGGGCGCTGGGAT
TGGGGAGCGTGATGGAATTATGCATAAGATTGACATCATCTCTGGAACCTTTGGCAAGGCCTTTGGCTGTG
TGGGCGGCTACATTGCCAGCACCCGTGACTTGGTGGACATGGTGCCTCCTATGCTGCAGGCTTCATCTTT
ACCACTTCTCTGCCCCCATGGTGCTCTCTGGAGCTCTAGAATCTGTGCGGCTGCTCAAGGGAGAGGAGGG
CCAAGCCCTGAGGCGAGCCCACCAGCGCAATGTCAAGCACATGCGCCAGCTACTCATGGACAGGGGCCTTC
CTGTATCCCCTGCCCCAGCCACATCATCCCCATCCGGGTGGGCAATGCAGCACTCAACAGCAAGCTCTGT
GATCTCCTGCTCTCCAAGCATGGCATCTATGTGCAGGCCATCAACTACCCAAGTGTCCCCGGGGTGAAGA
GCTCCTGCGCTTGGCACCCCTCCCCCACCACAGCCCTCAGATGATGGAAGATTTTGTGGAGAAGCTGTGTC
TGGCTTGGACTGCGGTGGGGCTGCCCCCTCCAGGATGTGTCTGTGGCTGCCTGCAATTTCTGTGCGCGTCT
GTACACTTTGAGCTCATGAGTGAGTGGGAACGTTCTACTTCGGGAACATGGGGCCCCAGTATGTCA**CCAC**
CTATGCTGAGAAGCCAGCGCCGCTCGAGTCTAGAGGGCCCGTTTTAAACCCGCTGATCAGCCTCGACTGT
GCCTTCTAGTTGCCAGCCATCTGTTGTTTGGCCCTCCCCCGTGCCTTCCCTTGACCCTGGAAGGTGCCACTC
CCACTGTCCTTTTCTAATAAAAATGAGGAAATGCATCGCATTGTCTGAGTAGGTGTCATTCTATTCTGGGG
GGTGGGGTGGGGCAGGACAGCAAGGGGGAGGATTGGGAAGACAATAGCAGGCATGCTGGGGATGCGGTGGG
CTCTATGGCTTCTGAGGCGGAAAGAACCAGCTGGGGCTCTAGGGGGTATCCCCACGCGCCCTGTAGCGGCG
CATTAAAGCGCGGGGTGTGGTGGTTACGCGCAGCGTGACCGCTACACTTGCCAGCGCCCTAGCGCCCGCT
CCTTTTCGCTTTTCTCCCTTCTTTCTCGCCACGTTCCCGGCTTTCCCCGTCAAGCTCTAAATCGGGGGCT
CCCTTTAGGGTTCCGATTTAGTGCTTTACGGCACCTCGACCCCAAAAACTTGATTAGGGTGTGGTTTCCAC
GTAGTGGGCCATCGCCCTGATAGACGGTTTTTTCGCCCTTTGACGTTGGAGTCCACGTTCTTTAATAGTGGA
CTCTTGTTCAAAATGGAACAACACTCAACCCTATCTCGGTCTATTCTTTTATTATAAGGGATTTTGCC
GATTTTCGGCCTATTGGTTAAAAAATGAGCTGATTTAACAATAAATTAACGCGAATTAATTCTGTGGAATGT
GTGTGAGTTAGGGTGTGGAAAGTCCCCAGGCTCCCCAGCAGGCAGAAGTATGCAAAGCATGCATCTCAATT
AGTCAGCAACCAGGTGTGGAAAGTCCCCAGGCTCCCCAGCAGGCAGAAGTATGCAAAGCATGCATCTCAAT
TAGTCAGCAACCATAGTCCCGCCCTAACTCCGCCCATCCCGCCCTAACTCCGCCCAGTTCCGCCCATTC

TCCGCCCCATGGCTGACTAATTTTTTTTTATTTATGCAGAGGCCGAGGCCGCCTCTGCCTCTGAGCTATTCC
AGAAGTAGTGAGGAGGCTTTTTTGGAGGCCTAGGCTTTTGC AAAAAGCTCCCGGGAGCTTGTATATCCATT
TTCGGATCTGATCAGCACGTGTTGACAATTAATCATCGGCATAGTATATCGGCATAGTATAATACGACAAG
GTGAGGAATAAACCATGGCCAAGTTGACCAGTGCCGTTCCGGTGCTCACCGCGCGCGACGTGCGCCGGAGC
GGTCGAGTTCTGGACCGACCGGCTCGGGTTCTCCCGGGACTTCGTGGAGGACGACTTCGCCGGTGTGGTCC
GGGACGACGTGACCCTGTTTCATCAGCGCGGTCCAGGACCAGGTGGTGCCGGACAACACCCTGGCCTGGGTG
TGGGTGCGCGGCCCTGGACGAGCTGTACGCCGAGTGGTCGGAGGTCGTGTCCACGAACCTCCGGGACGCCTC
CGGGCCGGCCATGACCGAGATCGGCGAGCAGCCGTGGGGCGGGAGTTCGCCCTGCGCGACCCGGCCGGCA
ACTGCGTGCACTTCGTGGCCGAGGAGCAGGACTGACACGTGCTACGAGATTTTCGATTCCACC GCCCCTTC
TATGAAAGGTTGGGCTTCGGAATCGTTTTCCGGGACGCCGGCTGGATGATCCTCCAGCGGGGATCTCAT
GCTGGAGTTCTTCGCCACCCCAACTTGTTTTATTGCAGCTTATAATGGTTACAAATAAAGCAATAGCATCA
CAAATTTACAAATAAAGCATTTTTTTTACTGCATTCTAGTTGTGGTTTTGTCCAAACTCATCAATGTATCT
TATCATGTCTGTATAACCGTCGACCTCTAGCTAGAGCTTGGCGTAATCATGGTCATAGCTGTTTTCTGTGTG
AAATTGTTATCCGCTCACAATTCACACAACATACGAGCCGGAAGCATAAAGTGTAAGCCTGGGGTGCCT
AATGAGTGAGCTAACTCACATTAATTGCGTTGCGCTCACTGCCCGCTTTCAGTCGGGAAACCTGTCTGTG
CAGCTGCATTAATGAATCGGCCAACGCGCGGGGAGAGGCGGTTTTGCGTATTGGGCGCTCTTCGCTTCCTC
GCTCACTGACTCGCTGCGCTCGGTCTGTTCCGGCTGCGGCGAGCGGTATCAGCTCAAAAGGCGGTAATAC
GGTTATCCACAGAATCAGGGGATAACGCAGGAAAGAACATGTGAGCAAAAGGCCAGCAAAAGGCCAGGAAC
CGTAAAAAGGCCGCGTTGCTGGCGTTTTTCCATAGGCTCCGCCCCCTGACGAGCATCACAAAAATCGACG
CTCAAGTCAGAGGTGGCGAAACCCGACAGGACTATAAAGATACCAGGCGTTTTCCCCTGGAAGCTCCCTCG
TGCGCTCTCCTGTTCCGACCCTGCCGCTTACCGGATACCTGTCCGCTTTTCTCCCTTCGGGAAGCGTGGCG
CTTTCTCATAGCTCACGCTGTAGGTATCTCAGTTCGGTGTAGGTGCTTCGCTCCAAGCTGGGCTGTGTGCA
CGAACCCCGCTTCAGCCCCGACCGCTGCGCCTTATCCGGTAACTATCGTCTTGAGTCCAACCCGGTAAGAC
ACGACTTATCGCCACTGGCAGCAGCCACTGGTAACAGGATTAGCAGAGCGAGGTATGTAGGCGGTGCTACA
GAGTTCTTGAAGTGGTGGCCTAACTACGGCTACACTAGAAGAACAGTATTTGGTATCTGCGCTCTGCTGAA
GCCAGTTACCTTCGAAAAAGAGTTGGTAGCTTTGATCCGGCAAACAACACCACCGCTGGTAGCGGTTTTT
TTGTTTGCAAGCAGCAGATTACGCGCAGAAAAAAGGATCTCAAGAAGATCCTTTGATCTTTTTCTACGGGG
TCTGACGCTCAGTGGAACGAAAACTCAGTTAAGGGATTTTGGTCATGAGATTATCAAAAAGGATCTTCAC
CTAGATCCTTTTTAAATTAATAAATGAAGTTTTAAATCAATCTAAAGTATATATGAGTAAACTTGGTCTGACA
GTTACCAATGCTTAATCAGTGAGGCACCTATCTCAGCGATCTGTCTATTTTCGTTTCATCCATAGTTGCCTGA
CTCCCCGTCGTGTAGATAACTACGATACGGGAGGGCTTACCATCTGGCCCCAGTGCTGCAATGATACCGCG
AGACCCACGCTCACCGGCTCCAGATTTATCAGCAATAAACAGCCAGCCGGAAGGGCCGAGCGCAGAAGTG
GTCCTGCAACTTTATCCGCCTCCATCCAGTCTATTAATTGTTGCCGGAAGCTAGAGTAAGTAGTTCCGCA
GTTAATAGTTTTCGCAACGTTGTTGCCATTGCTACAGGCATCGTGGTGTACGCTCGTCTGTTGGTATGGC
TTCATTACGCTCCGGTTCCTAACGATCAAGGCGAGTTACATGATCCCCATGTTGTGCAAAAAAGCGGTTA
GCTCCTTCGGTCTCCGATCGTTGTGAGAAGTAAGTTGGCCGCGAGTGTATCACTCATGGTTATGGCAGCA
CTGCATAATTTCTTACTGTATGCCATCCGTAAGATGCTTTTTCTGTGACTGGTGAGTACTCAACCAAGTC
ATTCTGAGAATAGTGTATGCGGCGACCGAGTTGCTCTTGCCCGGCGTCAATACGGGATAATACCGCGCCAC
ATAGCAGAACTTTAAAAGTGCTCATCATTGGA AACGTTCTTCGGGGCGAAA ACTCTCAAGGATCTTACCG
CTGTTGAGATCCAGTTTCGATGTAACCCACTCGTGCACCCAACTGATCTTCAGCATCTTTTACTTTACCAG
CGTTTTCTGGGTGAGCAAAAACAGGAAGGCAAAATGCCGCAAAAAGGGAATAAGGGCGACACGGAAATGTT
GAATACTCATACTCTTCTTTTTCAATATTATTGAAGCATTATCAGGGTTATTGTCTCATGAGCGGATAC
ATATTTGAATGTATTTAGAAAAATAACAAATAGGGGTTCCGCGCACATTTCCCCGAAAAGTGCCACCTGA
CGTC

Sequence of pcDNA 4/TO-CDR1

GACGGATCGGGAGATCTCCCGATCCCCTATGGTGCCTCTCAGTACAATCTGCTCTGATGCCGCATAGTTA
AGCCAGTATCTGCTCCCTGCTTGTGTGTTGGAGGTCGCTGAGTAGTGCGCGAGCAAAATTTAAGCTACAAC
AAGGCAAGGCTTGACCGACAATTGCATGAAGAATCTGCTTAGGGTTAGGCGTTTTGCGCTGCTTCGCGATG
TACGGGCCAGATATACGCGTTGACATTGATTATTGACTAGTTATTAATAGTAATCAATTACGGGGTCATTA
GTTTCATAGCCCATATATGGAGTTCCGCGTTACATAACTTACGGTAAATGGCCCCGCTGGCTGACCGCCCAA
CGACCCCGCCATTGACGTCAATAATGACGTATGTTCCCATAGTAACGCCAATAGGGACTTTCCATTGAC
GTCAATGGGTGGAGTATTTACGGTAAACTGCCCACTTGGCAGTACATCAAGTGTATCATATGCCAAGTACG
CCCCCTATTGACGTCAATGACGGTAAATGGCCCCGCTGGCATTATGCCAGTACATGACCTTATGGGACTT

TCCTACTTGGCAGTACATCTACGTATTAGTCATCGCTATTACCATGGTGATGCGGTTTTGGCAGTACATCA
ATGGGCGTGGATAGCGGTTTTGACTCACGGGGATTTCCAAGTCTCCACCCATTGACGTCAATGGGAGTTTG
TTTTGGAACCAAAATCAACGGGACTTTCCAAAATGTCGTAACAACCTCCGCCCATTTGACGCAAATGGGCGG
TAGGCGTGTACGGTGGGAGGTCTATATAAGCAGAGCTCTCCCTATCAGTGATAGAGATCTCCCTATCAGTG
ATAGAGATCGTCGACGAGCTCGTTTTAGTGAACCGTCAGATCGCCTGGAGACGCCATCCACGCTGTTTTGAC
CTCCATAGAAGACACCGGGACCGATCCAGCCTCCGGACTCTAGCGTTTAAACTTAAGCTTGGTACCGAGCT
CGGATCCATGGCTTGGTTGGAAGACGTGGATTTTCTGGAAGACGTACCTTTGTTGGAAGACATACCTTTGT
TGAAGACGTACCTTTGTTGGAAGACGTACCTTTGTTGGAAGACACAAGTAGGCTGGAAGACATTAATTTG
ATGGAAGACATGGCTTTGTTGGAAGACGTGGATTTGCTGGAAGACACGGATTTCTGGAAGACCTGGATTT
TTCGGAAGCTATGGATTTGAGGGAAGACAAGGATTTTCTGGAAGACATGGATAGTCTGGAAGACATGGCTT
TGTTGGAAGACGTGGACTTGCTGGAAGACACGGATTTCTGGAAGACCCGGATTTTTTGGAAAGCTATAGAT
TTAAGGGAAGACAAGGATTTTCTGGAAGACATGGATAGTCTGGAAGACCTGGAGGCCATTGGAAGATGTGG
ATTTTCTGGAAGACATGGCTTTTTTGGAAAGACGTAGATTTTTCAGGAAGACCCAAATTATCCGGAAGACTTG
GATTTGTTGGGAAGACGTGGATTTTCTGGAAGACTGGGAGGTTACTGGAAGACATGGATTTTCTGGAAGACA
TGGATTTTCTGGAAGACGTGGATCTTCAGGAAGACATATATTGGCTGGAAGACCTGGATTTTTTCCGGAAG
ATGTGGATTGACTGGAAGACCTGGATTTGGTGGAAAGACGTAGATTTTTCTGGAAGACACTGACTGACTGGA
AGACCTGGATTTCTTTCTGGAAGACACTGATTGACTGGAAGACCTGGATTTCTTTCTGGAAG**ACACTGATT**
GACTGGAAGATCTAGCGGCCGCTCGAGTCTAGAGGGCCCGTTTTAAACCCGCTGATCAGCCTCGACTGTGC
CTTCTAGTTGCCAGCCATCTGTTGTTTGGCCCTCCCCCGTGCCTTCTTTGACCCTGGAAGGTGCCACTCCC
ACTGTCCTTTTCTAATAAAATGAGGAAATTGCATCGCATTGTCTGAGTAGGTGTCATTCTATTCTGGGGGG
TGGGGTGGGGCAGGACAGCAAGGGGGAGGATTGGGAAGACAATAGCAGGCATGCTGGGGATGCGGTGGGGCT
CTATGGCTTCTGAGGCGGAAAGAACCAGCTGGGGCTCTAGGGGGTATCCCCACGCGCCCTGTAGCGGGCGCA
TTAAGCGCGGGGGTGTGGTGGTTACGCGCAGCGTGACCGCTACACTTGCCAGCGCCCTAGCGCCCGCTCC
TTTTCGCTTTCTTCCCTTCTTTCTCGCCACGTTCCCGGCTTTCCCGCTCAAGCTCTAAATCGGGGGCTCC
CTTTAGGGTCCGATTTAGTGCTTTACGGCACCTCGACCCCAAAAACTTGATTAGGGTGTGGTTACAGT
AGTGGGCCATCGCCCTGATAGACGGTTTTTTCGCCCTTTGACGTTGGAGTCCAGCTTCTTTAATAGTGACT
CTTGGTTCCAACTGGAACAACACTCAACCTATCTCGTCTATTCTTTTATTATAAGGATTTTGGCGA
TTTTCGCCTATTGGTTAAAAAATGAGCTGATTTAAACAAAAATTTAACCGCAATTAATCTGTGGAATGTGT
GTCAGTTAGGGTGTGGAAGTCCCCAGGCTCCCCAGCAGGCAGAAGTATGCAAAGCATGCATCTCAATTAG
TCAGCAACCAGGTGTGGAAGTCCCCAGGCTCCCCAGCAGGCAGAAGTATGCAAAGCATGCATCTCAATTA
GTCAGCAACCATAGTCCCGCCCTAACTCCGCCATCCCGCCCTAACTCCGCCAGTTCGCCCCATTCTC
CGCCCCATGGCTGACTAATTTTTTTTTTATTTATGCAGAGGCCGAGGCCGCCTCTGCCTCTGAGCTATTCCAG
AAGTAGTGAGGAGGCTTTTTTGGAGGCCTAGGCTTTTGCAAAAGCTCCCGGGAGCTTGTATATCCATTTT
CGGATCTGATCAGCACGTGTTGACAATTAATCATCGGCATAGTATATCGGCATAGTATAATACGACAAGGT
GAGGAATAAACCATGGCCAAGTTGACCAGTGCCGTTCCGGTGCTCACCGCGCGGACGTCGCCGGAGCGG
TCGAGTTCTGGACCGACCGGCTCGGGTTCTCCCGGACTTCGTGGAGGACGACTTCGCCGGTGTGGTCCGG
GACGACGTGACCCTGTTTCATCAGCGCGGTCCAGGACCAGGTGGTGCCGGACAACACCCTGGCCTGGGTGTG
GGTGCGCGCCCTGGACGAGCTGTACGCCGAGTGGTCGGAGGTGCTGTCCACGAACCTCCGGGACGCTCCG
GGCCGGCCATGACCGAGATCGGCGAGCAGCCGTGGGGGCGGGAGTTTCGCCCTGCGCGACCCGGCCGGCAAC
TGCGTGCCTTCGTGGCCGAGGAGCAGGACTGACACGTGCTACGAGATTTTCGATTTCCACCGCCGCTTCTA
TGAAAGGTTGGGCTTCGGAATCGTTTTTCCGGGACCGCGGCTGGATGATCCTCCAGCGCGGGGATCTCATGC
TGGAGTTCTTCGCCACCCCAACTTGTTTTATTGCAGCTTATAATGGTTACAAATAAAGCAATAGCATCACA
AATTTACAAATAAAGCATTTTTTTCACTGCATTCTAGTTGTGGTTTTGTCCAACTCATCAATGTATCTTA
TCATGTCTGTATACCGTCGACCTCTAGCTAGAGCTTGGCGTAATCATGGTCATAGCTGTTTCTGTGTGAA
ATTGTTATCCGCTCACAATTCACACAACATACGAGCCGGAAGCATAAAGTGTAAGCCTGGGGTGCCTAA
TGAGTGAGCTAACTCACATTAATTGCGTTGCGCTCACTGCCCGCTTTCCAGTCGGGAAACCTGTCTGCCA
GCTGCATTAATGAATCGGCAACGCGCGGGGAGAGGCGGTTTTGCGTATTGGGCGCTCTTCCGCTTCTCGC
TCACTGACTCGCTGCGCTCGGTGCTTCCGGCTGCGGCGAGCGGTATCAGCTCACTCAAAGCGGTAATACGG
TTATCCACAGAATCAGGGGATAACGCAGGAAAGAACATGTGAGCAAAAGGCCAGCAAAAGGCCAGGAACCG
TAAAAGGCCGCTTGTGGCGTTTTTCCATAGGCTCCGCCCCCTGACGAGCATCAAAAATCGACGCT
CAAGTCAGAGGTGGCGAAACCCGACAGGACTATAAAGATAACCAGGCGTTTTCCCCCTGGAAGCTCCCTCGTG
CGCTCTCCTGTTCCGACCCTGCCGCTTACCGGATACCTGTCCGCTTTCTCCCTTCGGGAAGCGTGGCGCT
TTCTCATAGCTCACGCTGTAGGTATCTCAGTTCCGTGTAGGTGCTTCCGCTCCAAGCTGGGCTGTGTGCACG
AACCCCCGTTCCAGCCCGACCGCTGCGCCTTATCCGGTAACTATCGTCTTGAGTCCAACCCGGTAAGACAC
GACTTATCGCCACTGGCAGCAGCCACTGGTAACAGGATTAGCAGAGCGAGGTATGTAGGCGGTGCTACAGA
GTTCTTGAAGTGGTGGCCTAACTACGGCTACACTAGAAGAACAGTATTTGGTATCTGCGCTCTGCTGAAGC
CAGTTACCTTCGGAAAAGAGTTGGTAGCTCTTGATCCGGCAAACAACACCAGGCTGGTAGCGGTTTTTTTT

GTTTGCAAGCAGCAGATTACGCGCAGAAAAAAGGATCTCAAGAAGATCCTTTGATCTTTTCTACGGGGTC
TGACGCTCAGTGGAACGAAAACCTCACGTTAAGGGATTTTGGTCATGAGATTATCAAAAAGGATCTTCACCT
AGATCCTTTTAAATTAATAATGAAGTTTTAAATCAATCTAAAGTATATATGAGTAAACTTGGTCTGACAGT
TACCAATGCTTAATCAGTGAGGCACCTATCTCAGCGATCTGTCTATTTTCGTTTCATCCATAGTTGCCTGACT
CCCCGTCGTGTAGATAACTACGATACGGGAGGGCTTACCATCTGGCCCCAGTGCTGCAATGATACCGCGAG
ACCCACGCTCACCGGCTCCAGATTTATCAGCAATAAACCAGCCAGCCGGAAGGGCCGAGCGCAGAAGTGGT
CCTGCAACTTTATCCGCCTCCATCCAGTCTATTAATTGTTGCCGGGAAGCTAGAGTAAGTAGTTCCGCCAGT
TAATAGTTTGCACAACGTTGTTGCCATTGCTACAGGCATCGTGGTGTACGCTCGTCGTTTGGTATGGCTT
CATTCAGCTCCGGTTCCCAACGATCAAGGCGAGTTACATGATCCCCATGTTGTGCAAAAAAGCGGTTAGC
TCCTTCGGTCCCTCCGATCGTTGTCAGAAGTAAGTTGGCCGCGAGTGTATCACTCATGGTTATGGCAGCACT
GCATAATTCTCTTACTGTCATGCCATCCGTAAGATGCTTTTCTGTGACTGGTGAGTACTCAACCAAGTCAT
TCTGAGAATAGTGTATGCGGCGACCGAGTTGCTCTTGCCCGGCGTCAATACGGGATAATACCGCGCCACAT
AGCAGAACTTTAAAAGTGCTCATCATTGGAAAACGTTCTTCCGGGGCGAAAACCTCTCAAGGATCTTACCGCT
GTTGAGATCCAGTTCGATGTAACCCACTCGTGCACCCAACTGATCTTCAGCATCTTTTACTTTACCAGCG
TTTCTGGGTGAGCAAAAACAGGAAGGCAAAATGCCGCAAAAAAGGGAATAAGGGCGACACGGAAATGTTGA
ATACTCATACTCTTCCTTTTTTCAATATTATTGAAGCATTTATCAGGGTTATTGTCTCATGAGCGGATACAT
ATTTGAATGTATTTAGAAAAATAACAATAGGGGTTCCGCGCACATTTCCCCGAAAAGTGCCACCTGACG
TC

APPENDIX C

24.12.2014

Bilkent Webmail

Görüntülenen Klasör: **Gelen Kutusu**

[Oturumu Kapat](#)

[Mesaj Yaz](#) [Adresler](#) [Klasörler](#) [Seçenekler](#) [Ara](#) [Yardım](#) [Filters](#)

[Mesaj Listesi](#) | [Okunmamış](#) | [Sil](#) [Önceki](#) | [Sonraki](#) [İlet](#) | [Eklenti Olarak İlet](#) | [Cevap Yaz](#) | [Tümüne Cevap Yaz](#)

Konu: RE: Permission request

Gönderen: "PNAS Permissions" <PNASPermissions@nas.edu>

Tarih: 24 Aralık 2014, Çarşamba, 12:23 am

Alıcı: "Sinem Yılmaz" <syilmaz@fen.bilkent.edu.tr>

Öncelik: Normal

Allow Sender: [Allow Sender](#) | [Allow Domain](#) | [Block Sender](#) |

Create Filter: [Automatically](#) | [From](#) | [To](#) | [Subject](#)

Seçenekler: [Tüm Başlıklar Göster](#) | [Yazdırılabilir Şekilde Göster](#) | [Bunu dosya olarak indir](#) | [View Message Details](#) | [Add to Address Book](#) | [Spam](#)

Permission is granted for your use of the figure as described in your message. Please cite the PNAS article in full, and include "Copyright (2008) National Academy of Sciences, U.S.A." as a copyright note. Because this material published between 1993 and 2008, a copyright note is needed. Let us know if you have any questions.

Best regards,
Kay McLaughlin for
Diane Sullenberger
Executive Editor
PNAS

-----Original Message-----

From: Sinem Yılmaz [<mailto:syilmaz@fen.bilkent.edu.tr>]

Sent: Tuesday, December 23, 2014 8:43 AM

To: PNAS Permissions

Subject: Permission request

Dear Sir or madam,

I would like to get permission for the following article (necessary information is below) to be used in my PhD thesis.

Thanks in advance,

Sinem YILMAZ OZCAN
Bilkent University

Your full name, affiliation, and title: Sinem YILMAZ OZCAN PhD student

Your complete mailing address, phone number, fax number, and email address: Bilkent University Molecular Biology Department Bilkent Ankara Turkey, +905057749603, syilmaz@fen.bilkent.edu.tr

PNAS volume number, issue number, and issue date: 105, 51, 2008

PNAS article title: Genome-wide analysis of cancer/testis gene expression

PNAS authors' names: Oliver Hofmann, b, 1, Otavia L. Caballeroc, Brian J.

https://newmail.bilkent.edu.tr/src/read_body.php?mailbox=INBOX&passed_id=17854&star1Message=1

1/2

Stevenson^{d,e}, Yao-Tseng Chen^f, Tzeela Cohenc, Ramon Chua Christopher A. Maher^b, Sumir Panjib, Ulf Schaefer^b, Adele Kruger^b, Minna Lehtvaslaiahob, Piero Carninci^{g,h}, Yoshihide Hayashizaki^{g,h}, C. Victor Jongeneel^{d,e}, Andrew J. G. Simpson^c, Lloyd J. Old^{c,1}, and Winston Hidea^{a,b}

Page numbers of items to be reprinted: 1

Figure/table number or portion of text to be reprinted: Figure 1

Also include the following information about the intended use of the material:

Title of work in which PNAS material will appear: A NOVEL ROLE FOR 5-hmC IN THE REGULATION OF CANCER TESTIS GENE EXPRESSION IN CANCER AND MESENCHYMAL TO EPITHELIAL TRANSITION

Authors/editors of work: Sinem YILMAZ OZCAN

Publisher of work: PhD Thesis

Retail price of work: N/A

Number of copies of work to be produced: 6 print copies and soft copies

Intended audience: Academic

Whether work is for nonprofit or commercial use: nonprofit use

[Sil ve Öncekini Oku](#) | [Sil ve Sonrakini Oku](#)

Klasöre Taşı:

**American Society for Cell Biology LICENSE
TERMS AND CONDITIONS**

Dec 24, 2014

This is a License Agreement between Sinem YILMAZ OZCAN ("You") and American Society for Cell Biology ("American Society for Cell Biology") provided by Copyright Clearance Center ("CCC"). The license consists of your order details, the terms and conditions provided by American Society for Cell Biology, and the payment terms and conditions.

All payments must be made in full to CCC. For payment instructions, please see information listed at the bottom of this form.

License Number	3535300637481
License date	Dec 24, 2014
Licensed content publisher	American Society for Cell Biology
Licensed content title	MOLECULAR BIOLOGY OF THE CELL. ONLINE
Licensed content date	Dec 31, 1969
Type of Use	Thesis/Dissertation
Requestor type	Academic institution
Format	Print, Electronic
Portion	chart/graph/table/figure
Number of charts/graphs/tables/figures	2
Title or numeric reference of the portion(s)	Figure 1 and Figure 2
Title of the article or chapter the portion is from	Parallels between global transcriptional programs of polarizing Caco-2 intestinal epithelial cells in vitro and gene expression programs in normal colon and colon cancer.
Editor of portion(s)	N/A
Author of portion(s)	SÃf AM
Volume of serial or monograph.	18
Issue, if republishing an article from a serial	11
Page range of the portion	4245-60
Publication date of portion	2007
Rights for	Main product
Duration of use	Life of current and all future editions
Creation of copies for the disabled	no

With minor editing privileges	no
For distribution to	Worldwide
In the following language(s)	Original language of publication
With incidental promotional use	no
The lifetime unit quantity of new product	Up to 499
Made available in the following markets	Academic
The requesting person/organization is:	Sinem YILMAZ OZCAN
Order reference number	None
Author/Editor	Sinem YILMAZ OZCAN
The standard identifier	PhD Thesis
Title	A NOVEL ROLE FOR 5-hmC IN THE REGULATION OF CANCER TESTIS GENE EXPRESSION IN CANCER AND MESENCHYMAL TO EPITHELIAL TRANSITION
Publisher	PhD Thesis
Expected publication date	Dec 2014
Estimated size (pages)	132
Total (may include CCC user fee)	0.00 USD
Terms and Conditions	

TERMS AND CONDITIONS

The following terms are individual to this publisher:

None

Other Terms and Conditions:

None

STANDARD TERMS AND CONDITIONS

1. Description of Service; Defined Terms. This Republication License enables the User to obtain licenses for republication of one or more copyrighted works as described in detail on the relevant Order Confirmation (the "Work(s)"). Copyright Clearance Center, Inc. ("CCC") grants licenses through the Service on behalf of the rightsholder identified on the Order Confirmation (the "Rightsholder"). "Republication", as used herein, generally means the inclusion of a Work, in whole or in part, in a new work or works, also as described on the Order Confirmation. "User", as used herein, means the person or entity making such republication.

2. The terms set forth in the relevant Order Confirmation, and any terms set by the Rightsholder with respect to a particular Work, govern the terms of use of Works in

connection with the Service. By using the Service, the person transacting for a republication license on behalf of the User represents and warrants that he/she/it (a) has been duly authorized by the User to accept, and hereby does accept, all such terms and conditions on behalf of User, and (b) shall inform User of all such terms and conditions. In the event such person is a "freelancer" or other third party independent of User and CCC, such party shall be deemed jointly a "User" for purposes of these terms and conditions. In any event, User shall be deemed to have accepted and agreed to all such terms and conditions if User republishes the Work in any fashion.

3. Scope of License; Limitations and Obligations.

3.1 All Works and all rights therein, including copyright rights, remain the sole and exclusive property of the Rightsholder. The license created by the exchange of an Order Confirmation (and/or any invoice) and payment by User of the full amount set forth on that document includes only those rights expressly set forth in the Order Confirmation and in these terms and conditions, and conveys no other rights in the Work(s) to User. All rights not expressly granted are hereby reserved.

3.2 General Payment Terms: You may pay by credit card or through an account with us payable at the end of the month. If you and we agree that you may establish a standing account with CCC, then the following terms apply: Remit Payment to: Copyright Clearance Center, Dept 001, P.O. Box 843006, Boston, MA 02284-3006. Payments Due: Invoices are payable upon their delivery to you (or upon our notice to you that they are available to you for downloading). After 30 days, outstanding amounts will be subject to a service charge of 1-1/2% per month or, if less, the maximum rate allowed by applicable law. Unless otherwise specifically set forth in the Order Confirmation or in a separate written agreement signed by CCC, invoices are due and payable on "net 30" terms. While User may exercise the rights licensed immediately upon issuance of the Order Confirmation, the license is automatically revoked and is null and void, as if it had never been issued, if complete payment for the license is not received on a timely basis either from User directly or through a payment agent, such as a credit card company.

3.3 Unless otherwise provided in the Order Confirmation, any grant of rights to User (i) is "one-time" (including the editions and product family specified in the license), (ii) is non-exclusive and non-transferable and (iii) is subject to any and all limitations and restrictions (such as, but not limited to, limitations on duration of use or circulation) included in the Order Confirmation or invoice and/or in these terms and conditions. Upon completion of the licensed use, User shall either secure a new permission for further use of the Work(s) or immediately cease any new use of the Work(s) and shall render inaccessible (such as by deleting or by removing or severing links or other locators) any further copies of the Work (except for copies printed on paper in accordance with this license and still in User's stock at the end of such period).

3.4 In the event that the material for which a republication license is sought includes third party materials (such as photographs, illustrations, graphs, inserts and similar materials) which are identified in such material as having been used by permission, User is responsible for identifying, and seeking separate licenses (under this Service or otherwise) for, any of such third party materials; without a separate license, such third party materials may not be used.

3.5 Use of proper copyright notice for a Work is required as a condition of any license granted under the Service. Unless otherwise provided in the Order Confirmation, a proper copyright notice will read substantially as follows: "Republished with permission of [Rightsholder's name], from [Work's title, author, volume, edition number and year of copyright]; permission conveyed through Copyright Clearance Center, Inc. " Such notice must be provided in a reasonably legible font size and must be placed either immediately adjacent to the Work as used (for example, as part of a by-line or footnote but not as a separate electronic link) or in the place where substantially all other credits or notices for the new work containing the republished Work are located. Failure to include the required notice results in loss to the Rightsholder and CCC, and the User shall be liable to pay liquidated damages for each such failure equal to twice the use fee specified in the Order Confirmation, in addition to the use fee itself and any other fees and charges specified.

3.6 User may only make alterations to the Work if and as expressly set forth in the Order Confirmation. No Work may be used in any way that is defamatory, violates the rights of third parties (including such third parties' rights of copyright, privacy, publicity, or other tangible or intangible property), or is otherwise illegal, sexually explicit or obscene. In addition, User may not conjoin a Work with any other material that may result in damage to the reputation of the Rightsholder. User agrees to inform CCC if it becomes aware of any infringement of any rights in a Work and to cooperate with any reasonable request of CCC or the Rightsholder in connection therewith.

4. Indemnity. User hereby indemnifies and agrees to defend the Rightsholder and CCC, and their respective employees and directors, against all claims, liability, damages, costs and expenses, including legal fees and expenses, arising out of any use of a Work beyond the scope of the rights granted herein, or any use of a Work which has been altered in any unauthorized way by User, including claims of defamation or infringement of rights of copyright, publicity, privacy or other tangible or intangible property.

5. Limitation of Liability. UNDER NO CIRCUMSTANCES WILL CCC OR THE RIGHTSHOLDER BE LIABLE FOR ANY DIRECT, INDIRECT, CONSEQUENTIAL OR INCIDENTAL DAMAGES (INCLUDING WITHOUT LIMITATION DAMAGES FOR LOSS OF BUSINESS PROFITS OR INFORMATION, OR FOR BUSINESS INTERRUPTION) ARISING OUT OF THE USE OR INABILITY TO USE A WORK, EVEN IF ONE OF THEM HAS BEEN ADVISED OF THE POSSIBILITY OF SUCH DAMAGES. In any event, the total liability of the Rightsholder and CCC (including their respective employees and directors) shall not exceed the total amount actually paid by User for this license. User assumes full liability for the actions and omissions of its principals, employees, agents, affiliates, successors and assigns.

6. Limited Warranties. THE WORK(S) AND RIGHT(S) ARE PROVIDED "AS IS". CCC HAS THE RIGHT TO GRANT TO USER THE RIGHTS GRANTED IN THE ORDER CONFIRMATION DOCUMENT. CCC AND THE RIGHTSHOLDER DISCLAIM ALL OTHER WARRANTIES RELATING TO THE WORK(S) AND RIGHT(S), EITHER EXPRESS OR IMPLIED, INCLUDING WITHOUT LIMITATION IMPLIED WARRANTIES OF MERCHANTABILITY OR FITNESS FOR A PARTICULAR PURPOSE. ADDITIONAL RIGHTS MAY BE REQUIRED TO USE ILLUSTRATIONS, GRAPHS, PHOTOGRAPHS, ABSTRACTS, INSERTS OR OTHER PORTIONS OF THE WORK (AS OPPOSED TO THE ENTIRE WORK) IN A MANNER CONTEMPLATED BY USER; USER UNDERSTANDS AND AGREES THAT NEITHER CCC NOR THE

RIGHTSHOLDER MAY HAVE SUCH ADDITIONAL RIGHTS TO GRANT.

7. **Effect of Breach.** Any failure by User to pay any amount when due, or any use by User of a Work beyond the scope of the license set forth in the Order Confirmation and/or these terms and conditions, shall be a material breach of the license created by the Order Confirmation and these terms and conditions. Any breach not cured within 30 days of written notice thereof shall result in immediate termination of such license without further notice. Any unauthorized (but licensable) use of a Work that is terminated immediately upon notice thereof may be liquidated by payment of the Rightsholder's ordinary license price therefor; any unauthorized (and unlicensable) use that is not terminated immediately for any reason (including, for example, because materials containing the Work cannot reasonably be recalled) will be subject to all remedies available at law or in equity, but in no event to a payment of less than three times the Rightsholder's ordinary license price for the most closely analogous licensable use plus Rightsholder's and/or CCC's costs and expenses incurred in collecting such payment.

8. Miscellaneous.

8.1 User acknowledges that CCC may, from time to time, make changes or additions to the Service or to these terms and conditions, and CCC reserves the right to send notice to the User by electronic mail or otherwise for the purposes of notifying User of such changes or additions; provided that any such changes or additions shall not apply to permissions already secured and paid for.

8.2 Use of User-related information collected through the Service is governed by CCC's privacy policy, available online here:
<http://www.copyright.com/content/cc3/en/tools/footer/privacypolicy.html>.

8.3 The licensing transaction described in the Order Confirmation is personal to User. Therefore, User may not assign or transfer to any other person (whether a natural person or an organization of any kind) the license created by the Order Confirmation and these terms and conditions or any rights granted hereunder; provided, however, that User may assign such license in its entirety on written notice to CCC in the event of a transfer of all or substantially all of User's rights in the new material which includes the Work(s) licensed under this Service.

8.4 No amendment or waiver of any terms is binding unless set forth in writing and signed by the parties. The Rightsholder and CCC hereby object to any terms contained in any writing prepared by the User or its principals, employees, agents or affiliates and purporting to govern or otherwise relate to the licensing transaction described in the Order Confirmation, which terms are in any way inconsistent with any terms set forth in the Order Confirmation and/or in these terms and conditions or CCC's standard operating procedures, whether such writing is prepared prior to, simultaneously with or subsequent to the Order Confirmation, and whether such writing appears on a copy of the Order Confirmation or in a separate instrument.

8.5 The licensing transaction described in the Order Confirmation document shall be governed by and construed under the law of the State of New York, USA, without regard to the principles thereof of conflicts of law. Any case, controversy, suit, action, or proceeding arising out of, in connection with, or related to such licensing transaction shall be brought, at

CCC's sole discretion, in any federal or state court located in the County of New York, State of New York, USA, or in any federal or state court whose geographical jurisdiction covers the location of the Rightsholder set forth in the Order Confirmation. The parties expressly submit to the personal jurisdiction and venue of each such federal or state court. If you have any comments or questions about the Service or Copyright Clearance Center, please contact us at 978-750-8400 or send an e-mail to info@copyright.com.

v 1.1

Questions? customercare@copyright.com or +1-855-239-3415 (toll free in the US) or +1-978-646-2777.

Gratis licenses (referencing \$0 in the Total field) are free. Please retain this printable license for your reference. No payment is required.

**NATURE PUBLISHING GROUP LICENSE
TERMS AND CONDITIONS**

Dec 23, 2014

This is a License Agreement between Sinem YILMAZ OZCAN ("You") and Nature Publishing Group ("Nature Publishing Group") provided by Copyright Clearance Center ("CCC"). The license consists of your order details, the terms and conditions provided by Nature Publishing Group, and the payment terms and conditions.

All payments must be made in full to CCC. For payment instructions, please see information listed at the bottom of this form.

License Number	3534760900380
License date	Dec 23, 2014
Licensed content publisher	Nature Publishing Group
Licensed content publication	Nature Reviews Molecular Cell Biology
Licensed content title	TETonic shift: biological roles of TET proteins in DNA demethylation and transcription
Licensed content author	William A. Pastor, L. Aravind and Anjana Rao
Licensed content date	Jun 1, 2013
Volume number	14
Issue number	6
Type of Use	reuse in a dissertation / thesis
Requestor type	academic/educational
Format	print and electronic
Portion	figures/tables/illustrations
Number of figures/tables/illustrations	1

High-res required	no
Figures	Figure 1
Author of this NPG article	no
Your reference number	None
Title of your thesis / dissertation	A NOVEL ROLE FOR 5-hmC IN THE REGULATION OF CANCER TESTIS GENE EXPRESSION IN CANCER AND MESENCHYMAL TO EPITHELIAL TRANSITION
Expected completion date	Dec 2014
Estimated size (number of pages)	130
Total	0.00 USD
Terms and Conditions	

Terms and Conditions for Permissions

Nature Publishing Group hereby grants you a non-exclusive license to reproduce this material for this purpose, and for no other use, subject to the conditions below:

1. NPG warrants that it has, to the best of its knowledge, the rights to license reuse of this material. However, you should ensure that the material you are requesting is original to Nature Publishing Group and does not carry the copyright of another entity (as credited in the published version). If the credit line on any part of the material you have requested indicates that it was reprinted or adapted by NPG with permission from another source, then you should also seek permission from that source to reuse the material.
2. Permission granted free of charge for material in print is also usually granted for any electronic version of that work, provided that the material is incidental to the work as a whole and that the electronic version is essentially equivalent to, or substitutes for, the print version. Where print permission has been granted for a fee, separate permission must be obtained for any additional, electronic re-use (unless, as in the case of a full paper, this has already been accounted for during your initial request in the calculation of a print run). NB: In all cases, web-based use of full-text articles must be authorized separately through the 'Use on a Web Site' option when requesting permission.

3. Permission granted for a first edition does not apply to second and subsequent editions and for editions in other languages (except for signatories to the STM Permissions Guidelines, or where the first edition permission was granted for free).
4. Nature Publishing Group's permission must be acknowledged next to the figure, table or abstract in print. In electronic form, this acknowledgement must be visible at the same time as the figure/table/abstract, and must be hyperlinked to the journal's homepage.
5. The credit line should read:
Reprinted by permission from Macmillan Publishers Ltd: [JOURNAL NAME] (reference citation), copyright (year of publication)
For AOP papers, the credit line should read:
Reprinted by permission from Macmillan Publishers Ltd: [JOURNAL NAME], advance online publication, day month year (doi: 10.1038/sj.[JOURNAL ACRONYM].XXXXX)

Note: For republication from the *British Journal of Cancer*, the following credit lines apply.

Reprinted by permission from Macmillan Publishers Ltd on behalf of Cancer Research UK: [JOURNAL NAME] (reference citation), copyright (year of publication)
For AOP papers, the credit line should read:
Reprinted by permission from Macmillan Publishers Ltd on behalf of Cancer Research UK: [JOURNAL NAME], advance online publication, day month year (doi: 10.1038/sj.[JOURNAL ACRONYM].XXXXX)

6. Adaptations of single figures do not require NPG approval. However, the adaptation should be credited as follows:

Adapted by permission from Macmillan Publishers Ltd: [JOURNAL NAME] (reference citation), copyright (year of publication)

Note: For adaptation from the *British Journal of Cancer*, the following credit line applies.

Adapted by permission from Macmillan Publishers Ltd on behalf of Cancer Research UK: [JOURNAL NAME] (reference citation), copyright (year of publication)

7. Translations of 401 words up to a whole article require NPG approval. Please visit <http://www.macmillanmedicalcommunications.com> for more information. Translations of up to a 400 words do not require NPG approval. The translation should be credited as follows:

Translated by permission from Macmillan Publishers Ltd: [JOURNAL NAME] (reference citation), copyright (year of publication).

Note: For translation from the *British Journal of Cancer*, the following credit line applies.

Translated by permission from Macmillan Publishers Ltd on behalf of Cancer Research UK: [JOURNAL NAME] (reference citation), copyright (year of publication)

We are certain that all parties will benefit from this agreement and wish you the best in the use of this material. Thank you.

Special Terms:

v1.1

Questions? customercare@copyright.com or +1-855-239-3415 (toll free in the US) or +1-978-646-2777.

Gratis licenses (referencing \$0 in the Total field) are free. Please retain this printable license for your reference. No payment is required.

7 PUBLICATION



Epigenetic Mechanisms Underlying the Dynamic Expression of Cancer-Testis Genes, *PAGE2*, *-2B* and *SPANX-B*, during Mesenchymal-to-Epithelial Transition

Sinem Yilmaz-Ozcan¹, Asli Sade², Baris Kucukkaraduman¹, Yasemin Kaygusuz¹, Kerem Mert Senses¹, Sreeparna Banerjee², Ali Osmay Gure^{1*}

¹ Department of Molecular Biology and Genetics, Bilkent University, Ankara, Turkey, ² Department of Biological Sciences, Middle East Technical University, Ankara, Turkey

Abstract

Cancer-testis (CT) genes are expressed in various cancers but not in normal tissues other than in cells of the germline. Although DNA demethylation of promoter-proximal CpGs of CT genes is linked to their expression in cancer, the mechanisms leading to demethylation are unknown. To elucidate such mechanisms we chose to study the Caco-2 colorectal cancer cell line during the course of its spontaneous differentiation *in vitro*, as we found CT genes, in particular *PAGE2*, *-2B* and *SPANX-B*, to be up-regulated during this process. Differentiation of these cells resulted in a mesenchymal-to-epithelial transition (MET) as evidenced by the gain of epithelial markers CDX2, Claudin-4 and E-cadherin, and a concomitant loss of mesenchymal markers Vimentin, Fibronectin-1 and Transgelin. *PAGE2* and *SPANX-B* up-regulation was accompanied by an increase in Ten-eleven translocation-2 (TET2) expression and cytosine 5-hydroxymethylation as well as the disassociation of heterochromatin protein 1 and the polycomb repressive complex 2 protein EZH2 from promoter-proximal regions of these genes. Reversal of differentiation resulted in down-regulation of *PAGE2*, *-2B* and *SPANX-B*, and induction of epithelial-to-mesenchymal transition (EMT) markers, demonstrating the dynamic nature of CT gene regulation in this model.

Citation: Yilmaz-Ozcan S, Sade A, Kucukkaraduman B, Kaygusuz Y, Senses KM, et al. (2014) Epigenetic Mechanisms Underlying the Dynamic Expression of Cancer-Testis Genes, *PAGE2*, *-2B* and *SPANX-B*, during Mesenchymal-to-Epithelial Transition. PLoS ONE 9(9): e107905. doi:10.1371/journal.pone.0107905

Editor: Keping Xie, The University of Texas MD Anderson Cancer Center, United States of America

Received: May 17, 2014; **Accepted:** August 22, 2014; **Published:** September 17, 2014

Copyright: © 2014 Yilmaz-Ozcan et al. This is an open-access article distributed under the terms of the Creative Commons Attribution License, which permits unrestricted use, distribution, and reproduction in any medium, provided the original author and source are credited.

Data Availability: The authors confirm that all data underlying the findings are fully available without restriction. All relevant data are within the paper and its Supporting Information files.

Funding: This work was supported by grant nr. 1125023 from The Scientific and Technological Research Council of Turkey (TUBITAK) to AOG, a Young Investigator Award from The Turkish Academy of Sciences to SB, and by TUBITAK-BIDEP fellowships to SYO and BK. The funders had no role in study design, data collection and analysis, decision to publish, or preparation of the manuscript.

Competing Interests: The authors have declared that no competing interests exist.

* Email: agure@bilkent.edu.tr

Introduction

Cancer-testis (CT) or cancer-germline genes are expressed in tumors originating from various tissues, as well as in normal germline and trophoblast cells, but are generally silent in other normal tissues of the adult [1–3]. More than 100 different CT genes can be grouped according to homology into families [2]. Despite the lack of sequence similarity between CT genes from different families, re-expression of all CT genes in tumors has been associated with demethylation of CpG residues within their promoter-proximal regions [4]. This shared mechanism of expression regulation is most likely the reason for their coordinate expression in cancer [5–7]. However, the exact mechanism by which DNA demethylation occurs at CT gene promoter-proximal regions in cancers is unknown. CT genes show mostly a heterogeneous expression pattern in tumors [8–10]; in contrast to their expression in testis, which is demarcated and orderly [11]. A study in which stem-like and non-stem like cells of breast cancer were selectively killed, revealed that CT gene expression is generally a feature of more differentiated, non-stem cells [12]. Similarly, in melanoma, a subgroup of cells with more epithelial features express CT genes, when cells with mesenchymal features don't [13]. Interestingly, melanoma cells can switch between these

two classes *in vivo*, suggesting that tumor heterogeneity, as defined by CT gene expression, might represent a transitional phase similar to the switch between epithelial and mesenchymal phenotypes. Indeed, mesenchymal-to-epithelial transition (MET) is associated with the induction of CT gene expression [14]. To define mechanisms involved in regulating CT gene expression in cancer and during MET, we chose to study the Caco-2 spontaneous differentiation model which demonstrates features of MET and EMT during differentiation and de-differentiation, respectively. Our data reveal that the dynamic regulation of the two CT genes, *PAGE2* and *SPANX-B* in this model system, involves alterations of polycomb repressive complex 2 (PRC2) and heterochromatin protein 1 (HP1) occupancy within their promoter-proximal regions, with concordant changes in TET expression and cytosine hydroxymethylation (hmC) levels.

Methods

Cell lines, induction of differentiation and de-differentiation

The Caco-2 cell line was obtained from the SAP Enstitüsü (Ankara, Turkey). HCT116 (colorectal) and Mahlavu (hepatocellular) cancer cell lines were obtained from LGC Standards,

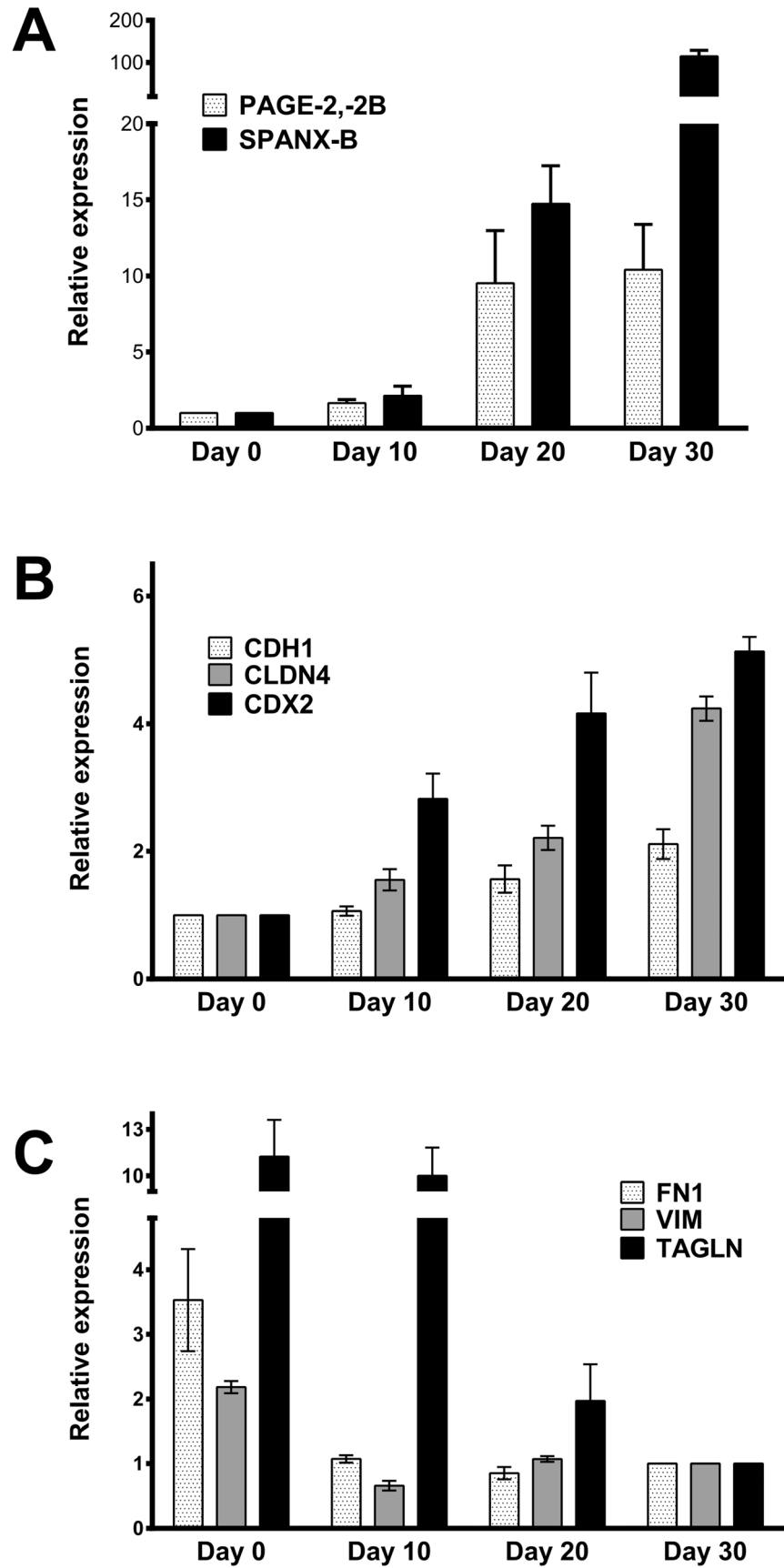


Figure 1. Up-regulation of CT genes in parallel to MET in the Caco-2 SD model. Relative mRNA expression of CT genes (*PAGE2*, *-2B* and *SPANXB*) (A), epithelial genes (*E-cadherin* (*CDH1*), *claudin 4*(*CLDN4*), *CDX2*) (B), and mesenchymal genes (*fibronectin 1* (*FN1*), *vimentin* (*VIM*), *transgelin* (*TAGLN*)) (C) as determined by quantitative PCR at days 0, 10, 20 and 30 post-confluence. Data represent average of two experiments. Change in expression levels for all genes between days 0 and 30 is statistically significant ($P < 0.0001$, by two way ANOVA with Tukey's post hoc test). doi:10.1371/journal.pone.0107905.g001

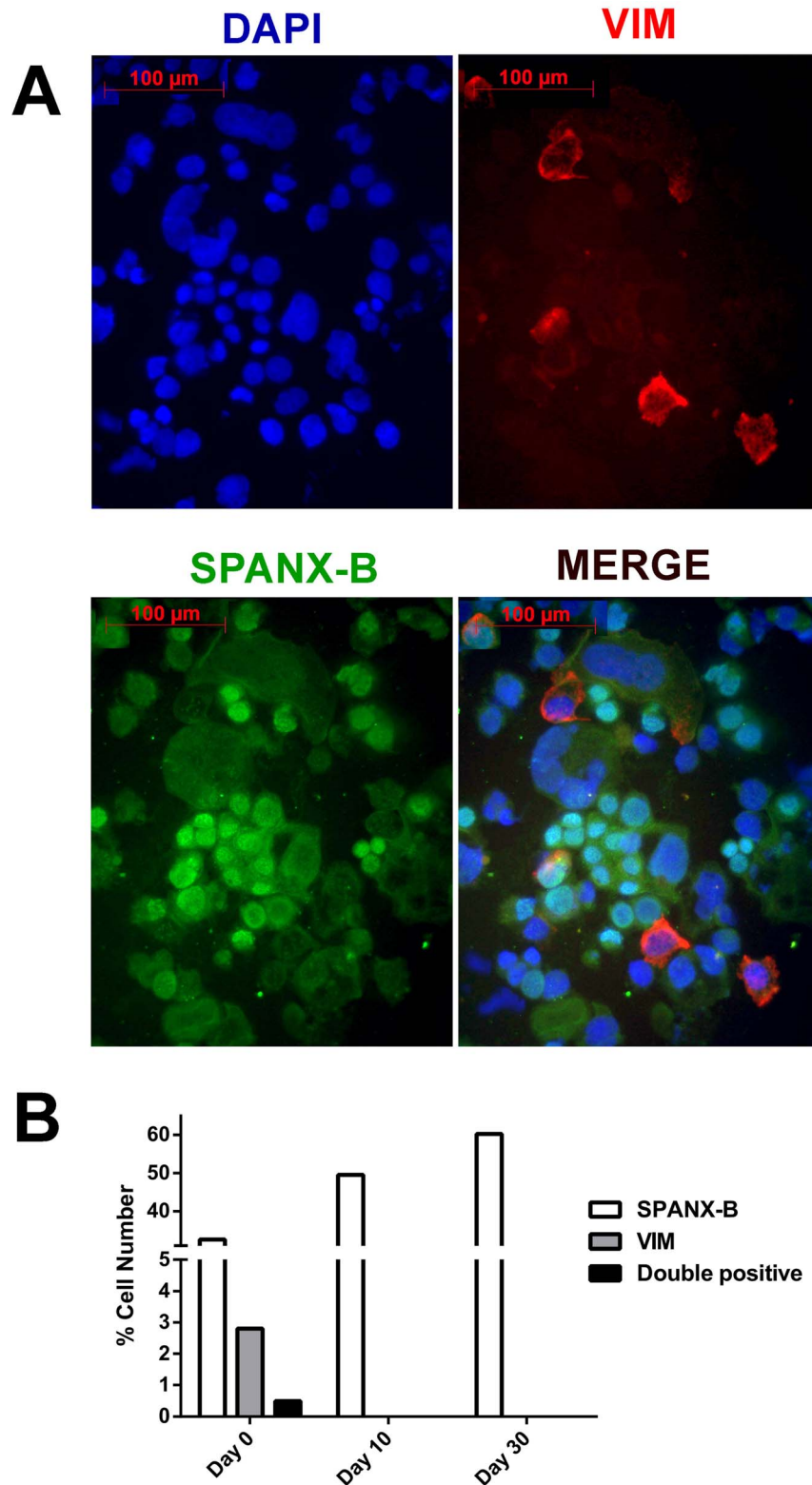


Figure 2. SPANX-B and vimentin expression are mutually exclusive in differentiating Caco-2 cells. Immunofluorescent staining of differentiating Caco-2 cells with DAPI counterstaining reveals a gradual increase in nuclear SPANX-B (green) with a concomitant decrease in cytoplasmic vimentin expression (red); (20× magnification) (A). Less than 1% of SPANX-B positive cells showed staining for vimentin on day 0 (B). doi:10.1371/journal.pone.0107905.g002

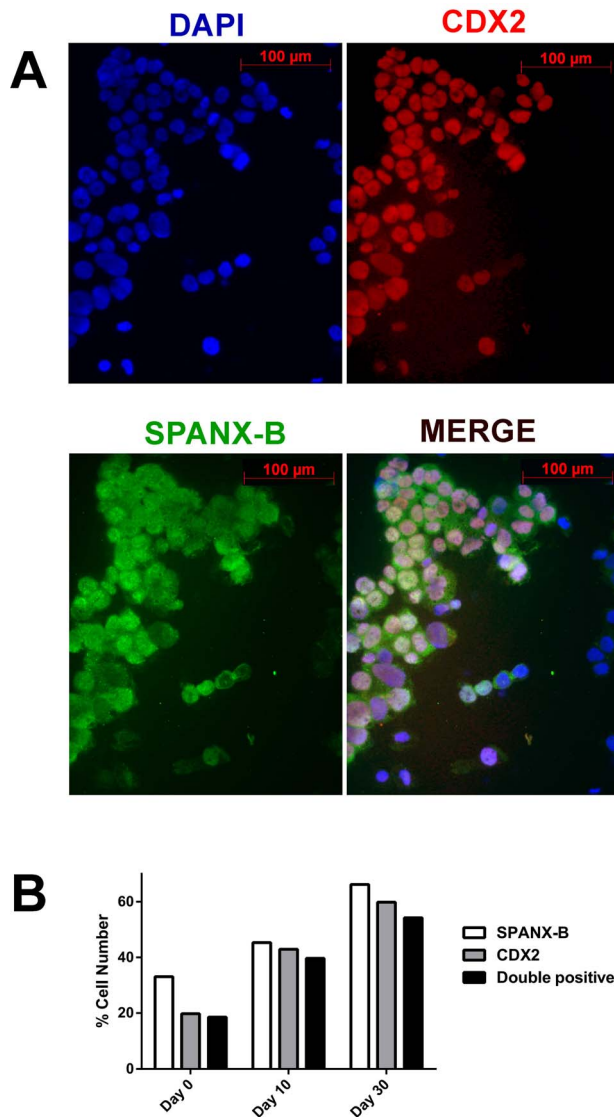


Figure 3. Nuclear co-localization of CDX2 and SPANX-B in differentiating Caco-2 cells. Immunofluorescent staining of differentiating Caco-2 cells with DAPI counterstaining reveals overlapping SPANX-B (Alexa Fluor 488: green) and CDX2 (Alexa Fluor 568: red) expression; (20 \times magnification) (A). More than 60 to 80% of the cells show double-labeling when analyzed quantitatively (B). doi:10.1371/journal.pone.0107905.g003

Middlesex, UK. A lung cancer cell line (SK-LC-17) was from the Memorial Sloan Kettering Cancer Center, NY, USA. Caco-2 cells were grown in EMEM and others in RPMI, supplemented with 20% FBS, 2 mM L-glutamine, 0.1 mM non-essential amino acids, 1.5 g/L sodium bicarbonate and 1 mM sodium pyruvate. All cell culture media and supplements were purchased from Biochrom AG, Berlin, Germany. The first day cells reached confluence was designated day 0. Cells grown in parallel cultures were used to determine phenotypic changes at days 0, 5, 10, 20 and 30, post-confluence. Additional measures of differentiation for cells used in this study have been reported elsewhere [15]. To induce dedifferentiation, cells at the 20th day of differentiation were detached and replated at about 50% confluence and RNA and protein were harvested 5 days following replating.

In silico analysis of CT and EMT gene expression

Expression data contained within GSE1614 [16] was GC-RMA normalized using GeneSpring v. 11.0. CT gene expression was analyzed based on 31 probesets in corresponding to 23 CT genes from 7 families (Figure S2). An interpretation was generated with an entity list composed of EMT related genes as defined by Loboda et al. [17], at three different time points. Genes for validation were selected among those for which significant differences of expression ($p < 0.05$) was observed by one way ANOVA test and Bonferroni FWER correction, when proliferating cells were compared to those at day 15.

Quantitative RT-PCR

Total RNA was isolated using the Trizol reagent (Ambion, Foster City, CA, USA) and treated with DNase I (Ambion, Foster City, CA, USA). 200 ng of RNA was reverse transcribed using Revert-Aid first strand cDNA synthesis kit (Thermo Fisher Scientific, Boston, MA, USA). PCR reactions were performed using an ABI 7500 thermal cycler (Applied Biosystems, Carlsbad, CA, USA). All reactions were performed according to manufacturer's recommendations. TaqMan Gene Expression Assays (Applied Biosystems, Carlsbad, CA, USA) were used for the following: GAPDH (4352934E), SPANX-B (Hs02387419_gH), PAGE2 and -2B (Hs03805505_mH), GAGE (Hs00275620_m1), SSX4 (Hs023441531_m1), NY-ESO-1 (Hs00265824_m1), and MAGE-A3 (Hs00366532_m1). SYBR Green master mix with ROX reference dye (Applied Biosystems, Carlsbad, CA, USA) was used to determine *CDH1*, *CDX2*, *CLDN4*, *VIM*, *FN1* and *TAGLN* expression (Table S1). Cycling conditions for these assays were 50°C for 2 min., 95°C for 10 min., followed by 40 cycles of 94°C for 15 sec., 60–65°C for 1 min. Relative expression was calculated by the $\Delta\Delta C_t$ method [18]. All samples were analyzed in triplicates and all experiments were repeated at least twice.

Promoter methylation analysis

Genomic DNA was isolated by Proteinase K treatment, following a phenol-chloroform extraction protocol. Bisulphite treatment of 200 ng genomic DNA was performed using Zymo DNA Methylation Gold Kit (Zymo Research, Irvine, CA, USA). Bisulphite modified DNA was stored at -20°C and used for PCR within 2 months. Two rounds of DNA amplification were performed using One Taq Hot Start DNA polymerase (New England Bioscience/NEB, Ipswich, MA, USA) using a Perkin Elmer 9700 thermal cycler (Applied Biosystems, Carlsbad, CA, USA). Primers used are given in Table S1. PCR products were gel extracted using the QIAGEN gel extraction kit (Qiagen, Hilden, Germany) and cloned into pCR2.1 (Invitrogen, Carlsbad, CA, USA). Plasmid DNA was purified using the QIAprep Spin Miniprep Kit (Qiagen, Hilden, Germany) from at least ten clones, and sequence analyzed by IONTEK (Istanbul, Turkey).

5-hydroxymethyl cytosine analysis

Caco-2 genomic DNA (gDNA) was sheared by probe sonication (30 sec. on, 30 sec. off, 5 cycles) to obtain 200–600 bp. fragments assessed by 1% agarose gel electrophoretic analysis. Immunoprecipitation was performed using the hMEDIP kit (Abcam, Cambridge, UK) according to manufacturer's instructions. 5 pg of control DNA was spiked into 500 ng of gDNA to use as an internal control. Positive and negative controls of the kit were included in all experiments. 2 μl from the eluted DNA was used as template for quantitative RT-PCR using 2 X SYBR Green master mix with ROX reference dye (Applied Biosystems, Carlsbad, CA,

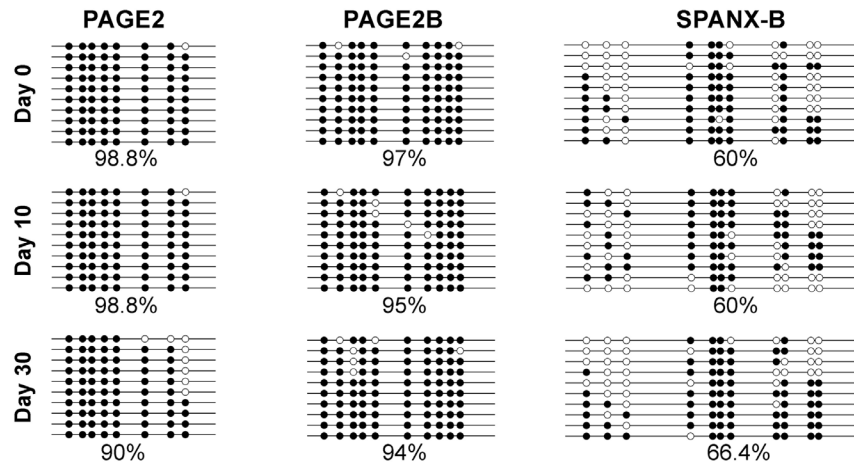


Figure 4. Bisulfide sequencing of *PAGE2*, *-2B* and *SPANX-B* promoter-proximal regions. Filled and empty circles represent methylated and unmethylated cytosines, respectively. % methylation within each analysed region, based on the 10 clones sequenced is indicated. CpG residues proximal to *PAGE2*, *-2B* and *SPANX-B* promoters during Caco2 differentiation at days 0, 10 and 30 reveals no statistically significant change (by one-way ANOVA). doi:10.1371/journal.pone.0107905.g004

USA) with the primers given in **Tables S1 and S2**. Primer efficiencies were controlled. Cycling conditions were 50°C for 2 min., 95°C for 10 min. followed by 40 cycles of 94°C for 15 sec., 60°C for 1 min. Shared genomic DNA was included in quantitative RT-PCR to calculate % input.

Immunofluorescence microscopy

Cells attached to glass slides by centrifugation using the Shandon CytoSpin3 (Thermo Scientific, Waltham, MA, USA) were immediately fixed in 2% formaldehyde/PBS at room temperature for 15 min. Fixed cells were permeabilized in 0.2% Triton X-PBS for 10 min. followed by blocking with 1% BSA in 0.1% PBS-Tween for 1 hour. Incubations with the primary antibody, diluted at 1:50, were performed overnight at 4°C. Secondary antibody was added at 1:200, following washing in 0.1% PBS-Tween for 5 min. for 3 times, and incubated with cells for 45 min. at room temperature (see **Table S3** for the complete antibody list). Stained samples were mounted with mounting medium (Santa Cruz Biotechnology, Santa Cruz, CA, USA) containing DAPI solution. Cell lines used as positive controls were Mahlavu (*PAGE-2,-2B* and *SPANXB*), MDA-MB 231 (VIM), MCF-7 (TAGLN) and SW620 (CDX2, FN1). Negative controls were combinations of primary antibodies with un-related secondary antibodies. All images were obtained using an AxioCam MRc5 image capture device (Carl Zeiss, Oberkochen, Germany).

Western analysis

Cell lysates (extracted with RIPA buffer) separated on 4–12% Novex Bis-Tris SDS gels (Invitrogen, Carlsbad, CA, USA) were transferred to Immobilon-PSQ membranes (Millipore Corp. Bedford, MA, USA) with an Invitrogen western blotting system (Invitrogen, Carlsbad, CA, USA). Following blocking with 5% milk powder in 0.02% PBS-T, blots were incubated with primary antibody overnight at 4°C. Primary antibody dilutions were 1:1000 for CDX2, fibronectin, vimentin and transgelin, 1:2500 for β -actin and 1:100 for *SPANX-B* and *PAGE-2,-2B* antibodies. HRP conjugated secondary antibody (Abcam, Cambridge, UK) was used at a 1:5000 dilution and incubated at room temperature for 1 hour. Signals were detected using the ECL luminescence assay (BioRad, Hercules, CA, USA).

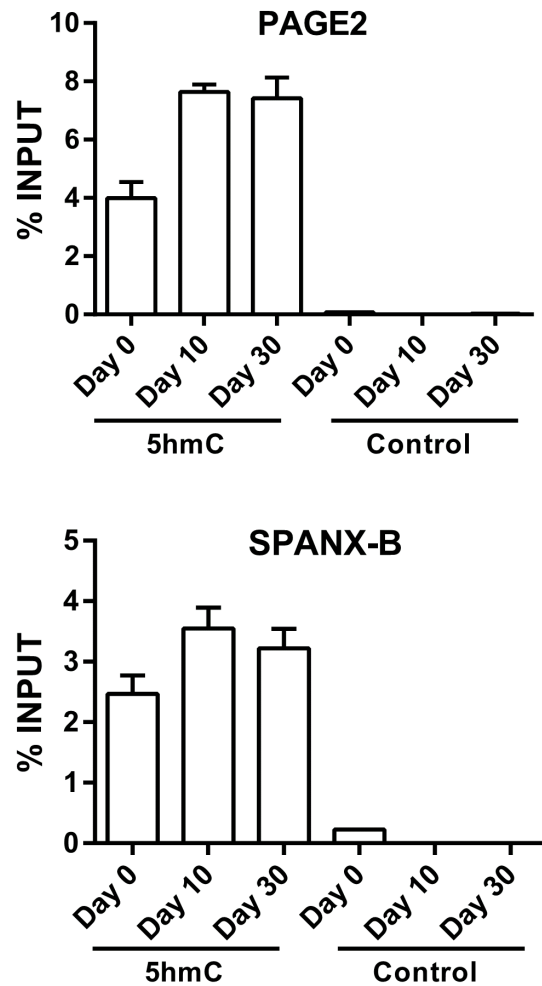


Figure 5. Increased hydroxymethylation of *PAGE2* and *SPANX-B* during Caco-2 spontaneous differentiation. CHIP experiments using an anti-hmC antibody and primers corresponding to +31 to +182 and +68 to +184 bp from the transcription start site of the *PAGE2* and *SPANX-B* genes, respectively. P values (one-way ANOVA) are 0.001 and 0.07 for *PAGE2* and *SPANX-B*, respectively. doi:10.1371/journal.pone.0107905.g005

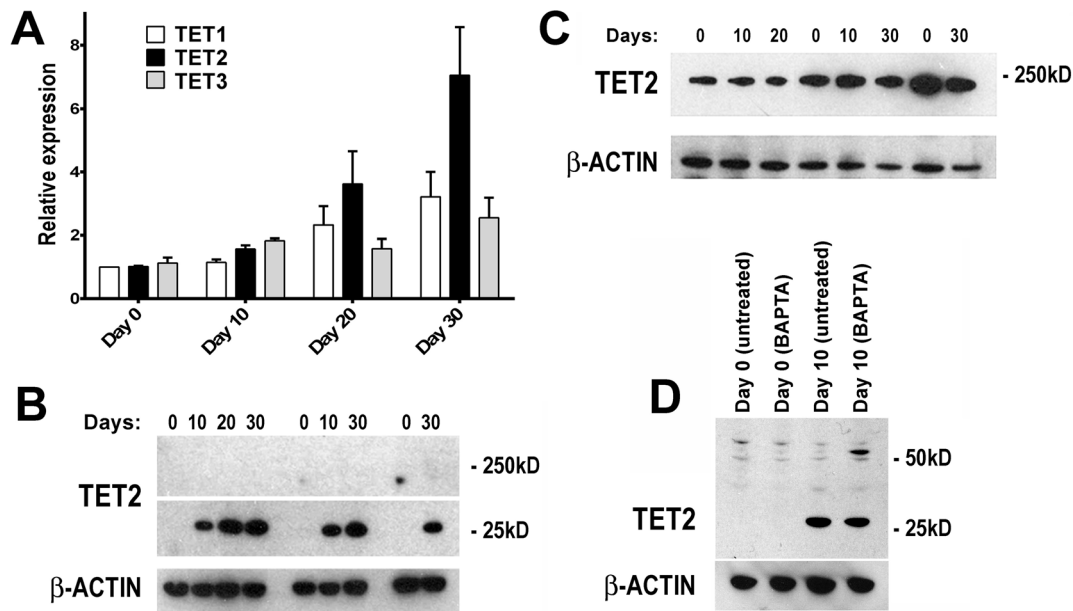


Figure 6. TET expression during Caco-2 SD. mRNA of all three TET genes increase gradually during Caco-2 SD (A). An increase in only a 25 kD version (B), but not the full-length TET2 protein (C) occurs simultaneously with the increase in mRNA. BAPTA-AM treatment results in a modest decrease in the 25 kD TET2 protein, with the generation of a larger mw version (D). P values, as determined by one-way ANOVA, are 0.03, 0.01, and 0.07, for Tet1, Tet2, and Tet3, respectively. doi:10.1371/journal.pone.0107905.g006

Chromatin Immunoprecipitation

Chromatin Immunoprecipitation (ChIP) was performed as previously described [15]. Briefly, formaldehyde cross-linked cell constituents were precipitated by protein A sepharose beads coupled to antibodies against EZH2, HP-1 or H3K27m3 (Abcam, Cambridge, UK), as well as isotype-specific control. Precipitated DNA was amplified using primers specific for *PAGE2*, *-2* or *SPANX-B* promoter sequences (Tables S1 and S2), following de-crosslinking.

Results

CT gene expression during Caco-2 spontaneous differentiation (Caco-2 SD)

The undifferentiated colorectal cancer cell line Caco-2 undergoes enterocytic differentiation upon reaching confluence *in vitro* [19,20]. Gradual differentiation has been observed up to 30 days post-confluence as evidenced by the up-regulation of various differentiation-associated genes including sucrase-isomaltase, alkaline phosphatase and carcinoembryonic antigen (CEA), (Figure S1) [15]. An *in silico* analysis of CT gene expression as defined by 31 probesets in the GSE1614 dataset, which contains gene expression data for the Caco-2 SD model obtained during differentiation (proliferating (2nd day), post-proliferation-undifferentiated (8th day), and post-proliferation-differentiated (15th day)) [16], revealed modest up-regulation of almost all CT genes during differentiation (Figure S2). We chose to validate the change in expression of six CT gene/gene families by quantitative RT-PCR in differentiating Caco-2 cells *in vitro*. *GAGE*, *MAGE-A3*, *NY-ESO-1* and *SSX4* transcripts were undetectable on the first day of confluence, as well as at later time points (data not shown). However, significant up-regulation of *PAGE2* (2 and 2B), and *SPANX-B* genes was evident (Figure 1).

PAGE2 and *SPANX-B* expression follow MET in the Caco-2 SD model

Spontaneous differentiation of Caco-2 *in vitro* has been reported to result in MET [21,22]. To determine if this occurred in parallel to the up-regulation of *PAGE2* and *SPANX-B*, we analyzed the GSE1614 dataset for the expression of genes representing EMT in colorectal cancer [17], and selected 6 genes to be validated in our model. Analysis of mRNA and protein expression of these revealed a decrease in mesenchymal genes (*vimentin*, *fibronectin 1* and *transgelin*) with a concomitant increase in expression of epithelial genes (*CDX2*, *claudin-4* and *E-cadherin*) as the cells differentiated, demonstrating that the increase in CT gene expression occurs simultaneously with MET in this model (Figure 1 & Figure S3).

PAGE2, *SPANX-B* and EMT gene expression *in situ*

To study if the changes in protein expression of CT and EMT genes occurred simultaneously in the same cells, we performed double immunofluorescence staining during differentiation. A gradual loss of mesenchymal markers was observed as cells differentiated, with a concomitant increase in epithelial genes and CT genes. *SPANX-B* and *PAGE-2* were frequently co-expressed with the epithelial marker *CDX2* in the same cells but almost never with *VIM* or *FN1* (Figures 2, 3 and Figures S4, S5, S6, S7).

PAGE2 and *SPANX-B* expression correlates with increased hmC and ten-eleven translocation methylcytosine dioxygenase (TET) up-regulation

Expression of all CT genes studied thus far including *PAGE2* and *SPANX-B* have been associated with the demethylation of CpG residues within regions proximal to the transcription start site [1,2,23–26]. In this line, both *PAGE2* and *SPANX-B* can be up-regulated by 5-aza 2'-deoxycytidine treatment (Figure S8).

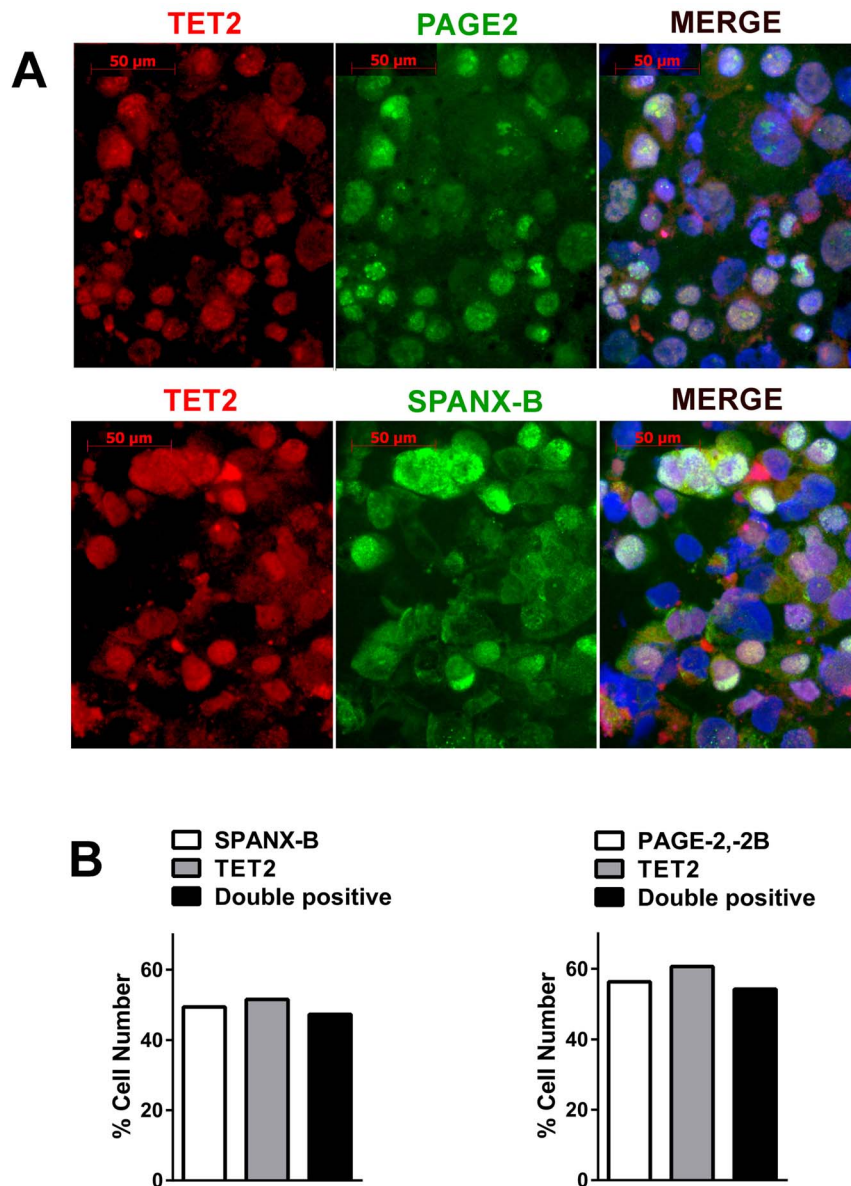


Figure 7. Overlapping TET2 and CT gene expression in differentiating Caco-2 cells. Double immunofluorescence staining for TET2 (Alexafluor 568: red) and SPANX-B or PAGE2 (Alexafluor 488: green) with DAPI counterstaining 20 days post-confluence show overlapping nuclear expression Magnification: 40× (**A**). More than 95% of cells expressing PAGE2 or SPANX-B were also positive for TET2 staining (**B**). doi:10.1371/journal.pone.0107905.g007

However, bisulfite sequencing of promoter-proximal regions of both *PAGE2* and *SPANX-B* revealed no differences at different stages of Caco-2 SD (**Figure 4**). As bisulfite sequencing is unable to distinguish methyl cytosine (mC) from hmC, we asked whether the change in CT gene expression could be related to altered hmC/mC ratios within their promoters. In fact, chromatin immunoprecipitation (ChIP) with a hmC specific antibody revealed an increase in hmC during differentiation in both *PAGE2* and *SPANX-B2* promoters (**Figure 5**). We next asked if the increase in hmC was related to an increase in TET1, -2, and -3 expression as these proteins are responsible for converting mC to hmC [27,28]. Indeed, the increase in hmC of *PAGE2* and *SPANX-B2* promoters were correlated with an up-regulation of *TET2* mRNA expression, together with modest increases in *TET1* and *3* (**Figure 6A**). Double immunofluorescence staining revealed

that the majority of cells expressing PAGE2 or SPANX-B were positive for TET2 staining; indicating these two events occurred in the same cells (**Figure 7**). It is therefore, likely that the increase in TET2 expression causes increased hmC in these genes. Interestingly, only a low molecular weight translation product (~25 kD) of TET2 was increased in the differentiating cells, when no clear difference in levels of the full-length TET2 protein was observed (**Figure 6B & C**). The peptide used for generating the commercial TET2 antibodies could specifically inhibit recognition of the 25 kD product confirming its identity with TET2 (data not shown). TET2 has recently been shown to undergo proteolytic cleavage by calpain 1 and 2, generating a 25 kD product *in vitro* [29]. To test if a cation-dependent protease is responsible for the generation of the 25 kD protein, we treated differentiating cells with an intracellular Ca²⁺ chelator (BAPTA-AM). This resulted in

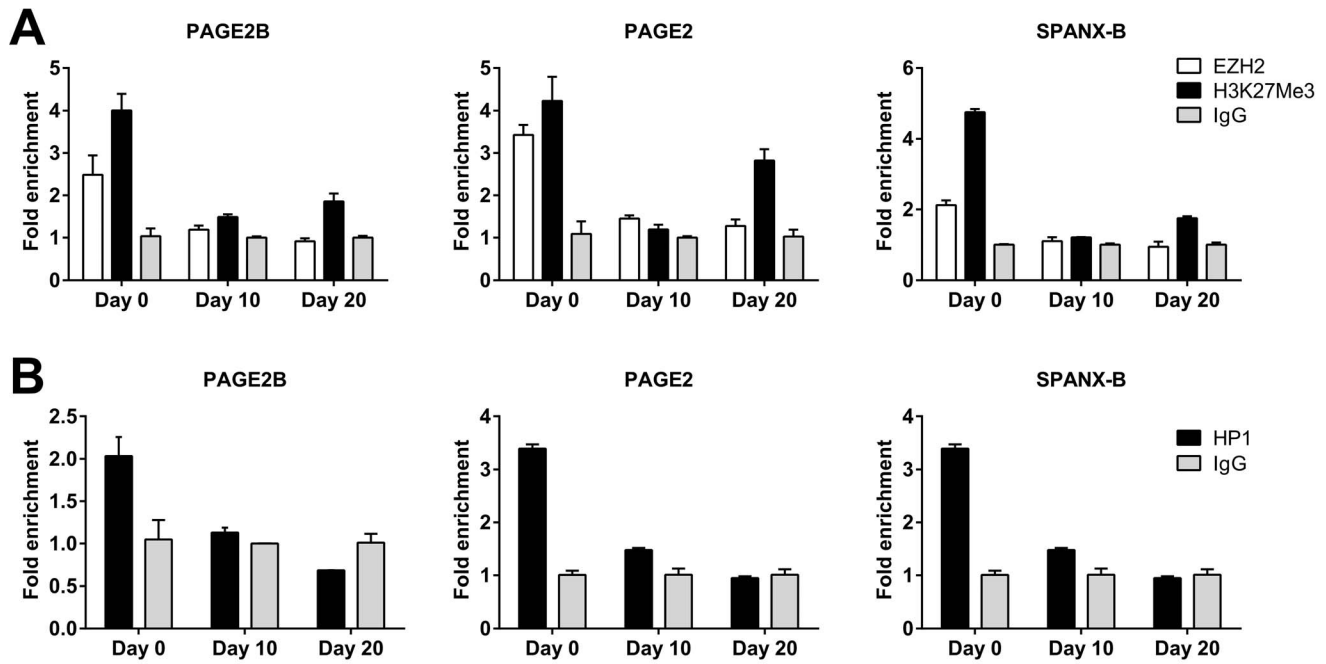


Figure 8. Chromatin modifications within *PAGE2* and *SPANX-B* during Caco-2 differentiation. CHIP analysis of *PAGE2*, *-2B* and *SPANX-B* transcription-start site-proximal regions reveals decreased EZH2 occupancy and H3K27m3 (A), as well as decreased HP-1 binding during differentiation (B). P values (one-way ANOVA) calculated for *PAGE2B*, *PAGE2*, and *SPANX-B*, are <0.001, 0.02, and 0.001 for EZH2; 0.003, <0.001, and <0.0001 for H3K27m3; and 0.001, <0.001, and <0.001, for HP1, respectively. doi:10.1371/journal.pone.0107905.g008

a modest reduction in the 25 kD TET2 protein with the concomitant generation of a larger molecular weight product (~50 kD), suggesting that the 25 kD TET2 protein is a Ca⁺² dependent protease cleavage product with a 50 kD intermediate (Figure 6D).

EZH2 and HP-1 occupancy of *PAGE2* and *SPANX-B* promoter proximal regions decrease during differentiation

Hydroxymethylation has been reported to prevail in promoters with dual H3K4 and H3K27 trimethylation that also bind PRC2 proteins [30]. The PRC2 complex protein EZH2 has been implicated

in the repression of *GAGE*, another CT gene [31]. We therefore, asked whether increased hmC within CT gene promoters resulted in altered EZH2 binding to the same sites. Indeed, ChIP experiments demonstrated a decrease in EZH2 occupancy, as well as a decrease in H3K27m3 in both *PAGE2* and *SPANX-B* promoters during Caco-2 SD (Figure 8). The PRC2 component SUZ12 has been reported to regulate H3K9 methylation and in turn, heterochromatin protein 1 (HP1 α) binding. In fact, we observed a simultaneous decrease in HP1 binding to both *PAGE2* and *SPANX-B* promoters during differentiation, that correlated with *PAGE2* and *SPANX-B* upregulation (Figure 8). Thus, our data suggest that both PRC2 and HP-1 contribute to maintaining *PAGE2* and *SPANX-B* in a transcriptionally silent state when the

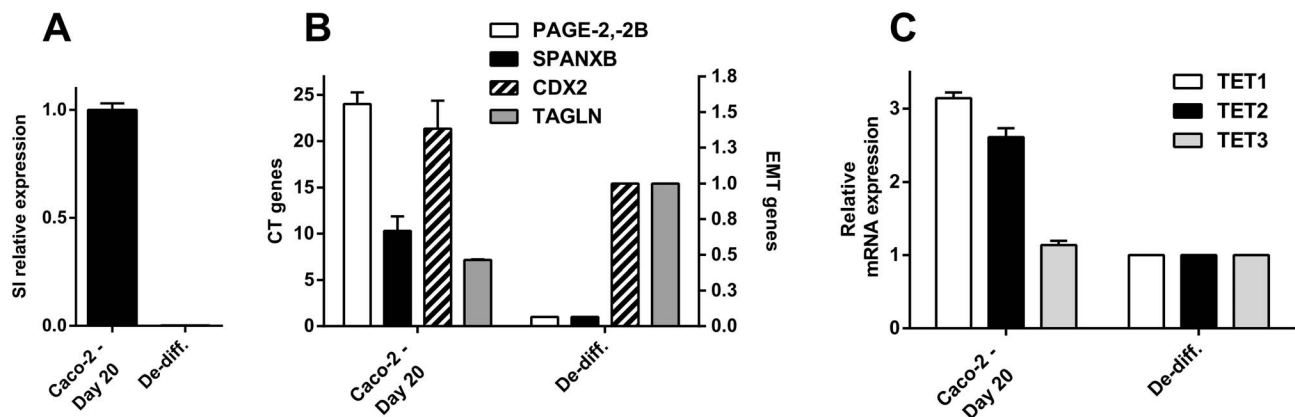


Figure 9. De-differentiation induced EMT and down-regulation of CT and TET genes. De-differentiation induced by growth under non-confluent conditions indicated by decreased *sucrose isomaltase* (SI) mRNA levels (A), leads to down-regulation of *CDX2*, *PAGE2*, *-2B* and *SPANX-B*, with concomitant up-regulation of *TGLN* (B). *TET1* and *-2* mRNAs are also down-regulated during de-differentiation (C). doi:10.1371/journal.pone.0107905.g009

cells have a mesenchymal phenotype, and that increased TET2 expression and hmC mediated transcriptional activation are related to PRC2 and HP-1 dissociation from the promoters of these CT genes during differentiation.

PAGE2 and SPANX-B up-regulation is reversed during EMT

We hypothesized that if the epigenetic alterations underlying CT gene expression happened in parallel to MET, that this process could be reversed if cells entered EMT. To test this hypothesis, differentiated Caco-2 cells were detached and allowed to proliferate for 5 days. This resulted in their rapid de-differentiation as evidenced by down-regulation of SI. De-differentiated cells down-regulated *PAGE2* and *SPANX-B*, as well as *CDX*, as they up-regulated *TAGLN*, in line with ongoing EMT (Figure 9). Although transcription of all three *TET* genes decreased during de-differentiation (Figure 9), we did not observe a decrease in hmC during this period (data not shown). We, therefore, conclude that the up-regulation of CT gene expression is reversible in this model.

Discussion

Previous studies revealed that CT gene expression correlated with an epithelial rather than a mesenchymal phenotype, and showed the up-regulation of CT genes during MET [12,14]. To our knowledge, this is the first report describing alterations in several epigenetic mechanisms within promoters of two CT genes during MET-like differentiation concordant with a dynamic change in gene expression. As bisulfite sequencing of *PAGE2* and *SPANX-B* promoters revealed no change upon differentiation, the increased hmC must strictly involve methylated CpG residues. This is in line with the fact that TET enzymes are responsible for the conversion of 5-methyl cytosine to 5-hydroxymethyl cytosine [27,28]. Conversion of hmC to mC is a far more complex process and might not happen with similar kinetics [32,33]. This is likely the reason why we did not observe a change in hmC during the 5 day de-differentiation process of Caco-2 cells despite the decrease observed in global TET levels. Our finding that *PAGE2*, *SPANX-B* and *TET2* induction is reversible is similar to another study in embryonic stem cells where Vitamin C was shown to induce TET2 expression, which in turn, resulted in up-regulation of CT genes. Both events were reversible upon Vitamin C withdrawal [34].

Although hydroxymethylation within gene promoters has been reported to decrease during differentiation of normal cells, a recent study revealed that about 20% of all modified cytosines in most CT genes in human brain, where they are not expressed, consist of hmC [35]. Up-regulation of TET2 expression in cancer has been associated with MET [36,37]; and therefore, a more differentiated state [30]. Similar to the inverse correlation between EZH2 and CT/TET2 expression we report here, others have shown EZH2 and TET enzymes to repress and induce differentiation of neuronal precursors, respectively [38]. CT genes are up-regulated during the initial stages of development in the human embryo, but decrease as tissues differentiate further [39]. As adult colon tissue does not show *PAGE2* or *SPANX-B* expression (data not shown), had Caco-2 cells the capability of differentiating further, both genes might have been down-regulated completely. On the other hand, the fact that we could not demonstrate up-regulation of *GAGE*, *MAGE-A3*, *NY-ESO-1* or *SSX4* expression in this model might be because these genes are expressed at earlier stages of differentiation. We believe this because *SPANX-B* expression is primarily in post-meiotic cells of the testis (i.e. spermatocytes,

spermatids, or sperm), whereas *GAGE*, *MAGE-A3*, *NY-ESO-1* or *SSX* expression is primarily in spermatogonia [11].

Our data and that of several others' indicate that cancer cells that express CT genes have more of an epithelial rather than a mesenchymal phenotype. We suggest that CT genes *PAGE2* and *SPANX-B* are induced during a window of differentiation that correlates with up-regulation of epithelial markers of differentiation. The Caco-2 SD model has made it possible to observe the actively changing epigenetic landscape within the promoters of these CT genes. However, as CT gene expression in tumors has closely been related to the methylation state of their promoter, the process that leads to CT gene induction *in vivo* might ultimately result in "fixing" of the epigenetic state which would in turn result in CpG methylation. Yet, via dynamic MET in tumors [40], it is conceivable that even this might change over the course of the disease.

From a clinical perspective, data from our lab as well as from others reveal that sub-grouping of tumors based on gene expression profiles can clearly identify cells with different chemosensitivity profiles [12,41,42]. In this line, we predict future studies will reveal distinct drug sensitivity profiles for colorectal cancer subtypes as possibly defined by *PAGE2* and *SPANX-B* expression, for which the Caco-2 SD model could be used.

Supporting Information

Figure S1 Post-confluence differentiation of Caco-2 *in vitro*. Up-regulation of *sucrase-isomaltase* (A), and carcinoembryonic antigen (CEA) (B) in cells collected at indicated days post confluence (DPC) as determined by quantitative RT-PCR, and Western analysis, respectively. Alkaline phosphatase expression is also upregulated as determined by immunohistochemistry revealing differentiation (C). Other measures of differentiation for the cells used in this study have been reported previously (ref. 17). *P<0.001 (ANOVA with Tukey's post hoc test). (DOCX)

Figure S2 Up-regulation of CT gene expression during Caco-2 spontaneous differentiation *in vitro*. Heat map based on 31 probesets in GSE1614 corresponding to 23 CT genes from 7 families. As compared to proliferating cells, gene expression incrementally increases in at confluence (8th day) and further during post-confluence differentiation (15th day). (DOCX)

Figure S3 Western analysis of differentially expressed genes during Caco-2 SD. A gradual increase in *SPANX-B* and *CDX2* in parallel to a decrease in expression of *FN*, *VIM* and *TGLN* up to day 30 post-confluence. Results from 3 independent differentiation experiments are shown. (DOCX)

Figure S4 *SPANX-B* and Fibronectin expression show limited overlap in differentiating Caco-2 cells. Immunofluorescent staining of differentiating Caco-2 cells with DAPI counterstaining reveals a gradual increase in nuclear *SPANX-B* (Alexa Fluor 488: green) with a concomitant decrease in cytoplasmic fibronectin expression (Alexa Fluor 568: red); (20× magnification) (A). Less than 10% of cells expressing *SPANX-B* stained for fibronectin at day 0 (B). (DOCX)

Figure S5 *PAGE2*, -2B and Vimentin expression are mutually exclusive in differentiating Caco-2 cells. Immunofluorescent staining of differentiating Caco-2 cells with DAPI counterstaining reveals a gradual increase in nuclear *PAGE2*, -2B (Alexa Fluor 488: green) with a concomitant decrease in

cytoplasmic vimentin expression (Alexa Fluor 568: red); (20× magnification) (A). Less than 10% of cells showed double fluorescence when staining was analyzed quantitatively at day 0. At later time points, none of the cells showed double staining (B). (DOCX)

Figure S6 PAGE2, -2B and fibronectin expression are mutually exclusive in differentiating Caco-2 cells. Immunofluorescent staining of differentiating Caco-2 cells with DAPI counterstaining reveals a gradual increase in nuclear PAGE2, -2B (Alexa Fluor 488: green) with a concomitant decrease in cytoplasmic fibronectin expression (Alexa Fluor 568: red); (20× magnification) (A). Less than 15% of cells showed double fluorescence when staining was analyzed quantitatively at day 0 (B). (DOCX)

Figure S7 Nuclear co-localization of CDX2 and PAGE2, -2B in differentiating Caco-2 cells. Immunofluorescent staining of differentiating Caco-2 cells with DAPI counterstaining reveals overlapping PAGE2, -2B (Alexa Fluor 488: green) and CDX2 (Alexa Fluor 568: red) expression; (20× magnification) (A). More than 80% of the cells show double-labeling when analyzed quantitatively (B). (DOCX)

Figure S8 Induction of PAGE2,-2B and SPANX-B gene expression by 5-aza-2'-deoxycytidine in HCT116 (top)

References

- Scanlan MJ, Gure AO, Jungbluth AA, Old LJ, Chen YT (2002) Cancer/testis antigens: an expanding family of targets for cancer immunotherapy. *Immunological Reviews* 188: 22–32.
- Caballero OL, Chen YT (2009) Cancer/testis (CT) antigens: potential targets for immunotherapy. *Cancer Sci* 100: 2014–2021.
- Hofmann O, Caballero OL, Stevenson BJ, Chen YT, Cohen T, et al. (2008) Genome-wide analysis of cancer/testis gene expression. *Proceedings of the National Academy of Sciences of the United States of America* 105: 20422–20427.
- Loriot A, Reister S, Parvizi GK, Lysy PA, De Smet C (2009) DNA methylation-associated repression of cancer-germline genes in human embryonic and adult stem cells. *Stem Cells* 27: 822–824.
- Mashino K, Sadanaga N, Tanaka F, Yamaguchi H, Nagashima H, et al. (2001) Expression of multiple cancer-testis antigen genes in gastrointestinal and breast carcinomas. *Br J Cancer* 85: 713–720.
- Gure AO, Chua R, Williamson B, Gonen M, Ferreira CA, et al. (2005) Cancer-testis genes are coordinately expressed and are markers of poor outcome in non-small cell lung cancer. *Clinical Cancer Research* 11: 8055–8062.
- Woloszynska-Read A, Mhawech-Fauceglia P, Yu JH, Odunsi K, Karpf AR (2008) Intertumor and intratumor NY-ESO-1 expression heterogeneity is associated with promoter-specific and global DNA methylation status in ovarian cancer. *Clinical Cancer Research* 14: 3283–3290.
- Jungbluth AA, Busam KJ, Kolb D, Iversen K, Coplan K, et al. (2000) Expression of MAGE-antigens in normal tissues and cancer. *Int J Cancer* 85: 460–465.
- Jungbluth AA, Chen YT, Busam KJ, Coplan K, Kolb D, et al. (2002) CT7 (MAGE-C1) antigen expression in normal and neoplastic tissues. *Int J Cancer* 99: 839–845.
- Jungbluth AA, Stockert E, Chen YT, Kolb D, Iversen K, et al. (2000) Monoclonal antibody MA454 reveals a heterogeneous expression pattern of MAGE-1 antigen in formalin-fixed paraffin embedded lung tumours. *Br J Cancer* 83: 493–497.
- Chen YT, Chiu RT, Lee P, Beneck D, Jin BQ, et al. (2011) Chromosome X-encoded cancer/testis antigens show distinctive expression patterns in developing gonads and in testicular seminoma. *Human Reproduction* 26: 3232–3243.
- Gupta PB, Onder TT, Jiang G, Tao K, Kuperwasser C, et al. (2009) Identification of selective inhibitors of cancer stem cells by high-throughput screening. *Cell* 138: 645–659.
- Hoek KS (2007) DNA microarray analyses of melanoma gene expression: a decade in the mines. *Pigment Cell Res* 20: 466–484.
- Argast GM, Krueger JS, Thomson S, Sujka-Kwok I, Carey K, et al. (2011) Inducible expression of TGF beta, Snail and Zeb1 recapitulates EMT in vitro and in vivo in a NSCLC model. *Clinical & Experimental Metastasis* 28: 593–614.
- Astarci E, Sade A, Cimen I, Savas B, Banerjee S (2012) The NF-kappaB target genes ICAM-1 and VCAM-1 are differentially regulated during spontaneous differentiation of Caco-2 cells. *FEBS J* 279: 2966–2986.
- Fleet JC, Wang L, Vitek O, Craig BA, Edenberg HJ (2003) Gene expression profiling of Caco-2 BBe cells suggests a role for specific signaling pathways during intestinal differentiation. *Physiol Genomics* 13: 57–68.
- Loboda A, Nebozhyn MV, Watters JW, Buser CA, Shaw PM, et al. (2011) EMT is the dominant program in human colon cancer. *BMC Medical Genomics* 4.
- Livak KJ, Schmittgen TD (2001) Analysis of relative gene expression data using real-time quantitative PCR and the 2^{-Delta Delta C(T)} Method. *Methods* 25: 402–408.
- Pinto M, Robineleon S, Appay MD, Kedinger M, Triadou N, et al. (1983) Enterocyte-Like Differentiation and Polarization of the Human-Colon Carcinoma Cell-Line Caco-2 in Culture. *Biology of the Cell* 47: 323–330.
- Simon-Assmann P, Turck N, Sidhoum-Jenny M, Gradwohl G, Kedinger M (2007) In vitro models of intestinal epithelial cell differentiation. *Cell Biology and Toxicology* 23: 241–256.
- Halleib JM, Saaf AM, Brown PO, Nelson WJ (2007) Transcriptional modulation of genes encoding structural characteristics of differentiating Enterocytes during development of a polarized epithelium in vitro. *Molecular Biology of the Cell* 18: 4261–4278.
- Saaf AM, Halleib JM, Chen X, Yuen ST, Leung SY, et al. (2007) Parallels between global transcriptional programs of polarizing Caco-2 intestinal epithelial cells in vitro and gene expression programs in normal colon and colon cancer. *Mol Biol Cell* 18: 4245–4260.
- Fratta E, Coral S, Covre A, Parisi G, Colizzi F, et al. (2011) The biology of cancer testis antigens: putative function, regulation and therapeutic potential. *Mol Oncol* 5: 164–182.
- Cannuyer J, Loriot A, Parvizi GK, De Smet C (2013) Epigenetic Hierarchy within the MAGEA1 Cancer-Germline Gene: Promoter DNA Methylation Dictates Local Histone Modifications. *Plos One* 8.
- Wang ZQ, Zhang J, Zhang YN, Lim SH (2006) SPAN-Xb expression in myeloma cells is dependent on promoter hypomethylation and can be upregulated pharmacologically. *International Journal of Cancer* 118: 1436–1444.
- Wang ZQ, Zhang J, Zhang Y, Srivenugopal K, Lim SH (2006) SPAN-XB core promoter sequence is regulated in myeloma cells by specific CpG dinucleotides associated with MeCP2 protein. *Blood* 108: 628a–628a.
- Iyer LM, Tahiliani M, Rao A, Aravind L (2009) Prediction of novel families of enzymes involved in oxidative and other complex modifications of bases in nucleic acids. *Cell Cycle* 8: 1698–1710.
- Loenarz C, Schofield CJ (2009) Oxygenase catalyzed 5-methylcytosine hydroxylation. *Chem Biol* 16: 580–583.
- Wang Y, Zhang Y (2014) Regulation of TET Protein Stability by Calpains. *Cell Rep* 6: 278–284.

30. Jiang Y, Liu S, Chen X, Cao Y, Tao Y (2013) Genome-wide distribution of DNA methylation and DNA demethylation and related chromatin regulators in cancer. *Biochim Biophys Acta* 1835: 155–163.
31. Sun F, Chan E, Wu Z, Yang X, Marquez VE, et al. (2009) Combinatorial pharmacologic approaches target EZH2-mediated gene repression in breast cancer cells. *Mol Cancer Ther* 8: 3191–3202.
32. Tsukada Y (2012) Hydroxylation mediates chromatin demethylation. *J Biochem* 151: 229–246.
33. Solary E, Bernard OA, Tefferi A, Fuks F, Vainchenker W (2014) The Ten-Eleven Translocation-2 (TET2) gene in hematopoiesis and hematopoietic diseases. *Leukemia* 28: 485–496.
34. Blaschke K, Ebata KT, Karimi MM, Zepeda-Martinez JA, Goyal P, et al. (2013) Vitamin C induces Tet-dependent DNA demethylation and a blastocyst-like state in ES cells. *Nature* 500: 222–226.
35. Wen L, Li X, Yan L, Tan Y, Li R, et al. (2014) Whole-genome analysis of 5-hydroxymethylcytosine and 5-methylcytosine at base resolution in the human brain. *Genome Biol* 15: R49.
36. Ficiz G, Branco MR, Seisenberger S, Santos F, Krueger F, et al. (2011) Dynamic regulation of 5-hydroxymethylcytosine in mouse ES cells and during differentiation. *Nature* 473: 398–402.
37. Song SJ, Polisenio L, Song MS, Ala U, Webster K, et al. (2013) MicroRNA-antagonism regulates breast cancer stemness and metastasis via TET-family-dependent chromatin remodeling. *Cell* 154: 311–324.
38. Hahn MA, Qiu R, Wu X, Li AX, Zhang H, et al. (2013) Dynamics of 5-hydroxymethylcytosine and chromatin marks in Mammalian neurogenesis. *Cell Rep* 3: 291–300.
39. Gjerstorff MF, Harkness L, Kassem M, Frandsen U, Nielsen O, et al. (2008) Distinct GAGE and MAGE-A expression during early human development indicate specific roles in lineage differentiation. *Hum Reprod* 23: 2194–2201.
40. Yao D, Dai C, Peng S (2011) Mechanism of the mesenchymal-epithelial transition and its relationship with metastatic tumor formation. *Mol Cancer Res* 9: 1608–1620.
41. Isbilen M, Senses KM, Gure AO (2013) Predicting Chemotherapy Sensitivity Profiles for Breast Cancer Cell Lines with and Without Stem Cell-Like Features. *Curr Signal Transduct Ther* 8: 268–273.
42. Isbilen M, Gure AO (2014) Identifying effective molecularly targeted drugs for hematological cancers. *Turkiye Klinikleri J Hematol-SpecialTopics* 7: 1–7.